

THE IDENTIFICATION AND CHARACTERIZATION OF  
NOVEL PERSISTENCE GENES IN  
*CHLAMYDIA TRACHOMATIS*

Matthew Kazuyuki Muramatsu

Submitted to the faculty of the University Graduate School  
in partial fulfillment of the requirements  
for the degree  
Doctor of Philosophy  
in the Department of Microbiology and Immunology,  
Indiana University

March 2017

Accepted by the Graduate Faculty, Indiana University, in partial fulfillment of the requirements for the degree of Doctor of Philosophy.

---

David E. Nelson, Ph.D., Chair

---

Byron E. Batteiger M.D.

Doctoral Committee

---

C. Henrique Serezani Ph.D.

---

Stanley M. Spinola, M.D.

November 30, 2016

---

William J. Sullivan, Jr., Ph.D.

© 2017  
Matthew Kazuyuki Muramatsu

## DEDICATION

I would like to dedicate this dissertation to my family for their support not only during my time in graduate school but throughout my entire life. I will always be eternally grateful for their never-ending sacrifice and how they have inspired me to work hard to achieve my goals.

## ACKNOWLEDGEMENTS

I would like to thank my mentor for his patience and allowing me the opportunity to present my scientific discoveries in papers and at conferences. My committee for providing invaluable guidance throughout my time in graduate school, and for setting me on the path to becoming a better scientific writer. The amazing secretaries who helped to keep me on track and moving toward my degree. Lastly, my friends and lab mates for their personal and scientific advice, and generally being there to help me blow off steam.

Matthew Kazuyuki Muramatsu

THE IDENTIFICATION AND CHARACTERIZATION OF NOVEL PERSISTENCE  
GENES IN *CHLAMYDIA TRACHOMATIS*

*Chlamydia trachomatis* is an obligate intracellular bacterial pathogen that can infect the eyes, genital tract, and disseminate to lymph nodes in humans. Many *C. trachomatis* infections are clinically asymptomatic and can become chronic if left untreated. When humans are infected with *C. trachomatis*, a cytokine that is produced is interferon-gamma (IFN- $\gamma$ ). *In vitro*, IFN- $\gamma$  stimulates expression of the host enzyme indoleamine 2,3-dioxygenase. This enzyme converts free intracellular tryptophan to N-formylkynurenine. Tryptophan starvation induces *C. trachomatis* to enter a viable-but-nonculturable state termed persistence, which has been proposed to play a key role in chronic *Chlamydial* disease. To circumvent host induced tryptophan depletion, urogenital strains of *C. trachomatis* encode a functional tryptophan synthase (TS). TS synthesizes tryptophan from indole and serine, allowing *Chlamydia* to reactivate from persistence. Transcriptomic analysis revealed *C. trachomatis* differentially regulates hundreds of genes in response to tryptophan starvation. However, genes that mediate entry, survival, and reactivation from persistence remain largely unknown. Using a forward genetic screen, we identified six Susceptible to IFN- $\gamma$  mediated Persistence (Sip) mutants that have diminished capacities to reactivate from persistence with indole. Mapping the deleterious persistence alleles in three of the Sip mutants revealed that only one of the mutants had a mutation in TS. The two other Sip mutants mapped had

mutations in CTL0225, a putative integral membrane protein, and CTL0694, a putative oxidoreductase. Neither of these genes plays a known role in tryptophan synthesis. However, amino acid (AA) competitive inhibition assays suggest that CTL0225 may be involved in the transport of leucine, isoleucine, valine, cysteine, alanine, and serine. Additionally, metabolomics analysis indicates that all free amino acids are depleted in response to IFN- $\gamma$ , making this amino acid transporter essential during persistence. Taken together we have identified two new chlamydial persistence genes that may play a role in chronic chlamydial disease.

David E. Nelson, Ph.D., Chair

## TABLE OF CONTENTS

LIST OF TABLES.....	ix
LIST OF FIGURES.....	x
LIST OF ABBREVIATIONS.....	xii
CHAPTER I: INTRODUCTION	
Section I: A brief history of chlamydial disease.....	1
Section II: Global prevalence of <i>C. trachomatis</i> infections.....	2
Section III: Intracellular development of <i>C. trachomatis</i> .....	4
Section IV: Chlamydial persistence.....	7
Section V: Chlamydial genetics.....	13
CHAPTER II: RESEARCH GOALS/HYPOTHESIS.....	23
CHAPTER III: MATERIALS AND METHODS.....	24
CHAPTER IV: Isolation and characterization of persistence mutants.....	45
CHAPTER V: Characterization of CTL0225.....	71
CHAPTER VI: Discussion.....	90
CHAPTER VII: Future Directions.....	101
REFERENCES.....	107
CURRICULUM VITAE	



## LIST OF TABLES

Table 1. Primers used in this study.....	39
Table 2. Plasmids used in this study.....	43
Table 3. Bacteria used in this study.....	44
Table 4. Mutations in Sip mutants.....	69

## LIST OF FIGURES

Figure 1. Prevalence of active and suspected regions of trachoma in 2015 .....	19
Figure 2. Sexually transmitted <i>C. trachomatis</i> infections in the US.....	20
Figure 3. <i>In vitro</i> <i>C. trachomatis</i> L2 life cycle.....	211
Figure 4. IFN- $\gamma$ mediated persistence .....	222
Figure 5. IFN- $\gamma$ persistence screen .....	36
Figure 6. Counterselection LGT.....	37
Figure 7. AA competitive inhibition screen.....	38
Figure 8. <i>C. trachomatis</i> L2 was transformed with pGFP::SW2.....	56
Figure 9. Secondary screening.....	57
Figure 10. Sip mutants exhibit normal growth kinetics .....	58
Figure 11. Sip mutants make fewer EB following reactivation .....	59
Figure 12. Sip recombinants form similar numbers of inclusions as L2-GFP .....	60
Figure 13. Sip mutant make smaller inclusions following reactivation .....	61
Figure 14. Transmission electron microscopy of L2-GFP and Sip mutants .....	62
Figure 15. Sip mutant EB production cannot be rescued by Trp or indole .....	63
Figure 16. Genome replication is altered during Sip mutant reactivation.....	64
Figure 17. Sip 6 forms small inclusions in the presence of IFN- $\gamma$ + Trp.....	65
Figure 18. Trp starvation alone induces Sip mutants to enter persistence.....	66
Figure 19. Sip1 TrpB <sup>P221S</sup> aligned to <i>Salmonella typhimurium</i> TS.....	67
Figure 20. Sip6 CTL0694 <sup>P105L</sup> aligned to the crystal structure of <i>E. coli</i> CysJ. ....	68
Figure 21. G77E mutations alters CTL0225 membrane topology .....	77
Figure 22. Sip2 is sensitive to high concentrations of Ile .....	78
Figure 23. Only Val reverses the Sip2 small inclusion phenotype.....	79
Figure 24. Ala reverses formation of small inclusions induced by excess Ser ....	80

Figure 25. Ala reverses Sip2 small inclusion phenotype caused by Cys.....	81
Figure 26. Sip2 forms two populations of inclusions when treated with Ser.....	82
Figure 27. Ala does not reverse small inclusion phenotype caused by Ile .....	83
Figure 28. Sip2 does not form large inclusions in the presence of Val + Ser.....	84
Figure 29. Free AA concentrations remain stable over time.....	85
Figure 30. Free AA decrease over time in IFN- $\gamma$ treated HeLa cells.....	86
Figure 31. IFN- $\gamma$ decreases free AA pools in HeLa cells.....	87
Figure 32. <i>C. trachomatis</i> increases some free AA pools.....	88
Figure 33. Free AAs are not increased during IFN- $\gamma$ mediated persistence .....	89

## LIST OF ABBREVIATIONS

ABA.....	Aminobutyric acid
Ala.....	Alanine
Amp.....	Ampicillin
ATc.....	Anhydrous tetracycline
BACTH.....	Bacterial two-hybrid
BCAA.....	Branched chained amino acids
Bp.....	Base pair
Bpdl.....	2,2'-bipyridyl
Bsd.....	Blasticidin S deaminase
BV.....	Bacterial vaginosis
Cat.....	Chloramphenicol acetyltransferase
CDC.....	Centers for disease control
CdsF.....	Chlamydial needle-forming protein
ChxR.....	Chlamydial mid-cycle transcription factor
COMC.....	<i>Chlamydia</i> outer membrane complex
Cys.....	Cysteine
CysJ.....	<i>E. coli</i> sulfite reductase subunit alpha
DAM.....	Deferoxamine mesylate
DMEM-10.....	Dulbecco's modified Eagle's medium
DMEM-10G.....	DMEM-10 supplemented with IFN- $\gamma$
DMEM-TF.....	DMEM-10 without tryptophan
EB.....	<i>Chlamydia</i> elementary body
EMS.....	Ethyl methanesulfonate

ER.....	Endoplasmic reticulum
EVIHI.....	Anti-chlamydial LPS antibody
FACS.....	Fluorescence activated cell sorter
FBS.....	Fetal bovine serum
FRAEM.....	Fluorescence-reported allelic exchange mutagenesis
GFP.....	Green fluorescent protein
GyrA.....	DNA gyrase subunit A
HAP.....	6-N-hydroxylaminopurine
HeLa.....	HeLa229 - Henrietta Lacks cervical epithelial cells
HEPES.....	4-2-hydroxyethyl-1-piperazineethanesulfonic acid
Hpi.....	Hours post infection
HPLC.....	High performance liquid chromatography
IDO1.....	Indoleamine 2,3-dioxygenase
Ile.....	Isoleucine
Incs.....	Inclusion membrane proteins
ISG.....	Interferon stimulated genes
Kb.....	Kilobase
Ksm.....	Kasugamycin
L2-GFP.....	<i>Chlamydia trachomatis</i> L2/434Bu expressing GFP
LB.....	Luria-Bertani liquid medium
Leu.....	Leucine
LGT.....	Lateral gene transfer
mARC.....	Mitochondrial amidoxime reducing component
MCS.....	Multiple cloning site
Met.....	Methionine

MD-76R.....	Diatrizoic acid
MOI.....	Multiplicity of infection
NEAA.....	Non-essential amino acids
PBPs.....	Penicillin binding proteins
PBS.....	Phosphate-buffered saline
PCR.....	Polymerase chain reaction
PG.....	Peptidoglycan
Phe.....	Phenylalanine
PID.....	Pelvic inflammatory disease
PZ.....	Chlamydial plasticity zone
qPCR.....	Quantitative PCR
Rab1.....	Ras-related proteins in brain 1
Rab11.....	Ras-related proteins in brain 11
Rab4.....	Ras-related proteins in brain 4
Rab5.....	Ras-related proteins in brain 5
Rab7.....	Ras-related proteins in brain 7
Rab9.....	Ras-related proteins in brain 9
RB.....	Chlamydia reticulate body
RpoB.....	RNA polymerase subunit B
rSip.....	Recombinant Sip strain
Ser.....	Serine
Sip.....	Sensitive to IFN- $\gamma$ induced persistence
SNAREs.....	Soluble NSF attachment protein receptor
SNAT.....	Small neutral amino acid transporter
Spc.....	Spectinomycin

SPG.....	Sucrose-phosphate glutamic acid buffer
STI.....	Sexually transmitted infections
T3SS.....	Type three secretion system
TCA.....	Trichloroacetic acid
TEM.....	Transmission electron microscopy
TILLING.....	Targeted induced local lesions in genomes
TL.....	Tryptophan limiting
Trp.....	Tryptophan
TrpA.....	Tryptophan synthase $\alpha$ -subunit
TrpB.....	Tryptophan synthase $\beta$ -subunit
TS.....	Tryptophan synthase
Val.....	Valine
VAMP4.....	Vesicle-associated membrane protein 4
VBNC.....	Viable-but-non-culturable-state
WARS.....	Tryptophanyl-tRNA synthetase
WGS.....	Whole genome sequencing
WHO.....	World health organization
YcbX.....	<i>E. coli</i> base analog detoxification protein
ZeoR.....	Zeocin resistance

## Chapter I: Introduction

### Section I:

#### A brief history of chlamydial disease

*Chlamydia trachomatis* is an obligate intracellular bacterial pathogen that has been co-evolving with humans for thousands of years. Scarring in ancient Aboriginal Australian skulls, dating back to around 8000 BC, is the earliest evidence of chronic *C. trachomatis* eye infections [1]. Additionally, the ancient Egyptians were among the first to describe treatments for a Chlamydia-like disease known as *nehat* in the Ebers Papyrus around 1500 BC [2].

*C. trachomatis* is one of the most prolific human pathogens. The ebb and flow of human conquest and exploration have contributed to the global dissemination of *C. trachomatis*. Troops returning from the Napoleonic Wars (1803-1815) may have contributed to the spread of *C. trachomatis* from Egypt to Europe [3]. The fear of trachoma was so great that in 1897 the United States government classified *C. trachomatis* as a “loathsome and contagious disease” and increased screening of U.S immigrants in an attempt to control its spread [4].

In 1907, Halberstaedter and Prowazek noticed small inclusion bodies, later determined to be chlamydial inclusions, in the cytoplasm of cells from scrapings of apes and humans with trachoma [5]. Shortly after this, the detection of inclusion bodies in newborns with conjunctivitis [6] and people with non-gonococcal sexually transmitted disease [7, 8], suggested that there may be a link between ocular trachoma, neonatal conjunctivitis, and genital disease. Additionally, monkeys infected with material gathered from men and women presenting with non-gonococcal genital infections developed trachoma



[9]. Results from these studies suggest that trachoma and non-gonococcal genital disease were caused by the same etiological agent, later classified as *C. trachomatis*.

## **Section II:**

### ***Chlamydia trachomatis* infections**

#### **Ocular chlamydial disease**

*C. trachomatis* serovars differ in their tissue tropisms and pathogenic strategies. Serovars A-C are the etiological agents of trachoma and primarily infect the conjunctival epithelial cells in the eye. While trachoma is still a global public health problem, improvements in sanitation and hygiene have limited the spread of *C. trachomatis* in the past several decades [10]. Currently, trachoma is only endemic in poor and rural locations of 42 countries located in Africa, Central and South America, Asia, Australia, and the Middle East (Figure 1).

Despite the fall in the global prevalence of trachoma, *C. trachomatis* serovars A-C remain the leading cause of preventable blindness by an infectious agent. When left untreated, repeated infections can lead to conjunctival scarring, development of corneal opacities, and possible progression to trichiasis (i.e., inversion of the eyelashes), which can result in irreversible blindness. Approximately 7.2 million people live with advanced trachoma, while another 200 million are at risk by living in trachoma endemic areas. In 2015, roughly 54 million people were treated for conjunctival *C. trachomatis* infections. The loss of productivity and treatment costs associated with trachoma was recently estimated at 8 billion dollars [11, 12], indicating trachoma is still a significant global health and economic burden.

## **Sexually transmitted chlamydial disease**

### **Urogenital**

*C. trachomatis* serovars D-K are sexually transmitted and typically cause urogenital infections. According to the World Health Organization (WHO), there are approximately 131 million new cases of sexually transmitted *C. trachomatis* infections each year [13]. In the United States, the most common sexually transmitted bacterial infection is *C. trachomatis*. National surveillance data, provided by the Centers for Disease Control and Prevention (CDC), indicate that rates of *C. trachomatis* infection were among the highest in Washington DC, Alaska, and the Virgin Islands (Figure 2).

In 2014, the CDC documented 1,441,789 new sexually transmitted *C. trachomatis* infections across the United States. However, they estimate that the annual number of urogenital *C. trachomatis* infections may be closer to 2.8 million per year because the majority of infections are asymptomatic in men and women (50% and 70% of all infections, respectively) [14]. When symptoms are present, men usually present with urethritis and less commonly with epididymitis [15]. Symptomatic women may present with Bartholin's cystitis, cervicitis, and acute urethral syndrome [16]. Additionally, chronically infected women are at risk for pelvic inflammatory disease (PID), endometritis, and ectopic pregnancies [17, 18]. A smaller proportion of patients can also develop Reiter's syndrome (reactive arthritis) [19, 20]. The CDC recommends that *C. trachomatis* urogenital infections be treated with a single dose of 1 gram of azithromycin or 100 milligrams of doxycycline twice daily for seven days.

## **Rectal**

*C. trachomatis* urogenital strains can also infect the rectum, most commonly in men who have sex with men. In heterosexuals, detection of rectal infections is not as common as urogenital tract infections. However, the frequency of rectal infections in heterosexuals may be higher than what is appreciated because screening the rectum for *C. trachomatis* is not standard practice unless patients have specific risk factors. *C. trachomatis* D-K rectal infections are usually asymptomatic. In contrast, *C. trachomatis* L1-L3 strains, which frequently infect the rectum, can cause severe disease and pathology [21].

While rectal infections with *C. trachomatis* D-K are rarer than urogenital infections in women, there is increasing concern that some apparent urogenital treatment failures may arise because of autoinoculation from the rectum [22, 23]. Additionally, a meta-analysis of rectal chlamydia treatment studies indicates doxycycline may be more efficacious than azithromycin for rectal *C. trachomatis* infections [24]. These studies suggest that *C. trachomatis* GI tract infections may be refractory to treatment with azithromycin and that GI tissues may be acting as a chlamydial reservoir contributing to apparent azithromycin treatment failure in women.

### **Section III:**

#### **Intracellular development of *Chlamydia trachomatis***

##### ***In vitro* chlamydial developmental lifecycle**

*C. trachomatis* is an obligate intracellular pathogen that has a biphasic life cycle (Figure 3). The extracellular, infectious forms of *Chlamydia* spp. are known as elementary bodies (EBs). EBs contain an electron dense nucleoid [25] that is enveloped in a protein shell known as the chlamydial outer membrane

complex (COMC). The COMC is primarily composed of three highly cross-linked cysteine-rich proteins OmpA, OmcA, and OmcB. These proteins are connected by disulfide bonds to form a semi-permeable lattice. [26-28] The COMC also contains “rosette structures” [29] that are thought to be composed of the chlamydial type III secretion system (T3SS) pores and the needle-forming protein, CdsF [30]. T3SS is a critical virulence factor that facilitates the injection of chlamydial proteins into host cells [31]. Ultrastructural analysis indicates that EBs have a polarized architecture and that CdsF associated needle-like structures form at the pole closest to host cells [32], suggesting that the T3SS plays a role in cellular invasion.

After an EB has successfully entered a host cell, the COMC is reduced [26], and EBs transition into reticulate bodies (RBs). Unlike EBs, RBs are non-infectious, metabolically active, and can replicate [31, 33, 34]. Genes necessary for RB replication and EB production are temporally regulated in *C. trachomatis* and fall into three rough categories called early, mid, and late genes [35-37].

Transcription of early genes begins 1 to 3 hours after *C. trachomatis* infection. Functions of early genes include suppressing transcription of late genes, macromolecular synthesis (transcription, translation, DNA replication), and setting up the nascent chlamydial inclusion [36]. During this time, EBs are also transitioning into RBs, and early inclusion membrane proteins (Incs) begin to decorate the nascent inclusion [38]. The majority of Incs share low primary sequence similarity; however, they are capable of forming similar secondary bilobed structures with N- and C- termini facing the cytoplasmic side of the inclusion membrane [39, 40]. Early Incs may prevent endocytic maturation of the chlamydial inclusion and fusion with lysosomes by preventing the

recruitment of early (Rab5) and late (Rab7 and Rab9) endocytic markers [41]. Additionally, the Inc protein CT850 plays a role in relocating the inclusion from the periphery of the cell to the peri-Golgi region, in a dynein-dependent manner [42, 43]. By relocating to the peri-Golgi region, RBs have access to nutrients from exocytic vesicles that promote growth and development of RB and the inclusion.

By eight hours post infection, the majority of *C. trachomatis* genes involved with replication, metabolism, and inclusion development begin to be expressed [44]. Incs expressed during mid-development may facilitate inclusion and chlamydial growth by recruiting host Rab proteins. Some Rab proteins that associate with the inclusion membrane include Rab4 and Rab11, which are involved in receptor recycling, and Rab1, which participates in vesicle trafficking from the endoplasmic reticulum (ER) to the Golgi [41]. Recruitment of these Rabs promotes the association of SNAREs, syntaxin6, and VAMP4 proteins. These proteins facilitate eukaryotic vesicle interactions and lead to the fusion of nutrient rich vesicles containing sphingomyelin and cholesterol with the chlamydial inclusion [45-47].

Late in development (>24h), most RBs have undergone 8 to 10 rounds of replication by binary fission [48] and a yet undefined asymmetric-polarized budding process [49, 50] and have begun to transition back into EBs. Increased late gene products may influence RB to EB transition. Known roles of late genes include DNA condensation, the formation of the COMC, and EB maturation. Late gene transcription has been shown to be inversely related to the expression of the early gene *euo*, which binds to late gene promoters and represses transcription [51]. Additionally, sigma-28 is a transcription factor that promotes late gene transcription [52].

Once RBs have transitioned into EBs, these are then released by host cell lysis or by extrusion of the entire chlamydial inclusion [53]. The release of EB from mature inclusions and subsequent host cell lysis is dependent on the plasmid gene *pgp4*. Pgp4 is a transcription factor that regulates chromosomal and plasmid genes. One of these genes is a T3S effector that destabilizes actin surrounding the chlamydial inclusion [54]. In addition to the destabilization of actin, chlamydial phospholipases, expressed during mid and late development [37], may weaken the inclusion membrane. In contrast to inclusion lysis, extrusion is an actin-dependent process that preserves the chlamydial inclusion and releases it without killing the host cell [55]. By manipulating the myosin phosphatase pathway, *C. trachomatis* hijacks phosphorylated myosin light chain 2 (MLC2), myosin light chain kinase (MLCK), and myosin II to extrude from the host cell [56].

#### **Section IV:**

#### **Chlamydial persistence**

Various stimuli can disrupt the *C. trachomatis* biphasic development cycle and induce *C. trachomatis* to enter a viable-but-non-culturable (VBNC) state termed persistence [48]. When this occurs, three phenotypes characterize persistent chlamydial forms. First, persistent chlamydia forms small inclusions that contain enlarged and non-dividing RB [48]. Second, these aberrant RBs continue to replicate their genomes [57]. Third, these aberrant RBs can resume development and make infectious EB when the persistence inducing stimulus is removed [58].

Many stimuli can induce persistence *in vitro*. In the following paragraphs the most studied persistence models will be discussed (e.g. penicillin treatment,

iron and amino acid limitation). However, the focus of this dissertation will be on the IFN- $\gamma$  persistence model.

### **Penicillin-induced persistence**

Penicillin was the first stimulus identified that induces *Chlamydia* persistence [48]. Chlamydiae contain 3 PBPs (PBP1, PBP2, and PBP3). PBP1 and PBP2 have transpeptidase activity, while PBP3 has carboxypeptidase activity [59, 60]. When penicillin binds PBPs, RB replication and RB to EB differentiation is inhibited, leading to the formation of enlarged RB. Removal of penicillin allows persistent RB to reactivate and resume normal development [48]. These studies suggest that physically limiting RB division is sufficient to induce persistence. However, limiting available nutrients can also induce persistence, and may be more relevant *in vivo* as penicillin treatment is not routinely used to treat chlamydia.

### **Iron limitation induced persistence**

Iron is a key co-factor utilized in both eukaryotic and prokaryotic cellular processes. As obligate intracellular pathogens, chlamydiae are highly dependent on host cells for free iron. The iron chelating agent deferoxamine mesylate (DAM) reduces free iron and induces chlamydiae to enter persistence. Unlike in the penicillin induced persistence model, DAM treatment causes the inclusion to bleb vesicles and alters the morphology of RB and EB. Additionally, some of the chlamydial inclusions have a ruffled membrane and associate with an unknown electron dense material [61].

The phenotypes observed with DAM treatment are not consistent with other chlamydial persistence models. Further investigations revealed DAM does not passively diffuse through cellular membranes, suggesting the phenotypes

elicited by DAM may be caused by inadequate iron-chelation [62]. Consistent with this hypothesis, treatment with 2,2'-bipyridyl (Bpdl), a membrane permeable iron chelator, caused *C. trachomatis* to form aberrant RB that resemble those seen in other persistence models [63].

### **Amino acid limitation induced persistence**

Depletion of amino acids (AA) can induce *C. trachomatis* persistence. For example, depleting cells of any of the branched chained amino acids (BCAA), isoleucine (Ile), leucine (Leu), or Valine (Val) inhibited *Chlamydia pneumoniae* and *C. trachomatis* EB production [64, 65]. However, depleting cells of a second structurally similar AA partially restored EB production [66]. These results indicate that depletion of one AA can be partially reversed by removal of a second AA, suggesting that the depleted AA is competitively inhibiting the uptake of the second AA, whose unopposed uptake results in persistence.

High concentrations of AA can also induce persistence through competitive inhibition of chlamydial AA transporters. For example, elevated levels of Ile, Leu, phenylalanine (Phe), and methionine (Met) competitively inhibit the transport of Val into *C. trachomatis*. When this occurs, *C. trachomatis* forms small inclusions filled with aberrant RB similar to those seen in other persistence models. However, competitive inhibition is alleviated when cells are co-treated with Val, suggesting Val starvation induces *C. trachomatis* persistence [67].

Co-infection with other intracellular pathogens can also induce *C. trachomatis* persistence. For example, *C. trachomatis* enters persistence when HeLa cells are co-infected with *Toxoplasma gondii*. As *T. gondii* is an intracellular parasite, it likely outcompetes *C. trachomatis* for specific nutrients



such as iron, lipoic acid, cholesterol, and AA, inducing *C. trachomatis* persistence. Consistent with this hypothesis, when pyrimethamine killed *T. gondii*, *C. trachomatis* reactivated from persistence. Additionally, by supplementing the medium with essential AA, *C. trachomatis* was able to reactivate from persistence. These results suggest essential AA limitation was the key factor inducing persistence [68].

### **IFN- $\gamma$ mediated persistence**

The IFN- $\gamma$  mediated persistence model may be the most relevant model of chlamydial persistence model because this cytokine is essential to controlling *Chlamydia* infections in animals. Moderate concentrations of IFN- $\gamma$  induces *Chlamydia psittaci* and *C. trachomatis* to enter persistence in T24 and HeLa 229 (HeLa) cells, respectively [58, 69]. IFN- $\gamma$  treatment causes host cells to upregulate indoleamine 2,3-dioxygenase (IDO1) (Figure 4A), which catabolizes tryptophan (Trp) to N-formylkynurenine (Figure 4B). Additionally, IFN- $\gamma$  does not induce *C. trachomatis* persistence in IDO1 deficient cells [70], and supplementing the medium with Trp causes persistent RB to reactivate [58, 71]. Furthermore, decreasing the concentration of Trp in the medium in the absence of IFN- $\gamma$  can also induce *C. trachomatis* persistence [72]. These results indicate that IDO1 mediated Trp starvation is the persistence-inducing stimulus in the IFN- $\gamma$  mediated persistence model [58, 73].

Urogenital strains of *C. trachomatis* can circumvent Trp starvation because they encode a functional tryptophan synthase (TS), which can synthesize Trp from indole and serine (Ser) (Figure 4C) [74-78]. Neither humans nor *C. trachomatis* synthesizes indole, suggesting that indole is scavenged from

another source, possibly indole-producing microorganisms in the genital and GI tract [79-81].

### **Differential gene expression between persistence models**

All persistence inducing stimuli cause chlamydiae to form small inclusions filled with aberrant RB. However, it is unknown what genes mediate this transition. A transcriptomic study indicated many genes are up- or down-regulated in persistent RB, during IFN- $\gamma$  mediated persistence, as compared to normal RB, growing in the absence of IFN- $\gamma$ . The microarray data indicate that many of the up-regulated genes are involved in tryptophan synthesis, DNA repair, and phospholipid biosynthesis, while many of the down-regulated genes are involved in RB to EB differentiation, cell division, and the TCA cycle [82]. As this is the only transcriptome study focusing on *C. trachomatis* persistence, it is hard to determine if there are common and stimuli specific persistence genes.

Using different persistence inducing stimuli, several studies have examined the differential expression of a few specific genes during chlamydial persistence. Comparing the data from these studies suggests that gene expression varies between different persistence inducing stimuli [83-85]. For example, *ftsK*, an essential cell division gene, is up-regulated in the penicillin induced persistence model, but down-regulated in the IFN- $\gamma$  mediated persistence model [82, 83]. Additionally, *ftsW*, which encodes a lipid II flippase, remains unchanged in the penicillin model but is down-regulated in the IFN- $\gamma$  model [37, 86]. In contrast, some genes share the same transcriptomic profile such as *hctB*, a histone-like gene, which is down-regulated in both the penicillin and IFN- $\gamma$  persistence models. These data suggest that common persistence genes are likely involved with RB to EB differentiation, while stimuli specific

persistence genes may participate in alleviating the persistence inducing triggers.

### ***In vivo* evidence for persistence**

There has been concern that chlamydial persistence is an artifact elicited by *in vitro* stimuli because detecting persistent chlamydial forms in patients has proven challenging. Some challenges include detecting persistent RB forms in tissue and confirming that these are VBNC.

Animal models show the presence of VBNC *Chlamydia in vivo* [87] and that they can be reactivated to produce viable EB [88]. Additionally, VBNC *C. trachomatis* may have also been detected in tubal biopsy specimens. The majority of these samples contained chlamydial DNA and antigens, but *C. trachomatis* could only be cultivated from 3 out of 25 patient samples [89]. Furthermore, persistent RBs have been detected in other patient samples. Aberrant RBs have been observed in fibroblasts and macrophages gathered from the synovial tissue of patients with Reiter's syndrome [90], as well as macrophages collected from aortic valve tissue [91].

A recent study of cervical scrapings provided some of the best evidence that *C. trachomatis* persistence models may be relevant in humans. Transmission electron microscopy (TEM) of the cervical scrapings revealed multiple inclusions of varying size containing normal RB, EB, and aberrant RB. These samples also contained a high concentration of chlamydial genomes but produced few infectious EBs. Additionally, genital secretions of one patient were assayed and found to contain a high concentration of IFN- $\gamma$  and indole [92]. These results suggest that *in vivo* conditions exist to induce *C. trachomatis* to enter and reactivate from IFN- $\gamma$  mediated persistence. However, it remains

unclear if persistence occurs *in vivo* or is relevant to human disease because of the limited number of patient samples.

## **Section VI:**

### **Chlamydial genetics**

The *C. trachomatis* serovar D genome indicated it is A+T rich (58.7%), approximately one megabase in size, and encodes approximately 900 functional genes [78]. Comparisons of chlamydial genomes have indicated that they are highly conserved and that relatively few novel genes influence virulence and tropism between organisms. However, most of these genes have not been systematically characterized because the tools required for genetic manipulation of *Chlamydia* spp. have only been developed in the last few years [76, 93-95].

#### **Genetic manipulation of *C. trachomatis***

The Wyrick group used electroporation to transform *C. trachomatis* with a shuttle vector expressing a chloramphenicol acetyltransferase (*cat*) cassette [96]. However, the shuttle plasmid was not stably maintained. Subsequently, the Maurelli group used electroporation to transform *C. psittacci* with a mutated 16S rRNA gene that could confer resistance to spectinomycin (Spc) and kasugamycin (Ksm). Recombinants that integrated the foreign DNA were resistant to both Spc and Ksm. This study confirmed that electroporation could deliver linear DNA and that foreign DNA could be integrated into *Chlamydia* genomes.

Recently, *C. trachomatis* L2 was transformed with a recombinant shuttle plasmid (pBR325::L2) using CaCl<sub>2</sub>. This shuttle plasmid was a fusion of an *E. coli* plasmid (pBR325) containing a  $\beta$ -lactamase and a *cat* cassette and an endogenous *Chlamydia* plasmid, which allowed stable maintenance of the

plasmid in both *E. coli* and *C. trachomatis* [97]. The Clarke group also demonstrated that it was possible to stably express GFP from a shuttle vector (pGFP::SW2) [97]. Stable plasmid transformation of *C. trachomatis* led to the development of new approaches to mutate chromosomal and plasmid genes and express introduced genes in *Chlamydia*.

### **Mutagenizing *C. trachomatis***

Most *Chlamydia* spp. have a plasmid suggesting that these play vital roles in chlamydial pathogenesis. Systematic interrogation of *C. trachomatis* plasmid genes, using PCR-based deletion mutagenesis and transformation indicated that *pgp1*, *pgp2*, *pgp6*, and *pgp8* are essential for plasmid maintenance [98]. Other plasmid studies confirmed that plasmid genes contributed to virulence [99].

Identification of plasmid maintenance genes permitted the development of a reverse genetic method called fluorescence reported allelic exchange mutagenesis (FRAEM). In this approach, a suicide vector was constructed by modifying the pGFP::SW2 shuttle plasmid. Plasmid stability was regulated by placing *pgp6*, an essential plasmid maintenance gene, under the control of a tetracycline-inducible promoter. In the presence of anhydrotetracycline (ATc), *pgp6* expression increases and the suicide vector is stably maintained. However, in the absence of ATc, *pgp6* expression decreases and the suicide plasmid is lost. To inactivate specific genes by homologous recombination, regions of the chlamydial chromosome surrounding the targeted gene were introduced into the suicide plasmid on either side of a  $\beta$ -lactamase and GFP-expressing gene. Transformants that had homologously recombined out the target gene were enriched for by passing the recombinants in the absence of ATc and presence of penicillin G [100].

Stable transformation permitted adaptation of other genetic tools for *Chlamydia*. Sigma's TargeTron Gene Knockout System is a reverse genetic technique that can inactivate specific genes by inserting a group II intron. This approach takes advantage of group II introns' ability to self-splice from precursor RNAs and form RNA lariats, which can invade genomic DNA targets by reverse splicing. Self-splicing of group II introns is mediated by the intron-encoded protein LtrA, which acts as a DNA binding endonuclease, reverse transcriptase and RNA maturase [101]. In the TargeTron Gene Knockout System, the *ltrA* region of the group II intron is replaced with a selectable antibiotic marker, and *ltrA* is placed on a suicide vector with the modified group II intron.

TargeTron was used to inactivate *C. trachomatis incA*. A modified TargeTron vector, containing a  $\beta$ -lactamase cassette and *incA* targeting sequences, was transformed into *C. trachomatis*. Transformants, which incorporated the modified group II intron, were enriched for by growing them in the presence of penicillin G. Loss of the suicide vector and inactivation of *incA* by the group II intron was confirmed by PCR [102]. TargeTron mediated knockout (KO) of *incA* was the first report of targeted site-directed mutagenesis in *Chlamydia*. Subsequently, the same group developed a similar vector that encodes a Spc resistance cassette, allowing them to construct a double *incA/rsbVI* mutant [103].

Although the new plasmid-based site-directed mutagenesis methods are powerful, their use so far has been restricted to non-essential genes. In contrast, chemical mutagenesis has been employed in a variety of forward and reverse genetic applications to investigate essential and non-essential genes.

The most frequently used mutagen in the *Chlamydia* literature is ethyl methanesulfonate (EMS) [104, 105], although both N-ethyl-N-nitrosourea (ENU) [106] and nitrosoguanidine (NTG) [107] have also been used. EMS preferentially causes GC to AT transitions and can generate nonsense and missense mutations [108]. A *C. trachomatis* *trpB* nonsense mutant was isolated by screening pools of EMS mutagenized chlamydiae using a reverse genetic approach called targeted induced local lesions in genomes (TILLING) [109]. Other groups have used EMS mutagenesis to generate mutant libraries for forward genetic screens. Glycogen deficient [110], temperature sensitive [111], and interferon-sensitive [112] mutants have been isolated from EMS mutant libraries in recent studies.

### **Recombination and mapping mutant genes**

Chemical mutagens can elicit partial and total loss-of-function mutations in chlamydial genes. A limitation of using chemical mutagens is that the resulting mutants often contain multiple mutations [106], making it difficult to determine which mutated gene causes the phenotype of interest. Sometimes the relevant mutation can be identified by sequencing mutants that have the same phenotype [110].

A more robust method for linking mutations to phenotypes was developed based on observations that *Chlamydia* spp. encode recombination machinery [78], and that clinical *Chlamydia* strains can exchange DNA [77, 113-115]. Demars *et al.* first recapitulated natural chlamydial lateral gene transfer (LGT) *in vitro*. They showed that if cells were co-infected with *C. trachomatis* strains encoding different antibiotic resistance alleles, doubly resistant recombinants could be enriched in the presence of the cognate antibiotics. [116].

Subsequent studies showed that *in vitro* LGT involves the transfer of large contiguous regions of chlamydial genomes, up to 790 kilobases (kb) [77]. However, the utility of this approach for mutation mapping was limited by the location and scarcity of known endogenous resistance alleles, as well as the fitness costs associated with some of these alleles. The development of counterselection LGT circumvented some of these limitations. In contrast to antibiotic LGT, counterselection LGT enriches for recombinants that have a wild-type phenotype by selecting against mutants that still contain a deleterious mutation [111]. The mutation linked to the phenotype of interest can then be inferred by comparing the mutations in the parent and recombinant mutant strains.

### **Identifying critical *C. trachomatis* persistence genes**

In this study, we sought to expand upon the classical view of chlamydial persistence through the identification of additional genes that induce *C. trachomatis* to enter into, maintain, and reactivate from IFN- $\gamma$  mediated persistence. Using newly developed chlamydial genetic tools, we made an EMS mutagenized library and screened for loss-of-function mutants that formed fewer inclusions following reactivation with indole. From the persistence screen, we identified six mutants that were susceptible to IFN- $\gamma$  mediated persistence (Sip) mutants. We were able to map the persistence alleles in 3 of the Sip mutants using counterselection LGT.

One of the Sip mutants had a mutation in *trpB*. A mutation in *trpB* was expected because TrpB plays a critical role in the synthesis of Trp. However, the other two mapped Sip mutants had mutations in novel persistence genes



*CTL0225* and *CTL0694*. *In silico* analysis of these genes indicate that they might play a role in AA transport and DNA damage repair, respectively.

We used competitive inhibition to test the hypothesis that *CTL0225* may transport BCAA (Ile, Leu, and Val), as well as Ser, cysteine (Cys) and alanine (Ala). Additionally, metabolomics analysis comparing uninfected and infected HeLa cells in  $\pm$  IFN- $\gamma$  conditions indicated that AA pools might be limiting following IFN- $\gamma$  treatment. These results suggest that AA transport is critical during IFN- $\gamma$  mediated persistence, and that *C. trachomatis* utilizes multiple strategies to counteract the effects of host interferon-stimulated genes.

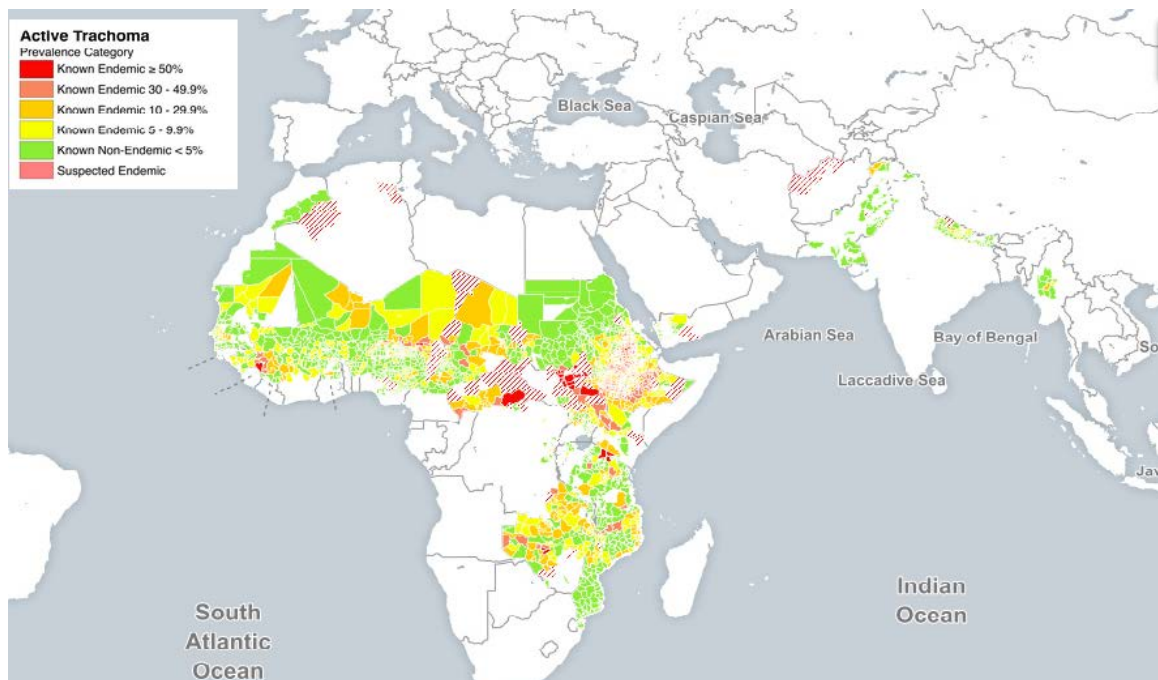


**Figure 1. Prevalence of active and suspected regions of trachoma in 2015.** Globally endemic trachoma infections are only prevalent in 42 countries with the highest rates of infection occurring in areas that are rural and have poor sanitation. (Trachoma Atlas - Last accessed September 2016)

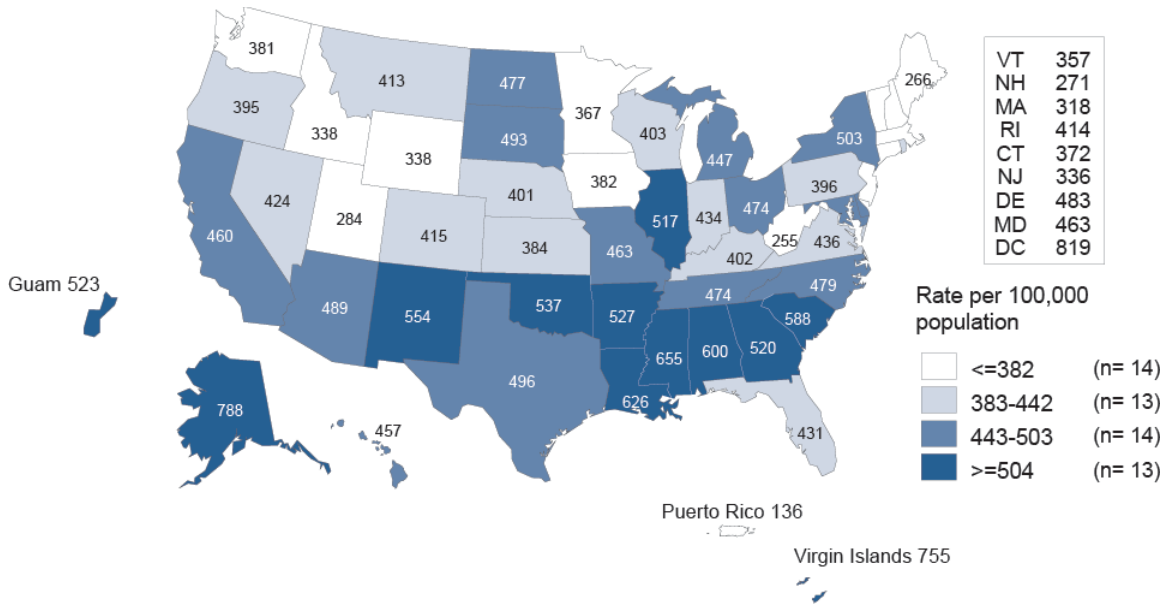


**Figure 2. Sexually transmitted *C. trachomatis* infections in the US.** National surveillance data indicate that rates of *C. trachomatis* infection were highest in Washington DC. The majority of the Southern states, such as Louisiana and Mississippi, had a higher incidence of infection than Northern states, such as Washington and New Hampshire (CDC-2014).

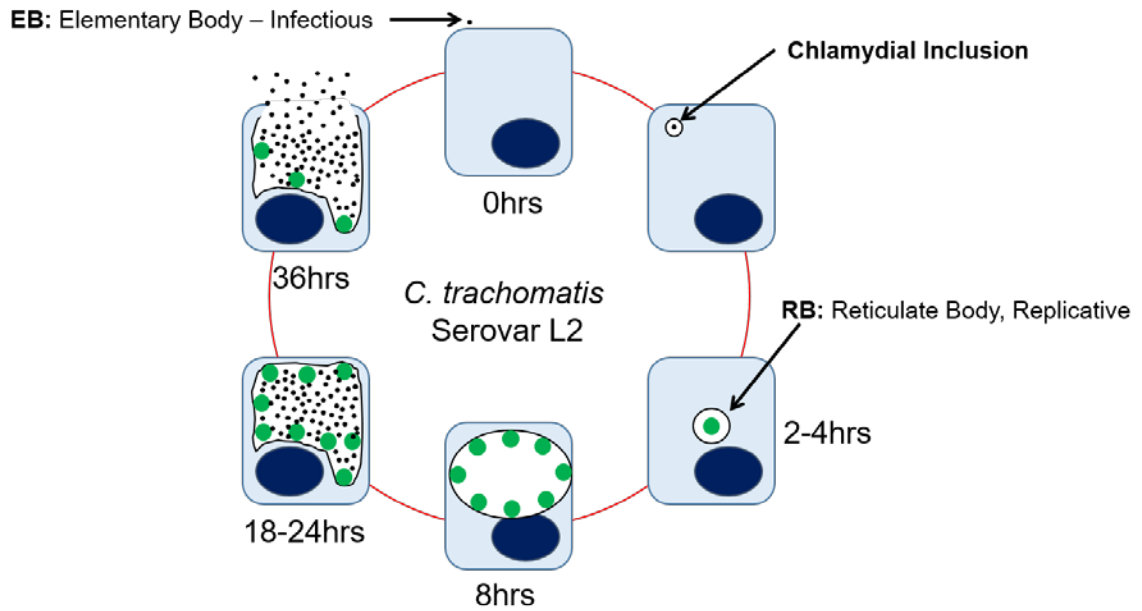


**Figure 3. *In vitro* *C. trachomatis* L2 life cycle.** *C. trachomatis* has a biphasic life cycle alternating between an infectious EB and replicative RB. Following the invasion of a susceptible eukaryotic cell, EB setup a protective niche known as the chlamydial inclusion. The EB then differentiates into an RB and begins to replicate. Following several rounds of replication, some RB asynchronously differentiate back into EB. By 36 hpi, most RBs have differentiated back into EBs. EBs are then released by host cell lysis or extrusion of the inclusion.

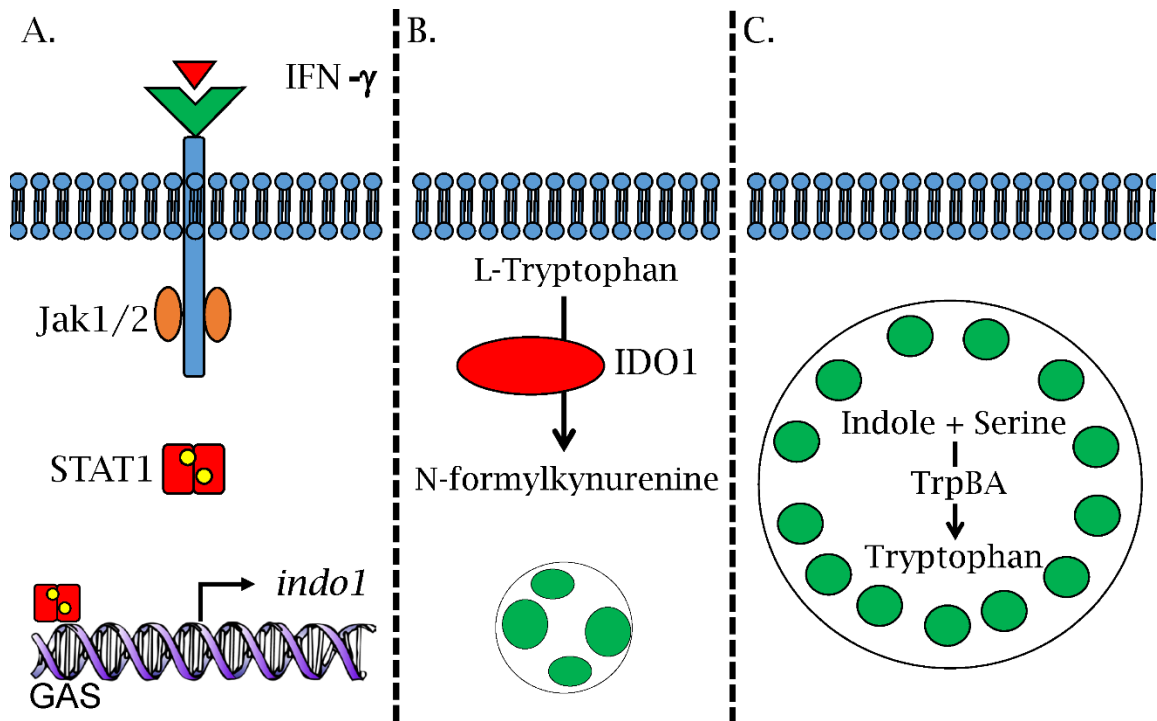


**Figure 4. IFN- $\gamma$  mediated persistence.** (A) IFN- $\gamma$  causes the dimerization of the IFN- $\gamma$  receptor and Janis Kinase 1 and 2 (Jak1/2), which induces the phosphorylation of STAT1. When phosphorylated STAT1 dimerizes and translocates to the nucleus where it binds to GAS elements and upregulates expression of *indo1*. (B) *Indo1* encodes the Trp catabolizing enzyme IDO1, which degrades free Trp to N-formylkynurenine. Trp starvation causes *C. trachomatis* to enter persistence and form aberrant RBs. (C) In response to low levels of Trp, urogenital strains upregulate expression of tryptophan synthase (TrpBA) and can reactivate from persistence by synthesizing Trp from Ser and indole.

## CHAPTER II: RESEARCH GOALS & HYPOTHESIS

Persistent *C. trachomatis* may contribute to the pathogenesis of chlamydial infections and treatment failure. Determining what genes play a critical role in chlamydial persistence is vital to the development of treatments that specifically inhibit persistent *C. trachomatis* and lessen the burden of chlamydia associated inflammation and disease. Transcriptomic analysis indicates persistent *C. trachomatis* RB up- and down-regulate many genes during IFN- $\gamma$  mediated persistence. However, none of these genes have been characterized except tryptophan synthase.

Our research goal was to identify susceptible to IFN- $\gamma$  mediated persistence (Sip) mutants and determine what genes play a critical role in *C. trachomatis* entering into, maintaining, or reactivating from IFN- $\gamma$  mediated persistence. We hypothesize that many of the Sip mutants will contain mutations in genes involved in tryptophan synthesis, DNA damage repair, protein synthesis, and nutrient acquisition.

**CHAPTER III:**  
**MATERIALS AND METHODS**

**Cell culture**

McCoy and HeLa cells were obtained from the American Type Culture Collection (ATCC) and were grown in 5% CO<sub>2</sub> humidified incubators at 37°C. Unless otherwise stated, the cells were cultivated in DMEM-high glucose medium supplemented with four mM L-glutamine (Hyclone), 10% Fetal Bovine Serum (FBS; Atlanta Biologicals), sodium pyruvate (Hyclone), 4-2-hydroxyethyl-1-piperazineethanesulfonic acid (HEPES; Hyclone) and non-essential amino acids (NEAA; Gibco) (DMEM-10).

***Chlamydia* Propagation and Purification**

*Chlamydia trachomatis* serovar L2 434/Bu (*C. trachomatis* L2) was obtained from the ATCC and propagated in either HeLa or McCoy cells. For infection experiments, *C. trachomatis* L2 EBs were suspended in sucrose-phosphate-glutamic acid buffer (SPG). Flask infections were performed by overlaying the cells with EBs in SPG and rocking the flask for 2 hours at 37°C. Plate infections were carried out by overlaying the cells with EBs in SPG and centrifuging the plate for 1 hour at 1600 x g at room temperature (RT), then rocking the plate for 30 minutes at 37°C. In both cases, the inoculum was then aspirated, and DMEM-10 infection medium was added unless indicated otherwise. When used, purified EBs were prepared by centrifugation over 30% diatrizoic acid (MD-76R) as previously described [26]. Purified and crude EB stocks were stored at -80°C.

### **Transformation of *C. trachomatis***

*C. trachomatis* L2 was transformed with the pGFP::SW2 plasmid, a kind gift from Dr. Ian Clarke, to produce L2-GFP using a CaCl<sub>2</sub> based protocol with some modifications [97]. Briefly, instead of mixing the transformation mixture with freshly trypsinized McCoy cells, confluent cell monolayers were infected with the transformation inoculum by centrifugation at 250 x g for 1 hour at RT.

### **Mutagenesis of L2-GFP**

Confluent monolayers of McCoy cells in T175 flasks were infected with L2-GFP at a multiplicity of infection (MOI) of two (MOI = 2). The medium was aspirated at 18 hours post-infection (hpi), and pre-warmed DMEM-10 + 4 mg/mL ethyl methanesulfonate (EMS) was added. The Flasks were rocked at 37°C for 1 hour, and then the monolayers were washed 3-times with 25 milliliters (mL) of phosphate-buffered saline (PBS). Twenty-five mL of pre-warmed DMEM-10 was added, and then the flasks were incubated for 15 hours. Thirty-four hpi, the medium was aspirated, and sterile SPG and ~ ¼ of an inch of 3 mm beads were added to the flasks. The McCoy cells were detached by manually shaking the flasks. EBs were released from the infected cells by transferring the cell SPG mixture into a 1.5 ml Eppendorf tube containing three 3mm glass beads and then agitating the tube for 2 min at 1600 rpm in an Eppendorf Thermomixer R *Shaker* Incubator Block Thermo Mixer (bead agitation). Host cell debris was pelleted by centrifuging the resulting cell lysates (250 x g for 10 minutes), and the supernatant containing EBs (mutagenized EB stock) was aliquoted into multiple tubes and frozen at -80°C.

### **Mutant isolation, library construction, and library expansion**



L2-GFP mutants were cloned from the mutagenized EB stock using a plaque cloning protocol developed by Matsumoto with a few modifications [117]. Confluent monolayers of McCoy cells in 6-well plates were infected with different doses of the stock to identify an inoculum that yielded 15 to 20 plaques per well. Multiple 6-well plates of McCoy cells were then infected with the same volume of inoculum using replicate aliquots of the mutant EB stock. Four thousand plaques were picked from these plates using a P200 pipet with large orifice low retention pipet tips (Fisher). EBs were released from the plaques by bead agitation in 200  $\mu$ l SPG and the plaque lysates were arrayed in deep well plates and stored at  $-80^{\circ}\text{C}$ . The isolates were expanded by thawing the plaque lysate plates in a  $37^{\circ}\text{C}$  water bath and then using 30  $\mu$ l of each lysate to infect a McCoy cell monolayer in a 96-well plate. Seventy hpi, the infectious media was aspirated and replaced with SPG (100  $\mu$ l) and infected monolayers were frozen at  $-80^{\circ}\text{C}$ .

### **Screening for Sensitive to IFN- $\gamma$ -induced Persistence (Sip) mutants**

HeLa cells were seeded in duplicate 96-well plates in DMEM-10. The following day, DMEM-10 was added to one plate (untreated) and DMEM-10 + 10 ng/mL IFN- $\gamma$  (Thermo Fisher; DMEM-10G) (IFN- $\gamma$  treated) was added to the other plate. Twenty-four hours later, the monolayers in the two plates were infected with equivalent inocula from the L2-GFP mutant library. The infections were then incubated for 24 hours in DMEM-10 or DMEM-10G. The untreated monolayers were fixed with 3.7% formaldehyde. In contrast, the IFN- $\gamma$  treated monolayers were rinsed with PBS and tryptophan-free DMEM-10 (UCSF Cell Culture Facility) (DMEM10-TF) + 10  $\mu$ M indole was added. Twenty-four hours later, these monolayers were fixed in 3.7% formaldehyde (Figure 5). In both

cases, GFP-positive inclusions were imaged using an automatic EVOS™ inverted fluorescent microscope at 4X magnification using a GFP filter set. Inclusions were counted using a custom program developed in FIJI.

### **Infectious progeny assays**

HeLa cell monolayers in 24-well plates were infected with various strains. Serial dilutions of the infectious inoculum were used to infect confluent monolayers of HeLa cells in 96-well plates to determine the exact input titer for the progeny assays. At various intervals post infection, the infectious medium was aspirated and replaced with SPG (250  $\mu$ l) and frozen at -80°C. Infected monolayers were thawed and detached by scraping with a pipet tip (scraping). EBs were released from the thawed cells by bead agitation. Cell debris was pelleted by centrifugation, and EB supernatants were isolated and serially diluted. Serial dilutions were used to infect HeLa cell monolayers in 96-well plates. The infected monolayers were fixed with methanol at 36 hpi. Inclusions were labeled with an anti-chlamydial LPS antibody (EVIH1), a kind gift from Dr. Harlan Caldwell at the National Institutes of Health in Bethesda MD, and a Dylight 488-conjugated anti-mouse IgG. Inclusions were imaged using an automatic EVOS™ inverted fluorescent microscope at 4X magnification using a GFP filter set. Inclusions were counted using a custom macro in FIJI.

### **Genome Sequencing**

Confluent monolayers of HeLa cells in 6-well plates were infected with various strains at an MOI = 1. Infected monolayers were detached 36 hpi by scraping with a rubber policeman in SPG, and EB supernatants were prepared using bead-agitation and centrifugation. Host cell DNA was depleted by treating the EB supernatants with RQ1 DNase (Promega) (37 °C, 5% CO<sub>2</sub> for 60 min).

DNase digestion was stopped by adding RQ1 stop buffer to the EB mixture. The EB were then lysed to release their chromosomes by heating the mixture to 65 °C for 10 minutes. Chlamydial DNA was then amplified using a REPLI-g kit (Qiagen), excluding the immunomagnetic cell separation step. Whole genome sequencing (WGS) libraries were prepared from the amplified chlamydial DNA using the NexteraXT DNA Library Preparation Kit. WGS libraries were sequenced at the Center for Genomic Research and Biocomputing Core, Corvallis, OR, on an Illumina HiSeq 2000 to obtain 100 base pair (bp) single-end reads. Genomes were assembled from the resulting reads using Geneious sequencing software version 7, as described previously [118].

### **Generating Sip recombinants**

Confluent HeLa cell monolayers in 12-well plates were infected with individual Sip mutants at an MOI = 4, or pairs of Sip mutants each at an MOI of 2. The infected cells were detached 36 hpi by scraping with a rubber policeman in 500  $\mu$ l SPG and EBs were released from cells by bead agitation and centrifugation.

The persistence screening method (Figure 5) was used to enrich for potential recombinants that had a wild-type phenotype following reactivation with indole. Briefly, EB supernatants were used to infect HeLa cell monolayers in 12 well plates that had been pre-incubated in DMEM-10G for 24 hours to deplete tryptophan. Fresh DMEM-10G was then added, and the infected monolayers were incubated for 24 hours. Infected monolayers were then washed with ice-cold PBS and incubated in DMEM-10TF + 10  $\mu$ M indole for an additional 24 hours to allow recombinants to reactivate and produce EB. The cells were detached by scraping in SPG, and bead agitation released the EBs. EB supernatants were

isolated by centrifugation and used to initiate another round of infection. This process was repeated until phenotypic revertants that had a wild-type persistence phenotype expanded in individual wells or if no inclusions were observed after five enrichments. The counterselection LGT strategy is outlined in (Figure 6).

### **Confirming loss of detrimental persistence allele**

Putative recombinant isolates identified during the co-infections and enrichments in the preceding section were plaque-cloned and expanded. *Chlamydia* DNA was isolated from EBs supernatants of these isolates by adding 50 µl of alkaline lysis buffer to 50 µl supernatant. This mixture was then heated to 95°C for 10 minutes, and the solution was neutralized by adding 50 µl neutralization buffer. The resulting mixture was used as a template for Sanger sequencing. *Chlamydia* genes of interest were amplified using Phusion™ High Fidelity Polymerase (NEB) and primers listed in Table 1. Cycling conditions recommended by the manufacturer were used, whereas the annealing temperature and extension times were determined by the annealing temperatures of the specific primer pairs and amplicon size, respectively. Primer annealing temperatures were calculated using an online T<sub>m</sub> calculator (ThermoFisher). The resulting amplicons were purified using a PCR purification kit (Bio Basic Inc) and sequenced by Eurofins Genomics. The sequences were manually analyzed using the SnapGene Viewer.

### **Transmission Electron Microscopy**

Confluent HeLa cell monolayers in 6-well plates were incubated in DMEM-10 or DMEM-10G for 24 hours. These monolayers were infected at an MOI = 0.1 with various strains. The infected monolayers were then treated as described in

the persistence mutant screen (Figure 5). Infected monolayers were fixed with 5% glutaraldehyde and 4% formaldehyde, either 24 hpi, for the untreated plates, or 24 hours post-reactivation (hpr) with indole, for the IFN- $\gamma$  treated plates. Fixed monolayers were carefully dislodged using a rubber policeman and pelleted in 1.5 mL tubes by centrifugation (250 x g for 10 minutes).

One-percent osmium tetroxide and 1% tannic acid was used to stain the fixed monolayers, which were then dehydrated, and embedded in epoxy resin. Ultrathin sections were made using a Leica ultracut UCT ultramicrotome. Sections were then stained with uranyl acetate and lead citrate. Sections were imaged using a JEOL JEM 1010 microscope with a Gatan 890 4k x 4k digital camera at the Indiana University Electron Microscopy Center in Bloomington, IN.

#### **Quantitative real-time PCR pre- and post- reactivation**

HeLa cell monolayers were treated using the persistence screening conditions (Figure 5). Monolayers in 6-well plates were infected with the indicated strains at an MOI = 0.1 and collected by scraping in SPG at various hpi. EB supernatants were prepared using bead agitation and centrifugation. DNA was purified from the clarified EB supernatants using a gMAX Mini Kit (IBI Scientific) and was then eluted with elution buffer (10mM Tris-HCl, pH 8.5) as suggested by the manufacturer. One microliter of this template DNA was then mixed with FastStart TaqMan Probe Master mix (Roche), nine pmol of primers (5'-GTAGCGGTGAAATGCGTAGA-3' and 5'-CGCCTTAGCGTCAGGTATAAA-3'), and a probe targeting the *C. trachomatis* 16S rRNA gene, (5'-FAM-ATGTGGAAG/ZEN/AACACCAGT-3'). Quantitative PCR (qPCR) was performed using an Eppendorf Realplex4 device. Standard curves were generated using a known concentration of plasmid that contained a cloned copy of *C. trachomatis*

16S rRNA gene. In both cases, the cycling conditions were: 10 min at 95°C, followed by 40 cycles of 95°C for 20 s, 60°C for 1 min, and 68°C for 20 s.

### **Tryptophan-free reactivation assays**

HeLa cells were seeded in 96-well plates in DMEM-10. The following day, the monolayers were rinsed with PBS and then incubated with either DMEM-10 or DMEM-10TF for twenty-four hours. The monolayers were then infected at an MOI = 0.1 with various strains. The infections incubated in DMEM-10 were fixed at 24 hpi, while the infections incubated in DMEM-10TF were rinsed with PBS and incubated for an additional 24 h in DMEM-10TF + 10  $\mu$ M indole before they were fixed. Inclusions were counted and compared between DMEM-10 and DMEM-10TF + 10  $\mu$ M indole treated monolayers. Persistence ratios were calculated as described above.

### **IFN- $\gamma$ free indole and tryptophan reactivation assays**

Confluent HeLa cell monolayers in 96-well plates were incubated for 24 h in DMEM-10 or DMEM-10G. The monolayers were then infected with various strains at an MOI = 0.1 and incubated in either DMEM-10 (untreated) or DMEM-10TF (TF). The untreated infections were fixed with 3.7% formaldehyde at 24 hpi, while the TF treated monolayers were washed with PBS and then incubated with DMEM-10TF, supplemented with 10  $\mu$ M indole or 128 mg/L-tryptophan. These infections were fixed 24 hours later. The numbers of inclusions these strains formed in untreated and TF conditions was used calculate a persistence ratio as described above.

### **Cross-sectional area of inclusions**

Infected monolayers were fixed with 3.7% formaldehyde and then permeabilized with 100% methanol. Inclusions were labeled with the anti-

chlamydial LPS antibody EVIH1 and Dylight488-conjugated anti-mouse IgG. Inclusions were then imaged at 20X using the automatic EVOS™ inverted fluorescent microscope. A custom macro was developed in FIJI to determine the area of each inclusion. An image scale bar was used to determine the relative pixel to micrometer distance observed in each picture.

### **IFN- $\gamma$ sensitivity assays**

HeLa cell monolayers in 96-well plates were incubated in DMEM-10G for 24 h. The monolayers were infected with various strains at an MOI = 0.1 then incubated in DMEM-10TF supplemented with 128 mg/L-tryptophan and 10 ng/mL IFN- $\gamma$ . Infected monolayers were fixed 24 hpi with 3.7% formaldehyde, permeabilized with 100% methanol, and the cross-sectional areas of inclusions were determined as described above.

### **AA competitive inhibition screen**

HeLa cells were seeded in 384-well plates and infected at an MOI = 0.5 with Sip2. DMEM-10 was supplemented with single AAs (10 mM) or with the indicated pairs (X 10 mM + Y 10 mM) (Figure 7). The AA solutions were adjusted to pH ~7.0 with 10M HCl or NaOH and were filter sterilized. The infected monolayers were fixed 46-48 hpi with 3.7% formaldehyde. Inclusions were permeabilized, stained and their cross-sectional area was measured as describe above. The effects of select AA was confirmed in a second experiment, performed in triplicate, in which the cross-sectional area of at least 1000 inclusions was determined for each unique assay condition and replicate.

### **Dose response amino acid competitive inhibition assays**

Hela cells were seeded in 96-well plates and were infected at an MOI = 0.1 with L2-GFP, Sip2, or rSip2, as described above. Infected monolayers were

treated with DMEM-10 supplemented with the indicated concentrations of AA of Ile, Leu, Val, Ala, Cys, Ser. The infected monolayers were fixed 44-48 hpi with 3.7% formaldehyde, permeabilized with 100% methanol, and stained. Cross-sectional areas of inclusions were measured as describe above.

### **Metabolomics assays**

#### **Infection and collection**

Confluent HeLa cell monolayers in T175 flasks (3 biological replicates for each condition ) were incubated in DMEM-10 or DMEM-10G for 24 hours to deplete tryptophan. The media was aspirated (time zero), and different sets of flasks that had been incubated in DMEM-10 or DMEM10 were either mock infected or infected with L2-GFP at an MOI = 0.5. Infected monolayers were harvested from the flasks at various times post infection. The monolayers were washed with ice-cold PBS and cells were detached by treating them with trypsin for five minutes. The cells were then washed with ice-cold PBS and pelleted by centrifugation at 500 x g for 5 minutes at 4°C. The supernatants were discarded, and the cell pellets were weighed and frozen -80°C.

#### **Processing of cell pellets and QQQ-HPLC Mass Spectrometry**

Cell pellets were thawed on ice and suspended in 100 µl (ddH<sub>2</sub>O, trichloroacetic acid (TCA) (500 mg/ 350 µl ddH<sub>2</sub>O) and aminobutyric acid (ABA) (10 ug)). The cell pellet mixture was then vortexed for 30 seconds, and cell debris was pelleted by centrifugation (500 x g for 10 minutes). The supernatant was then transferred to a new tube, and an equal volume of acetonitrile was added. Samples were then stored at -20°C.

Samples and AA standards were thawed on ice and separated on an Intrada AA column using an Agilent 6460 triple quadrupole mass spectrometer



coupled with the Agilent 1200 Rapid Resolution HPLC. Free AA concentrations (ng) were determined using Agilent software and normalized to pellet weight (ng/mg). Free AA concentrations were compared between the indicated conditions and time points.

### **Isolation of suppressor mutants**

Confluent monolayers of HeLa cells in T175 flasks were incubated in DMEM-10G for 24 hours and then infected at an MOI = 10 with various Sip mutants in SPG. The SPG was aspirated, and DMEM-10G was added. Twenty-four hpi, the flasks were washed with ice-cold PBS and then DMEM-10TF + indole was added. Twenty-four hours later, the infected monolayers were lysed using glass beads in SPG and centrifuged to produce EB supernatants. These supernatants were then used to infect fresh flasks of HeLa cells that had been pretreated with IFN- $\gamma$ . The process mentioned above was repeated until most of the HeLa cells in the flask were infected or if no inclusions were observed after five passages. Putative suppressor mutants were plaque cloned and expanded for further characterization similarly as described above.

### **Electroporation of *E. coli* strains**

Mutant and wild-type copies of CTL0225 and CTL0226 were cloned into *E. coli* expression vectors (Table 2). *E. coli* strains were ordered from the *E. coli* genetics stock center at Yale University (Table 3). The strains were made electrocompetent using a protocol from the Dr. Jeffery Barrick's Lab with some modifications (<http://barricklab.org/twiki/bin/view/Lab/ProtocolsElectrocompetentCells>). *E. coli* colonies were picked from plates and were then grown overnight in LB + Kanamycin broth (50  $\mu$ g/mL). Five-hundred microliters of the overnight cultures

were used to inoculate 250 mL of LB broth, and these were incubated shaking at 37°C until an OD<sub>600</sub> of ~0.6-1.0 was reached. The bacteria were pelleted by centrifugation (3220 x g for 10 minutes) in 50 mL conical tubes. The pellet was then suspended and washed with 30 mL of ice-cold 10% glycerol solution. The centrifugation and washing steps were repeated four times. The cells were then suspended in 500 µl of 10% glycerol and 50 µl aliquots were flash frozen in dry ice and stored at -80°C.

Electrocompetent *E. coli* strains were thawed on ice and transformed with ~70 ng of the desired vector using pre-chilled electroporation cuvettes (BioRad 0.1 cm gap). The transformation mixture was then added to 900 µl pre-warmed SOC media in 15 mL Falcon tubes and incubated for 60 minutes at 37°C with shaking. Fifty microliters were then plated on LB + Amp plates and incubated overnight at 37°C. Transformant colonies were picked to a patch plate and screened for the desired insert by colony PCR.

## **Bioinformatic Analysis**

### **Transmembrane prediction software TMHMM Server 2.0**

FASTA formatted AA sequences were submitted for analysis to the TMHMM Server 2.0 transmembrane prediction server (<http://www.cbs.dtu.dk/services/TMHMM/>). Transmembrane domains were graphed using TOPO2 transmembrane protein display software (<http://www.sacs.ucsf.edu/TOPO2/>).

## **Statistics**

Data were analyzed using GraphPad Prism version 6.0 for Windows. Statistics were calculated using One-Way and Two-way ANOVA and Dunnett's *post hoc* test for multiple comparisons.

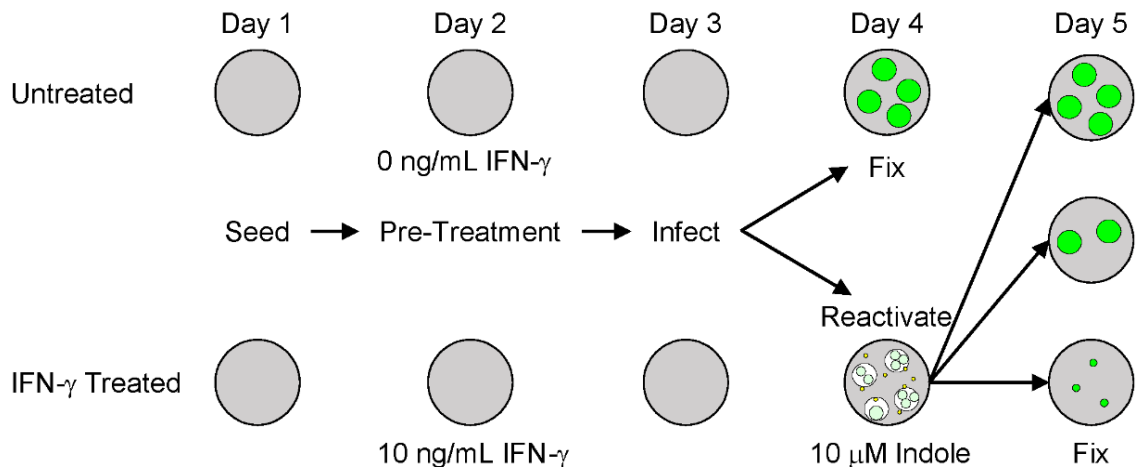


**Figure 5. IFN- $\gamma$  persistence screen.** HeLa cells were seeded in parallel plates. One plate was treated with IFN- $\gamma$  while the other plate received fresh DMEM-10. Untreated and IFN- $\gamma$  treated HeLa cell monolayers were then infected with equal volumes of mutant isolates from an EMS-mutagenized L2-GFP library. Untreated monolayers were fixed at 24 hpi, while the media from IFN- $\gamma$  treated monolayers was replaced with DMEM-TF supplemented with indole. Persistent chlamydiae were reactivated for 24 hours and then monolayers were fixed. Inclusions from the untreated and IFN- $\gamma$  treated plates were counted and compared. Copyright © American Society for Microbiology, [Infection and Immunity, 84, 2016, 2791-2801, and 10.1128/IAI.00356-16]

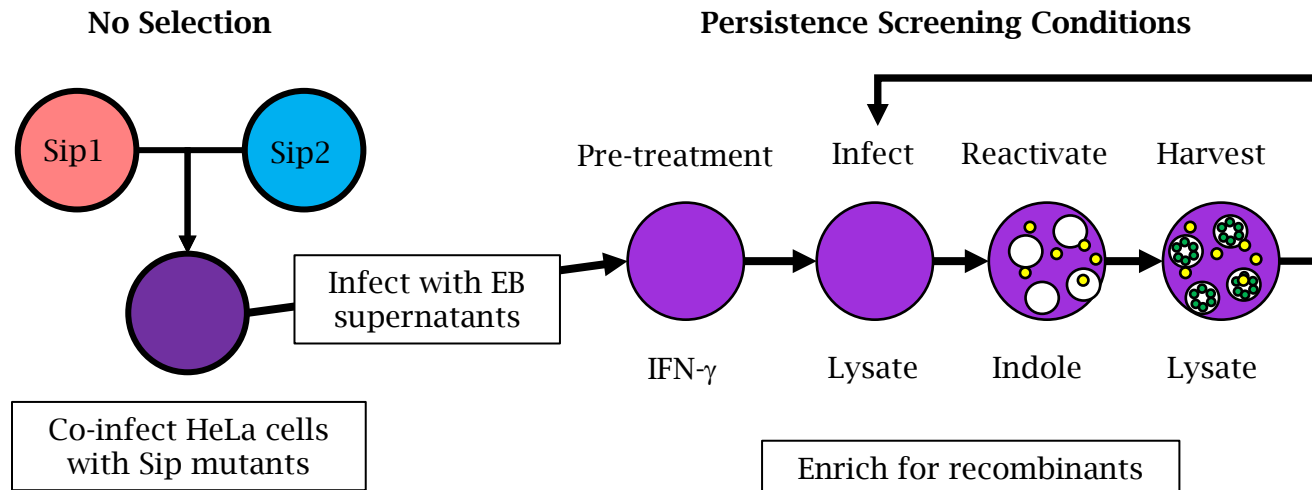


**Figure 6. Counterselection LGT.** HeLa cells were infected with pairs of Sip mutants (e.g. Sip1 x Sip2). Thirty six hpi, EBs were collected in SPG and then a portion was used to infect HeLa cell monolayers pre-treated with IFN- $\gamma$ . Twenty four hpi, infected monolayers were washed and treated with DMEM-10TF + 10  $\mu$ M indole to allow Sip recombinants to reactivate. Twenty four hours post reactivation, the infected monolayers were collected in SPG and the EB supernatants were then used to initiate another round of infection.

	A	R	N	D	C	E	Q	G	H	I	L	K	M	F	P	S	T	V
A					Green					Red	Red					Green		
R					Red					Red	Red					Red		
N					Red					Red	Red					Red		
D					Red					Red	Red					Red		
C	Green	Red	Red	Red	Red	Red	Red	Red	Red	Red	Red	Red	Red	Red	Red	Red	Red	Red
E					Red					Red	Red					Red		
Q					Red					Red	Red					Red		
G					Red					Red	Red					Red		
H					Red					Red	Red					Red		
I	Red	Red	Red	Red	Red	Red	Red	Red	Red	Red	Red	Red	Red	Red	Red	Red	Red	Green
L	Red	Red	Red	Red	Red	Red	Red	Red	Red	Red	Red	Red	Red	Red	Red	Red	Red	Green
K					Red					Red	Red					Red		
M					Red					Red	Red					Red		
F					Red					Red	Red					Red		
P					Red					Red	Red					Red		
S	Green	Red	Red	Red	Red	Red	Red	Red	Red	Red	Red	Red	Red	Red	Red	Red	Red	Red
T					Red					Red	Red					Red		
V					Red					Green	Green					Red		

**Figure 7. AA competitive inhibition screen.** HeLa cell monolayers in 384-well plates were infected with Sip2 and treated with the above combinations of AAs at a concentration of 10 mM. Blue boxes indicate wells with large inclusions, red boxes indicate wells that contained small inclusions, and green boxes indicate a combination of AAs that inhibited the formation of small inclusions.

**Table 1. Primers used in this study**

<b>Primer</b>	<b>Gene</b>	<b>Purpose</b>	<b>5' to 3' Sequence</b>
DN0247	<i>trpA</i>	PCR-Forward	ATCATCCGCAGAAACAGAGG
DN1593	<i>trpRBA</i>	PCR-Forward	GCTATGCGACATTACTGAAGACTAG
DN1594	<i>trpB</i>	Mutation confirmation-Reverse	GTCCATCGTCATCTTGAAGAAGATAC
DN1595	<i>trpB</i>	Sequencing-Forward	GTATCTTCTTCAAGATGACGATGGAC
DN1596	<i>trpRBA</i>	PCR-Reverse	GTCATCAAAGGATATGATTCCATG
DN1597	<i>trpB</i>	Sequencing-Forward	GCTATTGATGGCCCTAGAGTATTTT
DN1598	<i>trpB</i>	Sequencing-Reverse	GAAATACTCTAGGGCCATCAATAGC
DN1599	<i>trpA</i>	Sequencing-Reverse	CGGATACCTTCTACGATCTCTAAC
DN1621	<i>trpB</i>	Sequencing-Forward	GCATTGGAGTCTTCACATGC
DN1622	<i>trpA</i>	Sequencing-Reverse	ACACCTCCTTGAATCAGAGC
DN1623	<i>trpR</i>	Sequencing-Forward	AATCAAGAGGAGTCTGGCT
DN1624	<i>trpR</i>	Sequencing-Reverse	GAGGATCTGATCCTTTAAG
DN1626	16S rRNA	qRT-PCR-Forward	GGAGAAAAGGGAATTTACG
DN1627	16S rRNA	qRT-PCR-Reverse	TCCACATCAAGTATGCATCG
DN1639	CTL033	Mutation confirmation-Forward	CACTATTGGATAATAAGGTGATTATCG
DN1640	CTL033	Mutation confirmation-Reverse	GTCTGCACCTTACTCTGTAC
DN1641	CTL0124	Mutation confirmation-Forward	GAAGCGATGGTTAATAGAGAAC
DN1642	CTL0124	Mutation confirmation-Reverse	CTCCTATAGAACTGCCTCTAC
DN1643	CTL0133	Mutation confirmation-Forward	CCACTATGGGCTAATTTATGG
DN1644	CTL0133	Mutation confirmation-Reverse	CCTAACGCCTATTAAGACATTG
DN1645	CTL0209	Mutation confirmation-Forward	GATTTCTTACGATTATTCCAGTGG
DN1646	CTL0209	Mutation confirmation-Reverse	CTATAGCTTTGAATAATGGCCC
DN1647	CTL0129	Mutation confirmation-Forward	GCAAGTTTACCTACATCCTGAATTAG
DN1648	CTL0129	Mutation confirmation-Reverse	CCCAGAAACAACACCCAAG

Primer	Gene	Purpose	5' to 3' Sequence
DN1649	CTL0225	Mutation confirmation-Forward	GTCGATGTAATCATTGCTGGG
DN1650	CTL0225	Mutation confirmation-Reverse	CCTTCATGGCTATGTGCTTG
DN1651	CTL0233	Mutation confirmation-Forward	CTACCATAGCTCCTTCTATCAGG
DN1652	CTL0233	Mutation confirmation-Reverse	CATCCTGAGTCAGAATCATTCTATG
DN1653	CTL0257	Mutation confirmation-Forward	CATGATTGACCATGTTTAGGATGG
DN1654	CTL0257	Mutation confirmation-Reverse	CTAATTCTAAAGCACTCTTACGATAC
DN1655	CTL0325	Mutation confirmation-Forward	CCTATCAAGTAGGTGTGAGAG
DN1656	CTL0325	Mutation confirmation-Reverse	GATCACCTGAATGTCATCGATATAC
DN1657	CTL0447	Mutation confirmation-Forward	GCCAAATCTAATACCTCAGACTATC
DN1658	CTL0447	Mutation confirmation-Reverse	CGTCGTTACCAGTATTCTATTACCTATC
DN1659	CTL0722	Mutation confirmation-Forward	CTAGGAGGATGGAAGCGTATAC
DN1660	CTL0722	Mutation confirmation-Reverse	GTATCTAAGCATTGAGGAGTATGG
DN1661	CTL0176	Mutation confirmation-Forward	GTTCGTCAAGTTAGAATTTCTTTGTAG
DN1662	CTL0176	Mutation confirmation-Reverse	GGAATTGAGTTATAAATAGGTGTGTTG
DN1663	CTL0566	Mutation confirmation-Forward	GATCTCATGTGGAACAATAAACC
DN1664	CTL0566	Mutation confirmation-Reverse	GCTGAGGTAGAGCTTCATAACATC
DN1665	CTL0354	Mutation confirmation-Forward	GCACTACAAGTAATAAGATGCATCTC
DN1666	CTL0354	Mutation confirmation-Reverse	CGCAATGTATCTCTCCTATGAAC
DN1667	CTL0366	Mutation confirmation-Forward	CGCTCCTTAAATCTTACTTCACTCTC
DN1668	CTL0366	Mutation confirmation-Reverse	CATCAGCTCCTATGCTTAAAGC
DN1669	CTL0440	Mutation confirmation-Forward	GCTTATCTCCCACAACATGATAAC
DN1670	CTL0440	Mutation confirmation-Reverse	CGTCTTGTC AATCTTCGAGAAG
DN1671	CTL0175	Mutation confirmation-Forward	GAGAAAATGTAAGTACAAGAATG
DN1672	CTL0175	Mutation confirmation-Reverse	CTCTTTTAGGATATACTGAGACCTC
DN1673	CTL0641	Mutation confirmation-Forward	CGATACTCACAAAACGCATTC
DN1674	CTL0641	Mutation confirmation-Reverse	CTTTCTGTATGGGATAGTCAAG

Primer	Gene	Purpose	5' to 3' Sequence
DN1675	CTL0157	Mutation confirmation-Forward	GAACATTCCGGAGTTCATGG
DN1676	CTL0157	Mutation confirmation-Reverse	CTCCCTAACTTGTAGACAGGAG
DN1677	CTL0312	Mutation confirmation-Forward	GTAGAAGCGTCAGAGAGAGG
DN1678	CTL0312	Mutation confirmation-Reverse	CGATGGGTTATTCACAACGAC
DN1679	CTL0402	Mutation confirmation-Forward	GCTTACATGGCTTCCTATTATGC
DN1680	CTL0402	Mutation confirmation-Reverse	CTTGAGTATAATGAGCTTCTTGATGAG
DN1681	CTL0694	Mutation confirmation-Forward	GAACATGTTGGAGAAGAAGCTATAG
DN1682	CTL0694	Mutation confirmation-Reverse	GTAGATATTAAGATCAAGGCTGCC
DN2100	CTL0694	PCR Gene amplification- Forward	CAAGAGAATAGCCGAGGTTCTTC
DN2101	CTL0694	PCR Gene amplification - Reverse	GAGCAGTTTGAAATTCGTACTIONCAC
DN2102	CTL0225,	PCR Gene amplification - Forward	GTAAAGTTGTCGTAAATTATCAAGGG
DN2103	CTL0225	Sequencing Forward	CGAATAGTAGCAGCAAGAG
DN2104	CTL0226	Sequencing Reverse	CCATAGCCCTTCCTCATG
DN2105	CTL0226	PCR Gene amplification - Reverse	CTTTCTCGTTGATTATTAGGTTTC
DN2119	CTL0442	Mutation confirmation-Forward	GGTCTCGATCCCTGAATATAAATAGG
DN2120	CTL0442	Mutation confirmation-Reverse	GATACGCTTTTTATTAGGATAGTTATGG
DN2121	CTL0250	Mutation confirmation-Forward	GAATGCGCTGAAGATAAGAAC
DN2122	CTL0250	Mutation confirmation-Reverse	CCTCAATAGTAAACAGTCCATC
DN2123	CTL0352	Mutation confirmation-Forward	GAGCTAGTTTCTGTTTCAGTTTATC
DN2124	CTL0352	Mutation confirmation-Reverse	CAAGAGAGGCAGGATATCGAAC
DN2125	CTL0658	Mutation confirmation-Forward	GAAAGAGGACAATTATATGCCTGAG
DN2126	CTL0658	Mutation confirmation-Reverse	CCTACAGATCATCATCTTTGC
DN2127	CTL0737	Mutation confirmation-Forward	GATTGAAGAATGGCGATATGG
DN2128	CTL0737	Mutation confirmation-Reverse	CTCTTCACAGGTATGACGAGTG



<b>Primer</b>	<b>Gene</b>	<b>Purpose</b>	<b>5' to 3' Sequence</b>
DN2144	<i>trpBA</i>	Cloning pBAD18-EcoRI	GAAAAGGAATTCATGTTCAAACATAAACATCC
DN2145	<i>trpBA</i>	Cloning pBAD18-HindIII	CATAAAAAGCTTTTATCCAGGAATAACTGTTTGTGC
DN2146	CTL0225	Cloning pBAD18-EcoRI	GTATTTGAATTCATGCTACATTCACTATTTTCGTC
DN2147	CTL0225	Cloning pBAD18-HindIII	ATTTCCAAGCTTCTATCTCTTGACATAGAGAAG
DN2148	CTL0226	Cloning pBAD18-EcoRI	CGTCTCGAATTCATGGACTGGTCATTTTTTTTGTG
DN2149	CTL0226	Cloning pBAD18-HindIII	GCTTTCAAGCTTTTATAGGAAAGTTTGTGTAG
DN2150	CTL0694	Cloning pBAD18-EcoRI	TTAAAAGAATTCATGTCTTTATTTTCTAAATTCAAAGC
DN2151	CTL0694	Cloning pBAD18-XbaI	TCGGTATCTAGATTAGTATACGTCTGAAACTAGTC

<sup>a</sup>Bold faced text indicate inserted restriction enzyme site sequence

**Table 2. Plasmids used in this study**

<b>Plasmid Name</b>	<b>Description</b>	<b>Source</b>
pGFP::SW2	<i>C. trachomatis</i> shuttle plasmid	[97]
pBAD18	Arabinose inducible gene expression cloning vector	
pMM1	pBAD18 expressing wild-type <i>C. trachomatis</i> CTL0225	This study
pMM2	pBAD18 expressing mutant <i>C. trachomatis</i> CTL0225	This study
pMM3	pBAD18 expressing wild-type <i>C. trachomatis</i> CTL0226, CTL0225	This study
pMM4	pBAD18 expressing mutant <i>C. trachomatis</i> CTL0226, CTL0225	This study

**Table 3. Bacterial strains used in this study**

<b>Strains</b>	<b>Description</b>	<b>Source</b>
<i>E. coli</i>		
BW25113	Parent of JW strains	Yale Coli Genetic Stock Center #7636
JW2767	Keio collection knockout of serine transporter <i>sdaC</i>	Yale Coli Genetic Stock Center #10170
JW3060	Keio collection knockout <i>sstT</i>	Yale Coli Genetic Stock Center #10335
<i>C. trachomatis</i>		
L2-GFP	L2 434/Bu transformed with pGFP::SW2 plasmid	This study

## CHAPTER IV:

### Isolation and characterization of persistence mutants

Prior comparative transcriptomic studies identified a large number of *C. trachomatis* genes that are differentially expressed in normal and persistent RB [37, 82]. Except for tryptophan synthase (TS) genes, the roles these genes play during IFN- $\gamma$  mediated persistence have not been explored. Thus, we performed a forward genetic screen to identify genes that are essential for *Chlamydia* to enter into, maintain, and reactivate from IFN- $\gamma$  mediated persistence.

#### Mutant library construction

A urogenital lymphogranuloma venereum (serovar L2 434/BU) strain that expresses GFP (L2-GFP) was used as the library parent because inclusions of this strain can be visualized directly by GFP fluorescence (Figure 8). L2-GFP was mutagenized with the chemical mutagen ethyl methanesulfonate (EMS). EMS primarily causes GC to AT transition mutations, which can generate both missense and nonsense mutations, but rarely induces insertion and deletion (Indel) mutations [119]. An advantage of using a point mutagen was that it reduced the probability of causing polar effects.

L2-GFP infected McCoy cells were initially treated with EMS to produce a pool of mutant EBs. We observed that high concentrations of EMS substantially decreased chlamydial EB production. However, we were able to recover sufficient numbers of L2-GFP EBs from HeLa cells treated with 4 mg/mL EMS for library construction. EBs were cloned from this mutagenized stock using a plaque assay, and these were then expanded and arrayed in 96 deep-well plates to make the mutant library.

#### Screening for IFN- $\gamma$ persistence mutants

We screened a library of 2,016 chemically mutagenized L2-GFP isolates for mutants that had a reduced ability to reactivate from IFN- $\gamma$ -mediated persistence with indole. Briefly, we infected HeLa cells with the mutant library in  $\pm$  IFN- $\gamma$  conditions. We then compared the number of inclusions formed by each isolate in the (-) IFN- $\gamma$  condition, 24 hours post-infection (hpi), and in the (+) IFN- $\gamma$  condition, 24 hours post-reactivation (hpr). This comparison led us to calculate a mutant persistence ratio. Mutant and L2-GFP persistence ratios were then compared to normalize for differing MOIs. Similar to previous studies, we observed that L2-GFP produced approximately 50% fewer inclusions following reactivation from IFN- $\gamma$  mediated persistence than in untreated cells (data not shown) [74, 82]. In contrast, some library isolates formed markedly fewer inclusions following reactivation than in the untreated cells. We identified six persistence mutants from the primary screen and verified that their persistence phenotypes were statistically significant ( $p < 0.0001$ ) in subsequent assays (Figure 9). We named these isolates Sip mutants because they were sensitive to IFN- $\gamma$ -mediated persistence.

One-step growth curve analysis was used to compare the developmental kinetics of L2-GFP and these six Sip mutants during normal growth conditions. Untreated HeLa cells were infected with L2-GFP and each of the Sip mutants in parallel. The numbers of EBs generated by each Sip mutant were indistinguishable from the number produced by L2-GFP (Figure 10). These results indicated that the Sip mutants were not compromised in fitness and that the mutant persistence phenotypes we observed were related to their inability to enter, maintain, and be reactivated from, IFN- $\gamma$  mediated persistence.

### **Mapping deleterious persistence alleles in the Sip mutants**

A whole-genome sequencing (WGS) approach was used to compare the genomic sequences of L2-GFP and the Sip mutants. Sip mutants had between 2 to 8 mutations and contained at least two nonsynonymous mutations in predicted coding sequences (Table 4).

The lack of overlapping polymorphisms prevented us from using linkage analysis to map the deleterious persistence mutations in the Sip mutants. However, Sip1 had a missense mutation in *trpB*, which encodes the  $\beta$ -subunit of TS. A mutation in a TS related gene was expected and is a key datum that validates the efficacy of the screen we developed. However, because Sip1 contains two other missense mutations we could not definitively conclude that the mutation in *trpB* was causing Sip1 to form fewer inclusions following reactivation from persistence. Thus, we needed a way to link the persistence phenotype to a specific genotype.

We initially used an *in vitro* antibiotic lateral gene transfer (LGT) approach to isolate Sip recombinants and map the deleterious persistence alleles in each strain. Antibiotic LGT enriches for recombinants by selecting against strains that only have one endogenous resistance allele [110, 116]. A limitation of this approach is that endogenous antibiotic resistance alleles acquired by mutating genes such as *rpoB*, *gyrA*, and 16S rRNA are known to affect growth [120-124]. Unfortunately, the antibiotic-resistant Sip and recombinant mutant strains we generated had growth defects that confounded attempts to map persistence alleles.

We next sought to map causative persistence mutations by using a counterselection LGT approach. This technique produces markerless recombinants by enriching for strains that have a wild-type phenotype and

selecting against strains that still retain a deleterious persistence allele [111, 112]. As a proof of concept for this mapping strategy, we focused on the Sip mutants that had the strongest persistence phenotypes (Sip1, Sip2, and Sip6).

HeLa cells were co-infected with different pairs of Sip mutants (Sip1 x Sip2, Sip1 x Sip6, Sip2 x Sip6). Co-infections were then repeatedly passaged in HeLa cells cultivated in the persistence screen conditions (Figure 6). Phenotypic revertants arose from these co-infection experiments. In contrast, no revertants arose from control infections that used twice the amount of infectious inoculum of single Sip mutants after several passages. This observation suggested that the phenotypic revertants detected in co-infected wells resulted from recombination and were not genetic revertants or suppressor mutants.

We next attempted to use counterselection LGT to map the other Sip mutants. However, we were unable to enrich for recombinants using the attempted crossing strategy (Sip3 x Sip4, Sip3 x Sip5, and Sip4 X Sip5) because almost every HeLa cell was infected in the co-infected and Sip parent alone wells after the first passage using the persistence screen conditions. This trend continued for several passages. This observation indicated that EB production might influence the ease of enriching for recombinants. To address this hypothesis, we investigated how much infectious EB each of the Sip mutants produced following reactivation from persistence with indole.

Infectious progeny assays were used to compare Sip mutant EB production following IFN- $\gamma$  treatment and reactivation with indole. Sip1, Sip2, and Sip6 produced the fewest infectious EB as compared to L2-GFP (<5%). In contrast, the decline in EB production of Sip 3, Sip4 and Sip5 was relatively modest (19%, 40%, and 39%, respectively) (Figure 11). These data suggest that

enriching for recombinants is more efficient when Sip mutants produce little to no infectious EB after reactivating from persistence. Since we were unable to map the persistence alleles in Sip3, Sip4, and Sip5, all subsequent assays focus on characterizing Sip1, Sip2, and Sip6.

### **Allele mapping uncovers novel persistence genes**

L2-GFP and recombinant Sip (rSip) strains (rSip1, rSip2, and rSip6) formed similar numbers of inclusions after reactivation with indole (Figure 12). Sanger sequencing confirmed that each rSip strain differed from a Sip mutant parent by one nonsynonymous mutation. This analysis linked nonsynonymous mutations in genes encoding the  $\beta$ -subunit of TS (*trpB*), a putative integral membrane protein (*CTL0225*), and a putative oxidoreductase (*CTL0694*) to the persistence phenotypes of Sip1, Sip2, and Sip6, respectively (Table 4).

### **Sip mutants fail to reactivate from persistence**

Results from our secondary screen could not be used to determine whether the Sip mutants were compromised in their ability to enter, maintain, or be reactivated from, IFN- $\gamma$  mediated persistence. To address this issue, we used established methods to examine the inclusions of each mutant. Light microscopy indicated the inclusions of the Sip mutants were significantly smaller ( $p < 0.0001$ ) than those of L2-GFP following reactivation, despite being similar or larger in size under normal growth conditions (Figure 13 B-C). TEM revealed that there were no obvious differences in EB or RB morphology in untreated HeLa cells (Figure 14 A-D), consistent with the results of the one-step growth curve experiments (Figure 10). However, in IFN- $\gamma$  + indole treated HeLa cells, only Sip mutant inclusions still contained aberrant RB following reactivation. In contrast, dividing RB were frequently observed in HeLa cells



infected with L2-GFP, and rSip strains (Figure 14E-H). These results suggested that the Sip mutants could enter persistence, but could not reactivate from persistence.

Since the results from the TEM analysis indicated that the Sip mutants could not reactivate from IFN- $\gamma$  mediated persistence, we wanted to test if the remaining inclusions produced infectious EB. Untreated HeLa cells were infected with lysates from IFN- $\gamma$ -plus-indole-treated infections and inclusions were counted 34 hpi. All three of the Sip mutant strains produced significantly ( $p < 0.0001$ ) fewer infectious EBs than L2-GFP (Figure 15A). This result confirmed that the Sip mutants do not reactivate from persistence with indole and are impaired in their ability to produce infectious progeny.

Additionally, we tested if the Sip mutants produced infectious EBs following reactivation with Trp to determine if Sip2 and Sip6 had defects in acquiring or converting indole into Trp. Trp and indole similarly rescued L2-GFP EB production. In contrast, Trp did not enhance EB production of any of the Sip mutants ( $p < 0.0001$ ) (Figure 15B). Interestingly, Sip1 EB production was not fully rescued by treatment with Trp ( $p < 0.0001$ ), which was surprising because EB production of a *C. trachomatis* trpB null mutant can be reactivated with Trp [109]. These results suggest that the reason the Sip mutants are unable to reactivate from persistence is unrelated to Trp availability and that mutant TrpB (TrpB<sup>P221S</sup>) in Sip1 may have a deleterious alternative function.

### **Sip1 and Sip2 make fewer genomes following reactivation with indole and tryptophan**

Next, we wondered why the Sip mutants failed to reactivate from persistence with Trp. One possibility was they were dying during persistence. If

the Sip mutants were dying during persistence, then they should have reduced genome replication following reactivation from persistence. Using quantitative PCR (qPCR), we measured and compared the rate at which L2-GFP and the Sip mutants replicated their genomes during IFN- $\gamma$  treatment and reactivation from persistence with indole and tryptophan.

Consistent with previous reports that *C. trachomatis* genome replication continues during persistence, albeit more slowly [57], L2-GFP and the Sip mutants replicated their genomes slowly between 2 to 24 hpi in IFN- $\gamma$  treated HeLa cells (Figure 16). However, Sip1 genome replication diverged during reactivation with indole and Trp. Genome replication of Sip1 slightly increased 36 hpr with indole but increased approximately 5-fold during the same interval after the addition of Trp. This result suggested that Trp, but not indole, was able to mitigate the deleterious effects of mutant TrpB (TrpB<sup>p221S</sup>) expressed in Sip1. Genome replication of Sip2 was decreased and delayed during reactivation with indole and Trp, suggesting that this mutant might be dying during persistence and is unable to resume rapid replication of its genome. In contrast, Sip6 genome replication was similar to L2-GFP following reactivation with both indole and Trp. These data indicate that Sip6 can survive during persistence, but is unable to transition back into normal RB and EB, while both Sip1 and Sip2 may be dying during persistence due to an unknown mechanism.

### **Sip mutants are differentially sensitive to IFN- $\gamma$**

IFN- $\gamma$  upregulates the expression of many ISGs [125]. We tested if IFN- $\gamma$  treatment could inhibit the development of the Sip mutants in Trp replete conditions, as it could indicate if ISGs are playing a role in Sip1 and Sip2 dying during persistence. Untreated and IFN- $\gamma$  treated HeLa cells were infected with L2-

GFP and the Sip mutants in parallel. IFN- $\gamma$ -plus-Trp was added immediately following infection to prevent *C. trachomatis* from entering persistence. The numbers of inclusions formed (Figure 17A) and their relative sizes (Figure 17B) were assessed 24 hpi. Sip1 produced more inclusions ( $p < 0.01$ ) that were not significantly different in size than L2-GFP in the Trp-replete conditions. This result suggested that TrpB<sup>P221S</sup> expression in Sip1 was only detrimental to chlamydial survival during IFN- $\gamma$  mediated persistence. Sip2 also formed slightly more inclusions ( $p < 0.05$ ), which were significantly larger ( $p < 0.0001$ ) than those seen with L2-GFP in IFN- $\gamma$ -plus-tryptophan-treated cells. This result is consistent with the Sip2 inclusions being significantly ( $p < 0.0001$ ) larger than L2-GFP inclusions under normal growth conditions (Figure 13B). In contrast, the numbers of inclusions Sip6 formed were similar to L2-GFP (n.s), but Sip6 formed significantly smaller inclusions ( $p < 0.0001$ ). This result indicated that a Trp-independent effect of IFN- $\gamma$  might affect the development and subsequence size of Sip6 inclusions during persistence.

### **Trp starvation alone prevents Sip mutants from reactivating**

Next, we used a Trp-limiting (TL) persistence model to determine if Trp starvation alone was sufficient to inhibit the Sip mutants from reactivating from persistence with either indole or Trp [72]. We incubated HeLa cells in Trp-free medium (DMEM-10TF) for 24 hours to deplete Trp. Trp-replete and Trp-depleted HeLa cell monolayers were then infected with L2-GFP, Sip and rSip strains. We then compared the number of inclusions formed in Trp-replete conditions, 24 hpi, to the number of inclusions formed in the Trp-depleted conditions, 24 hpr, with indole or Trp. L2-GFP, Sip, and rSip strains formed similar ratios of inclusions following reactivation with either indole or tryptophan (Figure 18).

The ratios calculated from the TF persistence model were similar to ratios observed in the IFN- $\gamma$  mediate persistence model (Figure 9). These results suggest that Trp limitation alone is sufficient to inhibit the Sip mutants from reactivating from persistence. Additionally, these results indicate Trp starvation was responsible for the phenotypes observed with the Sip mutants in the IFN- $\gamma$  mediated persistence model.

### **The P221S mutation may disrupt substrate channeling of indole and Trp synthesis**

Indole is usually shuttled through a substrate tunnel to the active site of the  $\beta$ -subunit where it interacts with Ser to form Trp. However, in the absence of indole, the  $\beta$ -subunit of TS hydrolyzes Ser into pyruvate and ammonia [126]. We hypothesized that the P221S mutation in Sip1 disrupts indole from interacting with the active site of the  $\beta$ -subunit leading to the production of ammonia instead of Trp. If ammonia is being produced while Sip1 is in persistence, then this could explain why Sip1 does not fully reactivate from persistence with Trp.

Using Phyre2 and PyMOL analysis, we mapped the P221S mutation in TrpB onto the crystal structure of *Salmonella typhimurium* TS. Results from this *in silico* analysis suggested that the P221S mutation was located on the periphery of TrpB and did not directly interact with the substrate tunnel or the active site of the  $\beta$ -subunit. This observation suggests that the P221S mutation must cause a conformational change that disrupts indole from reaching the active site of TrpB<sup>P221S</sup> (Figure 19).

To gain a better understanding of the P221S mutation and how it may lead to the production of ammonia we generated suppressor mutants. HeLa cells were infected with Sip1, which was then induced to enter and reactivate

from IFN- $\gamma$  mediated persistence with indole. After several passages, suppressor mutants were isolated, and *trpB* was Sanger sequenced to determine the location of the suppressor mutation. One of these suppressor mutants had a Q52P mutation, also, located on the periphery of TrpB<sup>P221S</sup> (Figure 19). This result suggested that the Q52P mutation likely corrects the conformational change that prevented indole from interacting with the active site of the  $\beta$ -subunit.

#### **CTL0694 may be involved in DNA damage repair**

CTL0694 is annotated as a putative oxidoreductase [78]. Blastp analysis indicated that CTL0694 shares strong protein homology (47%) with an oxidoreductase in *Bacteroides fragilis* whose function is unknown. Other proteins that are similar to CTL0694 are annotated as being part of the sulfite reduction pathway, specifically the  $\alpha$ -subunit of the sulfite reductase complex, CysJ.

*E. coli* CysJ shares 28% protein homology to CTL0694. CysJ transfers reducing electrons to effector proteins in both the sulfite reduction and a DNA damage repair pathways. In the sulfite reduction pathway, CysJ helps to reduce sulfite to hydrogen sulfide by forming a multimeric complex with CysI (CysJ<sub>8</sub>CysI<sub>4</sub>), through its FMN domain. In a DNA damage repair pathway, CysJ forms a complex with YcbX (CysJYcbX) and helps to detoxify mutagenic nucleobases such as HAP to adenine. As CTL0694 lacks an FMN domain, we hypothesize CTL0694 is likely playing a role in DNA damage repair during IFN- $\gamma$  mediated persistence.

Using PyMOL analysis, we aligned mutant CTL0694 (CTL0694<sup>P105L</sup>) to *E. coli* CysJ, which revealed that the P105L mutation is close to an FAD-binding site (Figure 20). This observation suggests that the P105L mutation may interfere

with FAD binding to CTL0694. To determine if the this was the case, we generated Sip6 suppressor mutants as described above. We isolated a suppressor mutant that encoded a G75S mutation mapped to the periphery of CysJ, far from the FAD binding site (Figure 20). This result indicated that the P105L mutation likely does not disrupt FAD binding but may affect CTL0694 from binding to an effector protein.

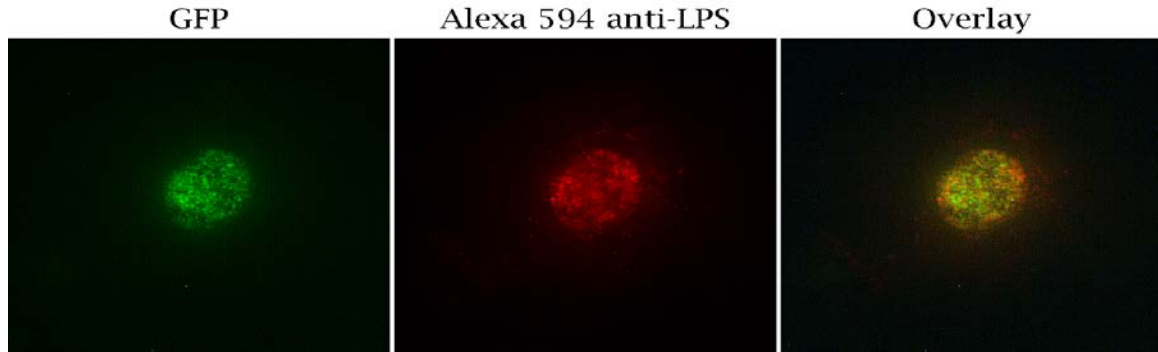


**Figure 8.** *C. trachomatis* L2 was transformed with pGFP::SW2. GFP expression (Green) and anti-chlamydial LPS Alexa 594 staining (Red) was compared 36 hpi. The pattern of GFP expression was similar to that of chlamydial LPS staining.

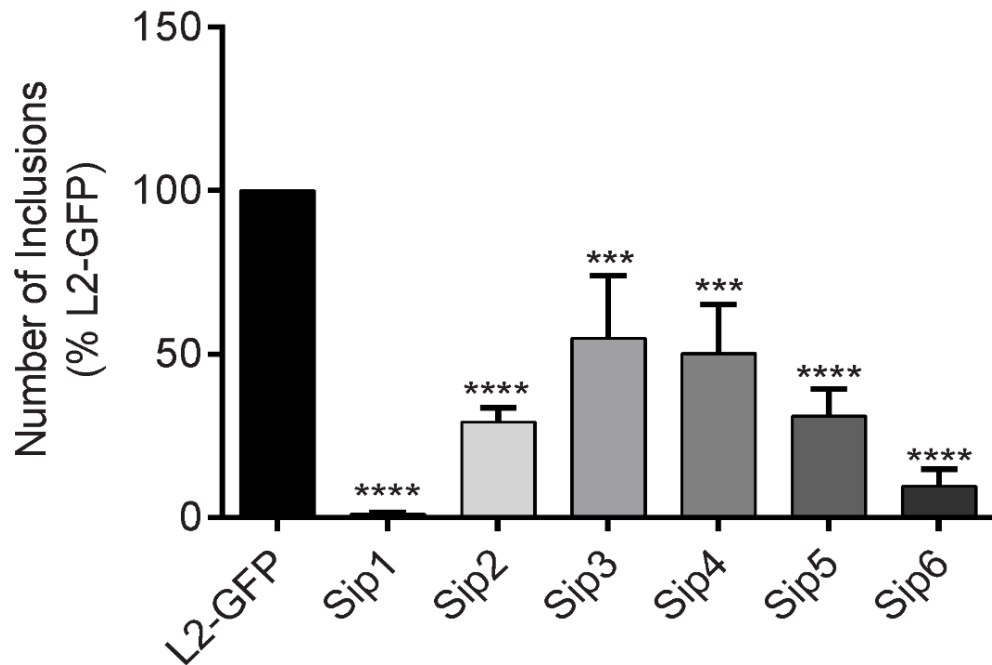


**Figure 9. Secondary screening confirmed that the Sip mutants made fewer inclusions following reactivation as compared to untreated wells and L2-GFP.** Bars represent the mean untreated/IFN- $\gamma$  treated inclusion ratios normalized to L2-GFP. n=3. Error bars indicate SD, \*\*\*,  $p < 0.001$ , \*\*\*\*,  $p < .0001$ . Copyright © American Society for Microbiology, [Infection and Immunity, 84, 2016, 2791-2801, and 10.1128/IAI.00356-16]



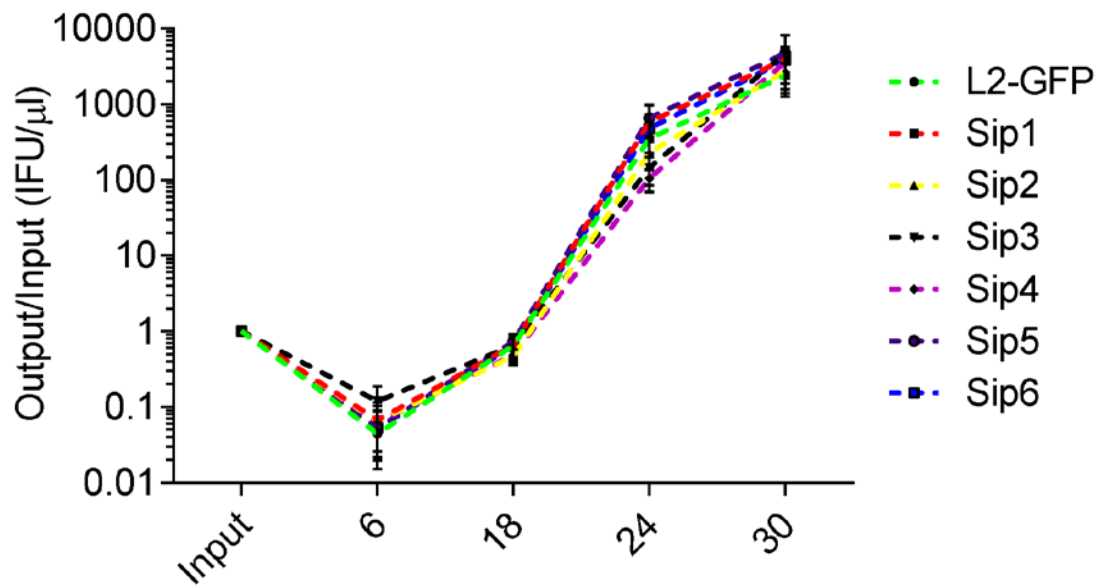


**Figure 10. Sip mutants exhibit normal growth kinetics.** The number of infectious EB produced by L2-GFP and Sip mutants was assessed at various intervals post infection. The number of inclusions formed for each strain was normalized to the initial inoculum. Data points represent the mean number of infectious progeny obtained from the indicated time points. n=3. Error bars indicate SD.

Copyright © American Society for Microbiology, [Infection and Immunity, 84, 2016, 2791-2801, and 10.1128/IAI.00356-16]

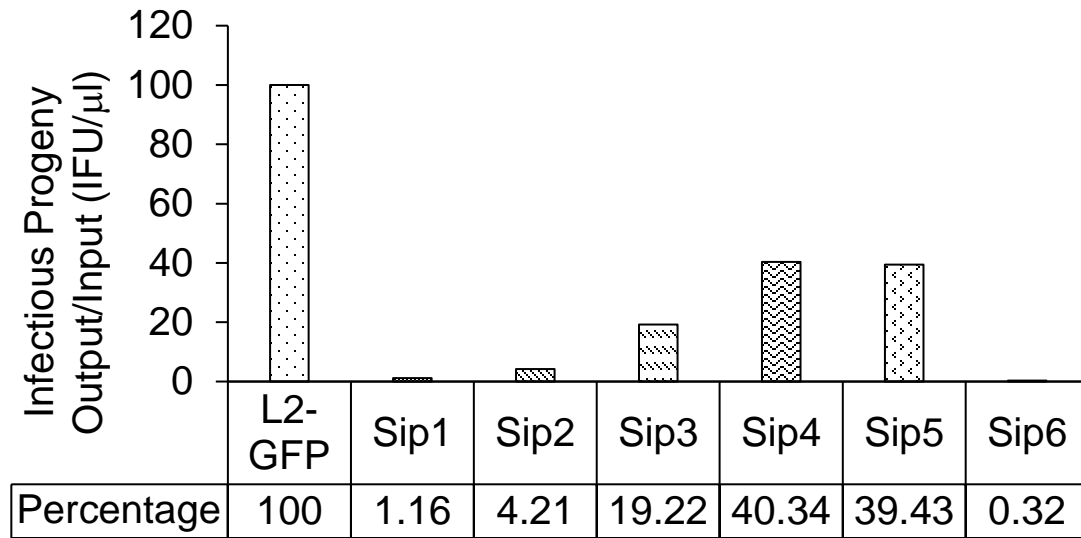


**Figure 11. Sip mutants make fewer EB following reactivation.** Cell lysates for L2-GFP and Sip mutants were harvested following reactivation with indole. Infectious EB was enumerated using an infectious progeny assay. Bars represent the mean percentage normalized to L2-GFP. n=3

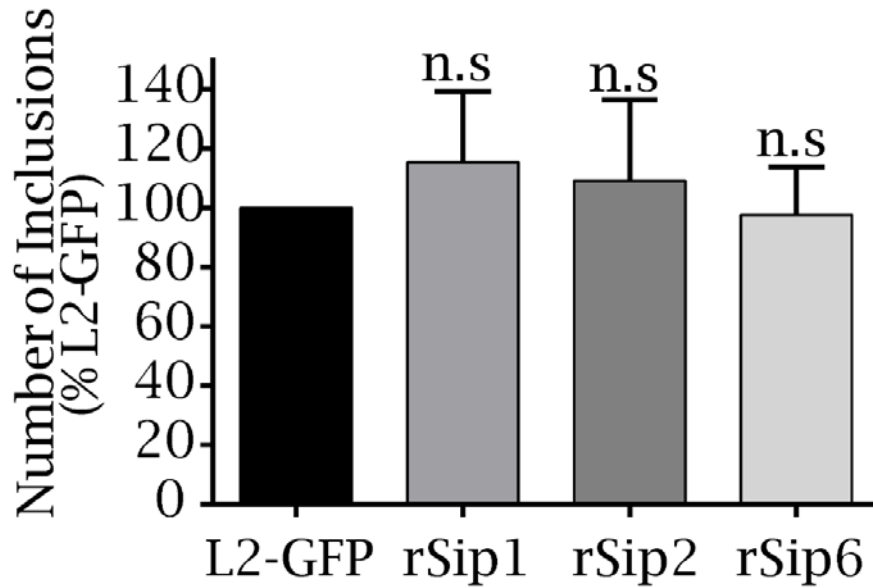


**Figure 12. Sip recombinants form similar numbers of inclusions as L2-GFP.** Sip mutant recombinants isolated from counter-selection LGT, make similar numbers of inclusions as L2-GFP following reactivation from IFN- $\gamma$  mediated persistence. Bars represent the mean percentage normalized to L2-GFP. n=3, Error bars indicate SD. n.s, non-significant.

Copyright © American Society for Microbiology, [Infection and Immunity, 84, 2016, 2791-2801, and 10.1128/IAI.00356-16]

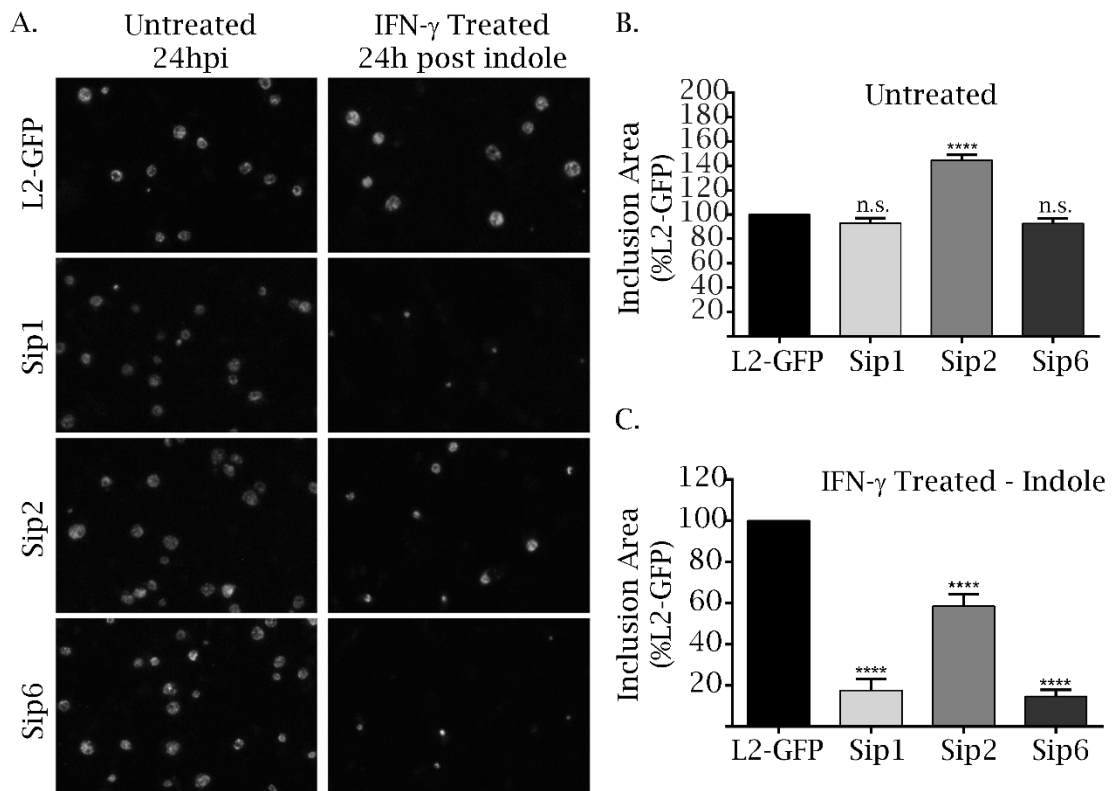


**Figure 13. Sip mutants make smaller inclusions following reactivation. (A)** Fluorescent images of inclusions under normal growth conditions and following reactivation from IFN- $\gamma$  mediated persistence with indole. **(B-C)** Quantification of the size of inclusions depicted in **(A)**. > 1000 inclusions were measured. Bars represent the mean percentage normalized to L2-GFP. Error bars indicate SD. \*\*\*\*,  $p < .0001$ , n.s, non-significant.

Copyright © American Society for Microbiology, [Infection and Immunity, 84, 2016, 2791-2801, and 10.1128/IAI.00356-16]

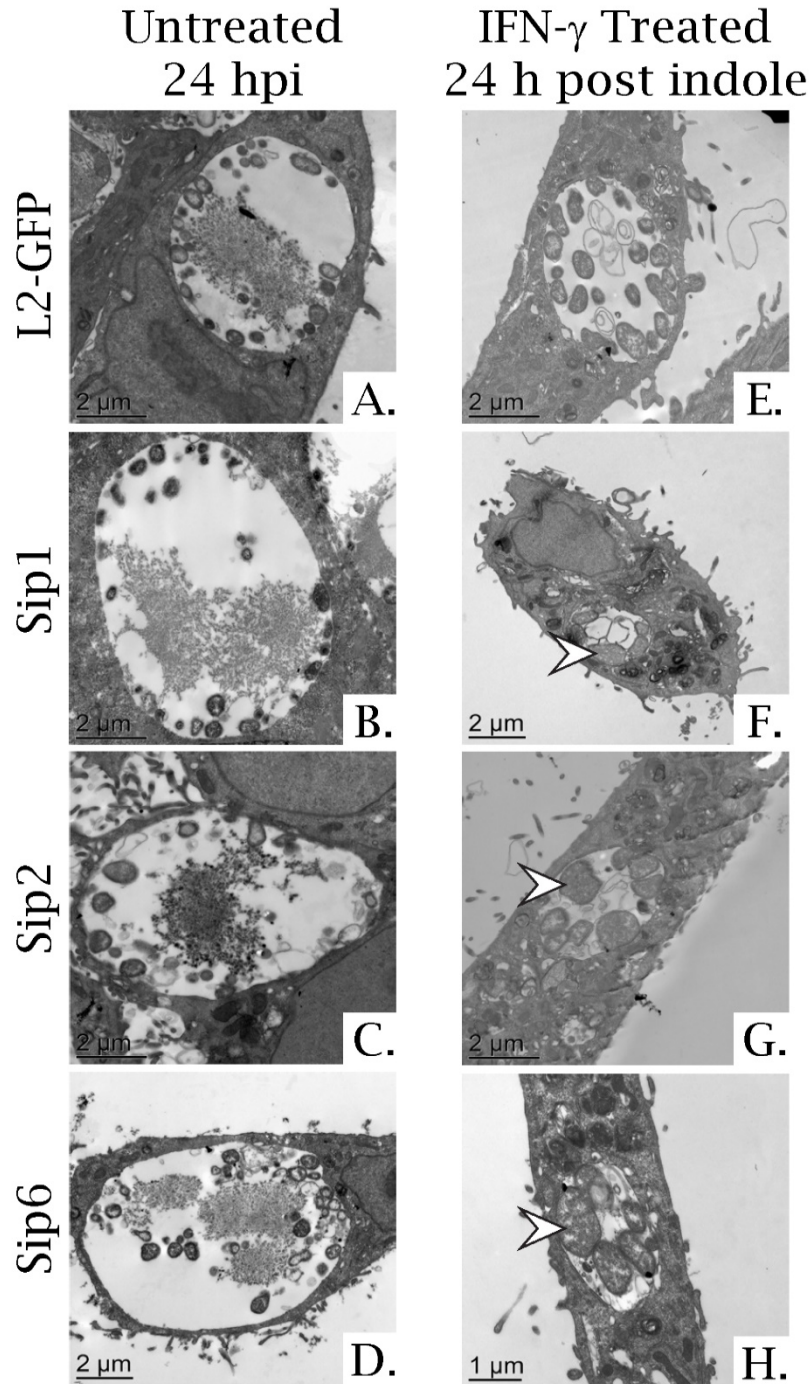


**Figure 14. Transmission electron microscopy of L2-GFP and Sip mutants. (A-D)** L2-GFP and Sip mutants form normal sized inclusions and RB in untreated HeLa cells 24hpi. **(E-H)** Only Sip mutants form small inclusions containing aberrant RB following reactivation with indole from IFN- $\gamma$  mediated persistence. White arrows indicate examples of aberrant RB.

Copyright © American Society for Microbiology, [Infection and Immunity, 84, 2016, 2791-2801, and 10.1128/IAI.00356-16]

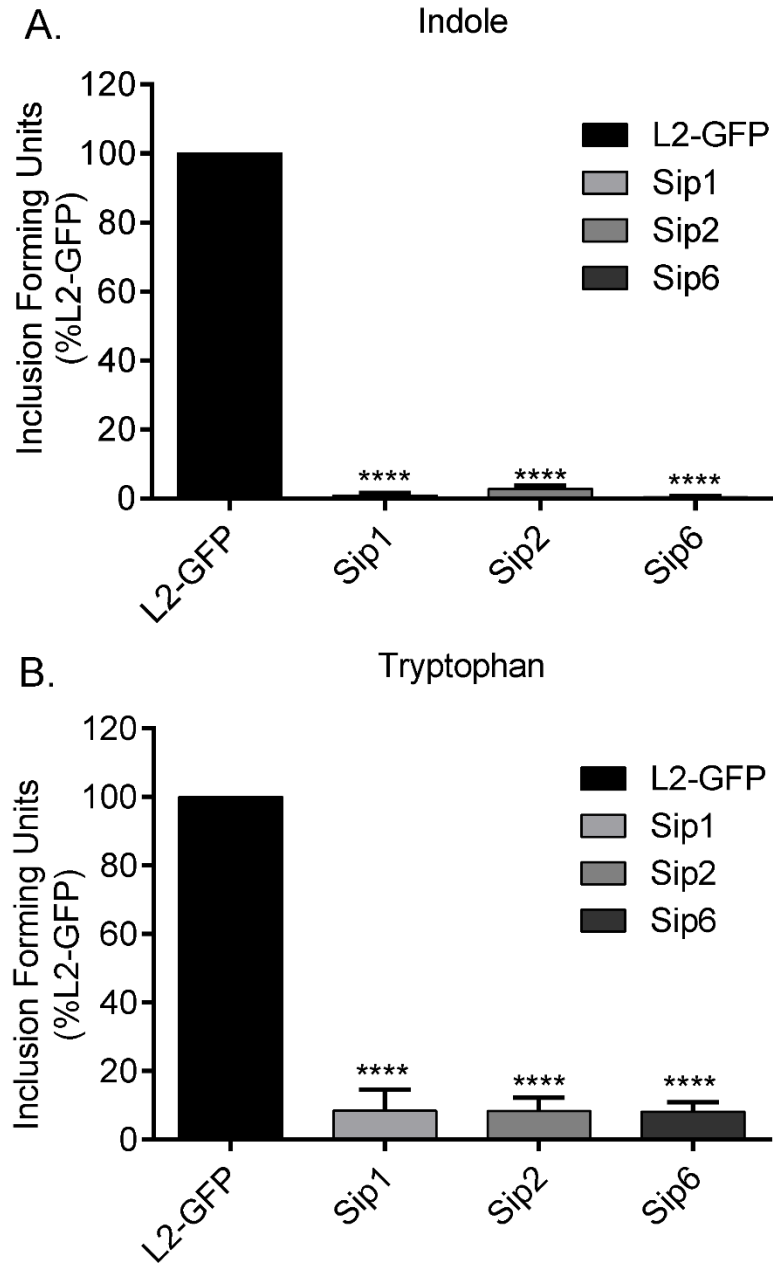


**Figure 15. Sip mutant EB production cannot be rescued by Trp or indole.** IFN- $\gamma$  treated HeLa cells were infected with L2-GFP or Sip mutants and then the infections were reactivated with (A) indole or (B) tryptophan. The infections were harvested 24 h post-reactivation and the EBs in the lysates enumerated in untreated HeLa cells. The number of inclusions each strain formed were normalized to the inoculum and then compared to L2-GFP. The graph depicts the mean of the results of three experiments performed in triplicate. The error bars indicate SD. \*\*\*\*,  $p < .0001$ .

Copyright © American Society for Microbiology, [Infection and Immunity, 84, 2016, 2791-2801, and 10.1128/IAI.00356-16]

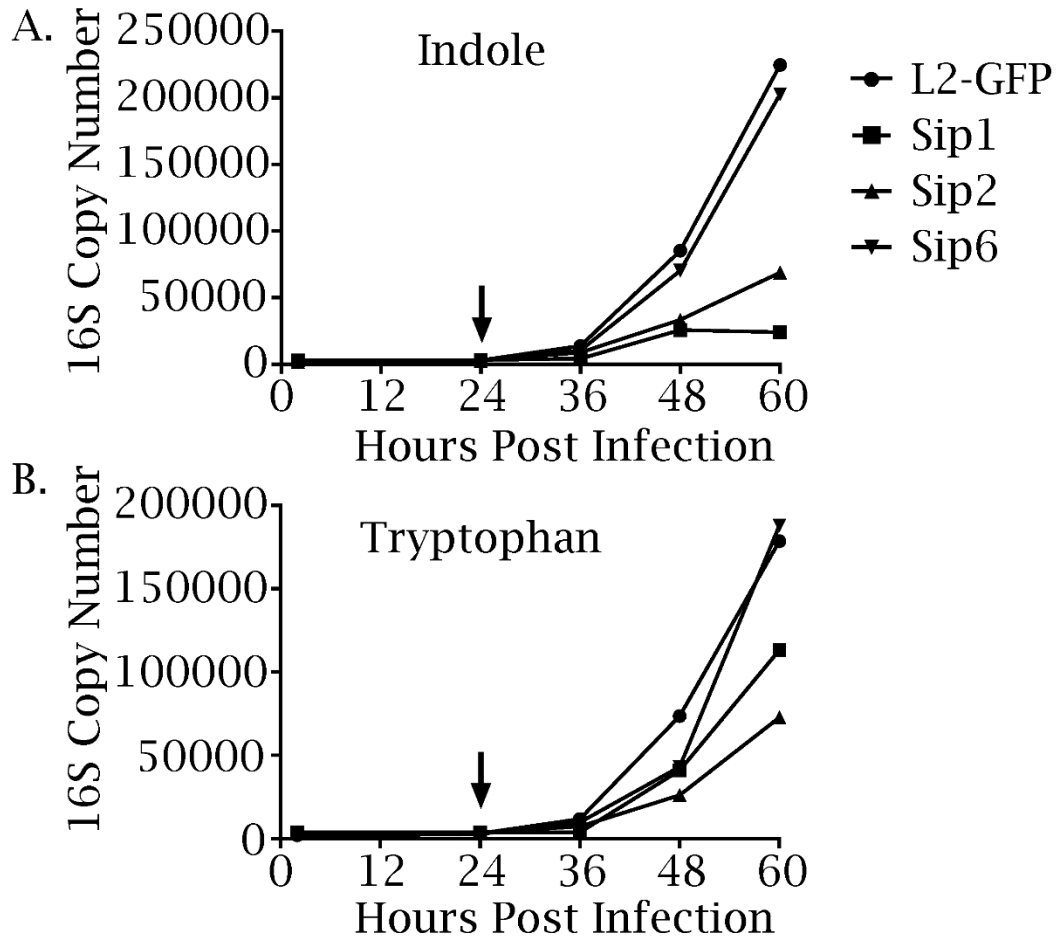


**Figure 16. Genome replication is altered during Sip mutant reactivation.** Genome copy numbers of L2-GFP and the Sip mutants were characterized pre- and post- (A) indole or (B) Trp reactivation using primers and a probe-set targeting the *C. trachomatis* 16S rRNA gene. The arrows indicate the time of indole or Trp addition. Data points represent the mean number of genome copies from two experiments performed in duplicate.

Copyright © American Society for Microbiology, [Infection and Immunity, 84, 2016, 2791-2801, and 10.1128/IAI.00356-16]

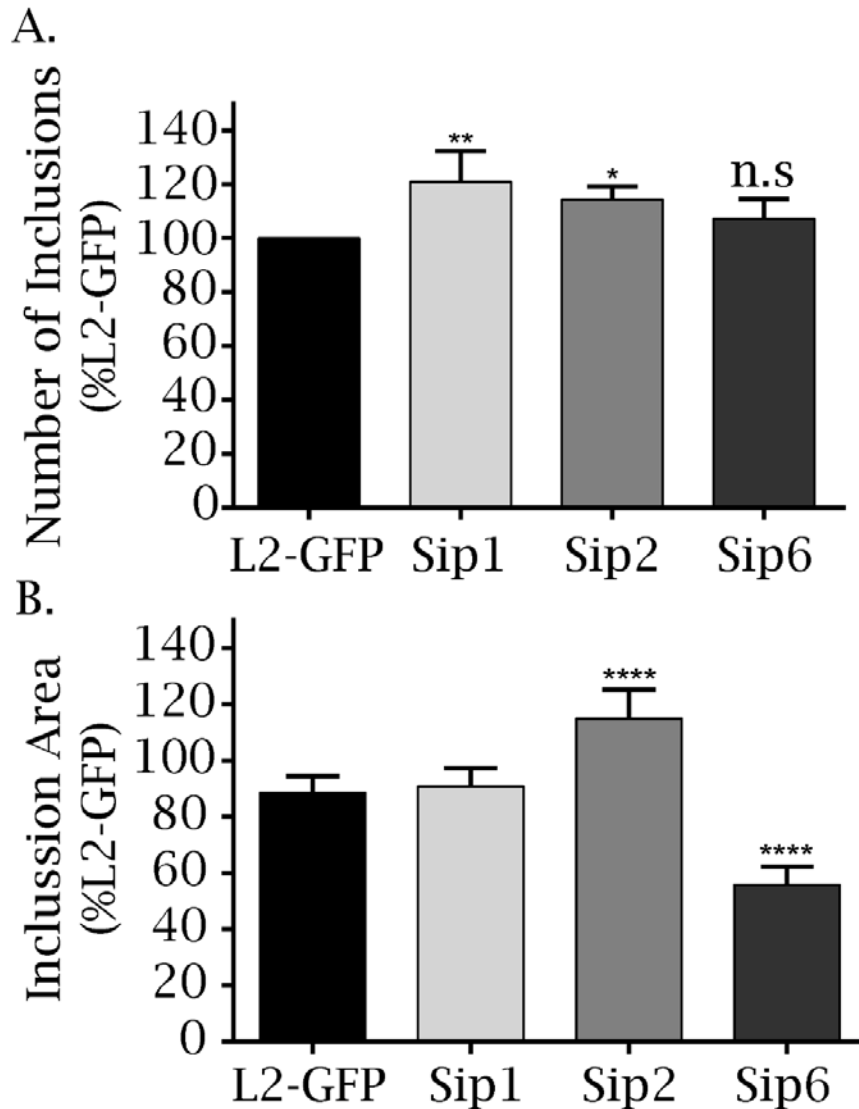


**Figure 17. Sip 6 forms small inclusions in the presence of IFN- $\gamma$  + Trp** (A) The Sip mutants form similar numbers of inclusions in the presence of IFN- $\gamma$  and excess Trp when compared to L2-GFP. (B) However, only Sip6 makes significantly smaller inclusions. Bars represent the mean percentage normalized to L2-GFP for the number of inclusions, and inclusion area. n=3. At least 1000 inclusions for each strain were analyzed for area of inclusion studies. Error bars indicate SD. \*,  $p < .05$ , \*\*,  $p < .01$ , \*\*\*\*,  $p < .0001$ , n.s, non-significant.

Copyright © American Society for Microbiology, [Infection and Immunity, 84, 2016, 2791-2801, and 10.1128/IAI.00356-16]



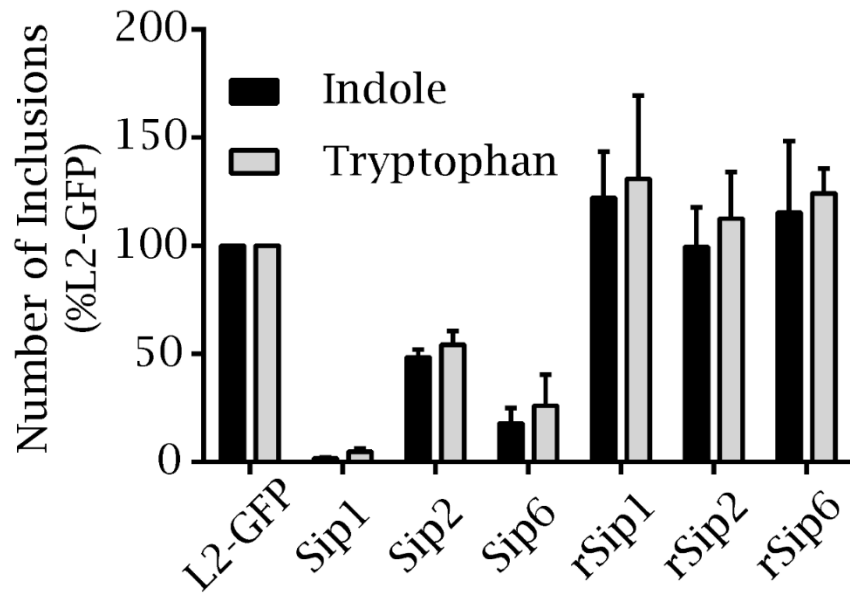


**Figure 18. Trp starvation alone induces Sip mutants to enter persistence** HeLa cells were depleted of Trp and infected with the indicated strains. The number of inclusions produced by each strain was compared to L2-GFP following reactivation with either indole or Trp. Bars represent the mean percentage normalized to L2-GFP. n=3. Error bars indicate SD.

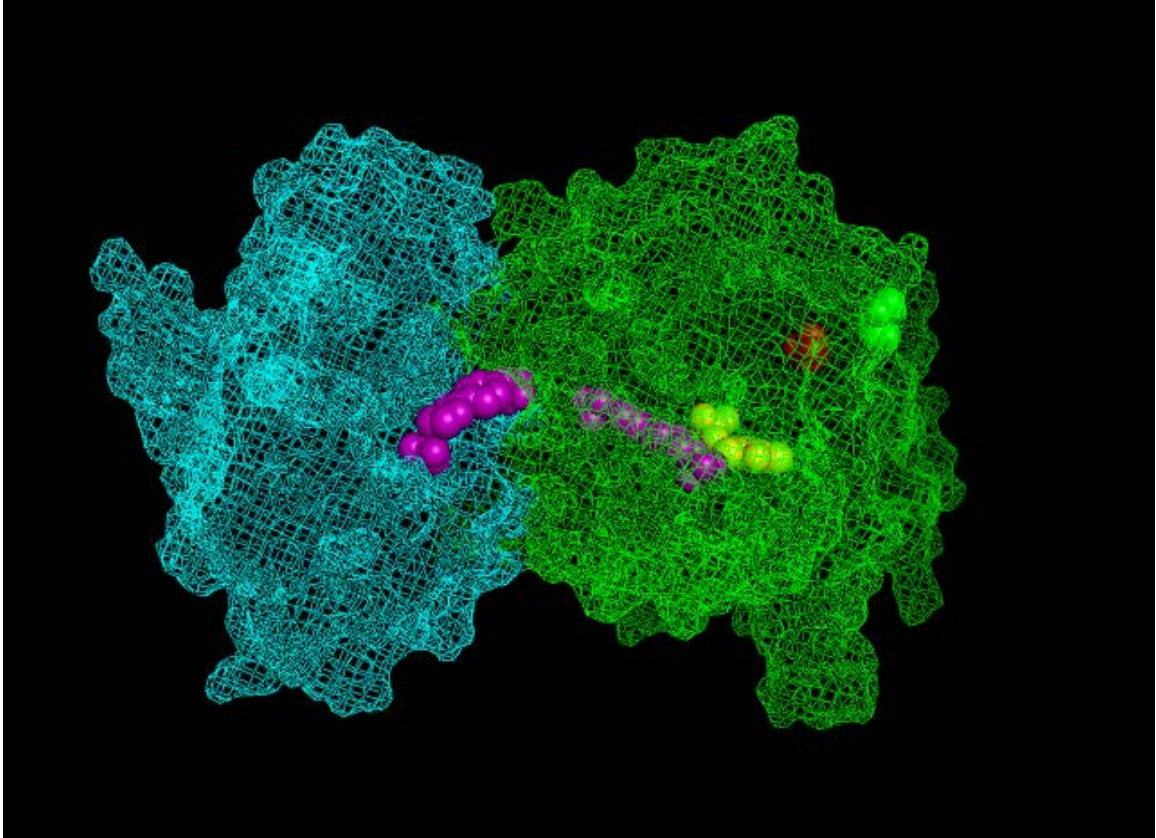


**Figure 19. Sip1 TrpBP221S aligned to *Salmonella typhimurium* TS.** The mesh crystal structures of the  $\alpha$ - and  $\beta$ - subunits of *S. typhimurium* TS are outlined in cyan and green, respectively. The purple spheres outline a bound substrate threaded through the substrate tunnel connecting the active sites of the  $\alpha$ - and  $\beta$ - subunits. The yellow spheres represent pyridoxal 5'-phosphate in the active site of the  $\beta$  subunit. The red spheres outline the location of the P221S mutation in TrpB<sup>P221S</sup>, and the green spheres indicate the location of the G52P suppressor mutation in Sip1. This image was generated using the PyMOL molecular graphics system.

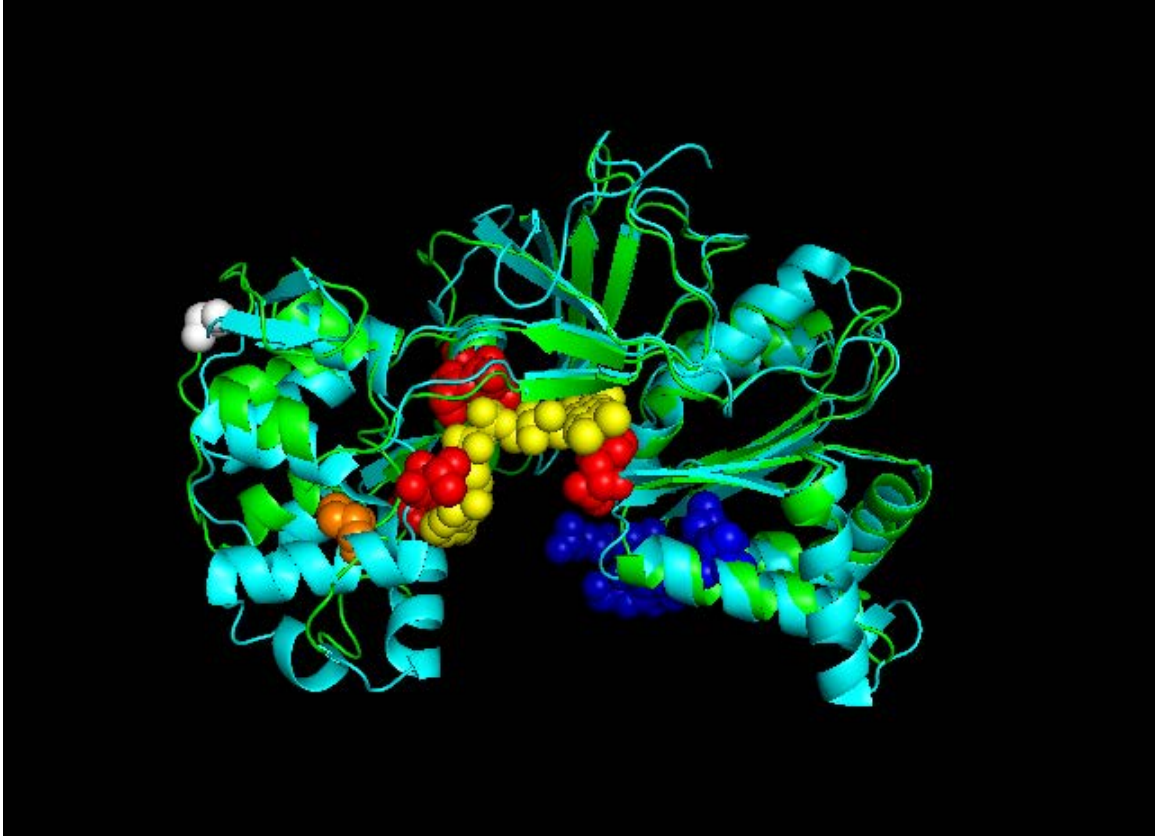


**Figure 20. Sip6 CTL0694<sup>P105L</sup> aligned to the crystal structure of *E. coli* CysJ.** The ribbon model outlines CTL0694<sup>P105L</sup> and CysJ in green and cyan, respectively. The blue spheres depict the location of a NAD binding site. The red spheres indicate the location of FAD binding sites with bound FAD, which is shown as yellow spheres. Orange and white spheres outline the location of the P105L mutation in CTL0694 and the G75S suppressor mutation in Sip6, respectively. This image was generated using the PyMOL molecular graphics system.

**Table 4. Mutations in Sip mutants.**

<b>Mutant</b>	<b>AA</b>	<b>Codon</b>	<b>Gene</b>	<b>Locus</b>	<b>Expected Function</b>
Sip1		818		CTL0033	Phosphopeptide binding protein
		341	<i>groEL</i>	CTL0124	60 kDa chaperonin GroEL
	A -> T	241		CTL0133	Hypothetical protein
	D -> N	62		CTL0209	Hypothetical protein
	P -> S	221	<i>trpB</i>	CTL0423 <sup>a</sup>	Tryptophan synthase subunit beta
Sip2	G -> R	298	<i>ftsW</i>	CTL0129	Cell division protein
	G -> E	77		CTL0225 <sup>a</sup>	Putative integral membrane protein
		258	<i>cpa</i>	CTL0233	Putative exported protease
		93	<i>gatC</i>	CTL0257	Aspartyl/glutamyl-tRNA amidotransferase subunit C
	S -> F	365		CTL0325	ABC transporter permease
	Intergenic				
	G -> E	299		CTL0447	Putative integral membrane protein
Sip3		64	<i>ispD</i>	CTL0722	2-C-methyl-D-erythritol 4-phosphate cytidyltransferase
	S -> N	246	<i>plsB</i>	CTL0176	Glycerol-3-phosphate acyltransferase
	Intergenic				
		245		CTL0291	Hypothetical protein
Sip4	P -> L	1,128	<i>rpoC</i>	CTL0566	DNA-directed RNA polymerase subunit beta'
	G -> R	37	<i>trxB</i>	CTL0354	Thioredoxin reductase
	G -> R	14	<i>groES</i>	CTL0366	Co-chaperonin GroES
Sip5	G -> E	39	<i>tmk</i>	CTL0440	Thymidylate kinase
	P -> S	831	<i>ptr</i>	CTL0175	Exported insulinase/protease
Sip6	H -> Y	37		CTL0641	Hypothetical protein
	S -> F	71		CTL0157	Putative integral membrane protein
		39	<i>pmpG</i>	CTL0250	Polymorphic outer membrane protein

Mutant	AA	Codon	Gene	Locus	Expected Function
Sip6	P -> S	225		CTL0312	Hypothetical protein
		381	<i>nusA</i>	CTL0352	Transcription elongation factor NusA
	D -> N	945		CTL0402	Putative integral membrane protein
		238	<i>gltT</i>	CTL0658	Sodium:dicarboxylate symport protein
	P -> L	105		CTL0694 <sup>a</sup>	Putative oxidoreductase
		296		CTL0737	Hypothetical protein
L2-GFP SNP	R -> C	131		CTL0882	Hypothetical protein

<sup>a</sup> Mapped persistence allele

Copyright © American Society for Microbiology, [Infection and Immunity, 84, 2016, 2791-2801, and 10.1128/IAI.00356-16]

## CHAPTER V:

### Characterization of Sip2

#### **The G77E mutation in CTL0225 may disrupt AA transport**

BLASTp identified CTL0225 as a putative integral membrane protein that is highly conserved among *Chlamydia* species (>89%) that is homologous to other intracellular and extracellular bacterial proteins in *E. coli* (31%), *B. aphidicola* (33%), and *C. burnetii* (35%). Additionally, CTL0225 shares homology with a small neutral AA transporter (SnatA) from *Thermococcus* strain KS-1 (29%).

SnatA is predicted to have six transmembrane domains and has been shown to transport glycine (Gly) and alanine (Ala) [127]. Similar to SnatA, THMHMM server 2.0 analysis indicated CTL0225 also contains six transmembrane domains (Figure 21A). Additionally, results from this *in silico* analysis suggested that the Gly77 to glutamate (G77E) mutation in Sip2 disrupts the 3<sup>rd</sup> transmembrane domain of CTL0225 (Figure 21B). This disruption may occur because Gly77 is located one AA away from a GXXXG motif, which is hypothesized to mediate helix-helix association and proper folding of integral membrane proteins [128]. Collectively, these observations suggest that CTL0225 is an AA transporter and that mutant CTL0225 (CTL0225<sup>G77E</sup>) is nonfunctional.

#### **Amino acid competitive inhibition causes Sip2 to form small inclusions.**

Typically, similar AAs are transported through the same AA transporters [129-131]. However, when one AA is present in excess, AA transport can be inhibited due to competitive inhibition. Braun *et al.* suggested that *C. trachomatis* formed small inclusions in the presence of excess Leu, Ile, Met, and Phe because these AAs are antagonists of Val. They speculated that these AAs

competitively inhibited the transport of Val, which led to a shortage of Val inside *Chlamydia* [67].

We speculated that CTL0225 transports a specific group of AAs and that the G77E mutation in Sip2 makes CTL0225 nonfunctional. Additionally, we hypothesized that Sip2 will form small inclusions in the presence of excess AA that CTL0225 normally transports, due to increased competitive inhibition of other chlamydial AA transporters. To test this hypothesis, we devised an AA competitive inhibition screen where Sip2 infected HeLa cells were treated with a high concentration (10 mM) of 18 single AAs alone or in the indicated pairs (Figure 7). Tyrosine (Tyr) or Trp could not be assessed because high concentrations were either insoluble or cytotoxic, respectively (data not shown).

Sip2 formed small inclusions in cells treated with excess Ile, Leu, Ser, and cysteine (Cys). Small inclusions were not detected in cells co-treated with Val + Ile and Leu or for Ala + Ser and Cys (Figure 7). These results confirm the observation made by Braun *et al.* that high concentrations of Ile and Leu cause Val starvation, and indicate Ser and Cys antagonize the transport of Ala. Additionally, these results indicate that CTL0225 may be playing a role in two different AA transport systems, as these AAs have not been previously described to be transported together.

### **Sip2 is hypersensitive to excess isoleucine**

The competitive inhibition screen indicated that Sip2 formed small inclusions in response to treatment with 10 mM Ile. However, it did not differentiate if the small inclusions observed were a normal *C. trachomatis* response to 10 mM Ile. Inclusion sizes of strains encoding a wild-type allele of CTL0225 (L2-GFP, Sip1, Sip6, rSip2) were compared to Sip2 in the presence of

increasing concentrations of Ile (0-30 mM). In the absence of Ile, all strains formed similar sized inclusions. However, when treated with 10 mM Ile, only Sip2 formed significantly smaller inclusions ( $p < 0.0001$ ). This trend continued even at the highest dose (30 mM) assayed ( $p < 0.0001$ ) (Figure 22).

#### **Excess isoleucine starves Sip2 of valine**

Some AA transporters can transport Ile, Leu, and Val [132-134]. However, the AA competitive inhibition screen indicated that only excess Ile antagonized the transport of Val and not Leu. To confirm our screening results, HeLa cells were infected with L2-GFP, Sip1, Sip2, Sip6, or rSip2 in the presence of 10 mM Ile and increasing concentrations (0-30 mM) of Val or Leu. Results from the competitive inhibition assays indicated that 5 mM Val was sufficient to allow Sip2 to form large inclusions in the presence of Ile (Figure 23A). However, even at the highest concentration of Leu assayed (30 mM), Sip2 did not form large inclusions (Figure 23B). These results indicate that 10 mM Ile starves Sip2 of Val and not Leu. Additionally, these results suggest that when Sip2 is treated with Ile, antagonism of Val transport increases due to the inability of CTL0225<sup>G77E</sup> to transport Ile.

#### **Excess cysteine or serine starve Sip2 of alanine**

The competitive inhibition screen indicated that Sip2 was sensitive to high concentrations of Ser and Cys. Using similar competitive inhibition assays as described above with Ile, we validated that treatment with 10 mM Ser (Figure 24) and Cys (Figure 25) caused Sip2 to form significantly smaller inclusions than L2-GFP ( $P < 0.0001$ ) 44-48 hpi. Additionally, we confirmed that when Sip2 was co-treated with 10 mM Ser or Cys + Ala, Sip2 formed large inclusions that were similar in size to L2-GFP (Figure 24 and 25). Interestingly, two distinct



populations of inclusions were evident when Sip2 was treated with 10 mM Ser. Most the Sip2 inclusions assayed, following treatment with Ser, were small; however, a minority of inclusions formed a distinct cluster of large inclusions. This phenomenon was only observed when Sip2 inclusions treated with Ser, as treatment with Cys, Ile, or Leu induce Sip2 to form a tighter cluster of small inclusions (Figure 26).

Next, we wanted to validate results of the AA competitive inhibition screen that suggested only structurally similar AAs (Ile, Leu, Val or Ala, Cys, Ser) mediate competitive inhibition and rescue of Sip2. HeLa cells were infected with Sip2 and then treated with either 10 mM Ile and Ala or Ser and Val. We confirmed that the addition of 10 mM Ala does not alleviate AA starvation caused by Ile treatment, as Sip2 still formed significantly smaller inclusions than L2-GFP ( $p < .0001$ ) (Figure 27). Similarly, Ser treatment still caused Sip2 to form small inclusions when co-treated with 10 mM Val (Figure 28). These results indicated that excess Ile exclusively antagonizes the transport of Val, while excess Ser only inhibits the transport of Ala. These results support the hypothesis that CTL0225 is involved in the transport of two classes of AA that have not been previously described as limited during IFN- $\gamma$  mediated persistence.

### **IFN- $\gamma$ depletes free amino acid pools**

Our competitive inhibition assays suggested that free AA may be limiting during IFN- $\gamma$  mediated persistence. HPLC-mass spectrometry was used to determine if free AA pools in HeLa cells deplete over time in  $\pm$  IFN- $\gamma$  conditions. Untreated and IFN- $\gamma$  treated monolayers were pelleted and weighed at each time point indicated. Following cell lysis, proteins were precipitated, and free AAs

were isolated from the supernatant. The concentration of free AAs was normalized to cell pellet weight to control for variability between samples. The average concentration of free AAs collected from 3 biological replicates was then compared between  $\pm$  IFN- $\gamma$  conditions.

Initially, we wanted to determine if free AA concentrations fluctuated during normal HeLa cell growth. If free AA concentrations fluctuated over time during normal growth, then this could confound our interpretations about the availability of free AA when HeLa cells are treated with IFN- $\gamma$  and/or infected with *C. trachomatis*. Metabolomics analysis of normally growing HeLa cells suggested that the concentrations of free AAs were stable (Figure 29).

Next, we wanted to determine if IFN- $\gamma$  depletes free AA in HeLa cells. Most AA decreased over time in IFN- $\gamma$  treated HeLa cells (Figure 30). This observation led us to speculate that CTL0225 may circumvent host AA limitation during IFN- $\gamma$  mediated persistence. Additionally, we observed that the concentration of free Trp was the low at every time point assayed in IFN- $\gamma$  treated cells compared to untreated HeLa cells (Figure 31). This result suggested that IDO1 was the only host factor actively degrading an AA. Furthermore, we speculate general AA depletion, caused by IFN- $\gamma$  treatment, might be due to an increase in protein synthesis and charging of unbound tRNAs.

### ***C. trachomatis* increases free amino acid pools**

Sip2 has normal growth kinetics in the absence of IFN- $\gamma$  (Figure 10), indicating that CTL0225 is nonessential during normal growth. Additionally, this suggests free AA pools are not limiting during *C. trachomatis* infection. To test this hypothesis, we used HPLC-mass spectrometry to determine the free AA concentrations in uninfected and infected HeLa cells over time, as described

above. The concentration of free AA was higher in *C. trachomatis* infected HeLa cells as compared to uninfected cells, 24 and 36 hpi (Figure 32). These results indicate *C. trachomatis* infection causes an increase in free AA and suggest that having multiple AA transporters may be dispensable during normal growth.

#### **IFN- $\gamma$ decreases AA pools in *C. trachomatis* infected cells**

Lastly, we tested if *C. trachomatis* could increase free AA pools in IFN- $\gamma$  treated HeLa cells. Free AA concentrations were determined as described above and compared to uninfected HeLa cells. The concentration of most of the free AAs resembled what was observed in uninfected IFN- $\gamma$  treated HeLa cells by 24 hpi (Figure 33). This result showed that *C. trachomatis* did not counteract the effects of IFN- $\gamma$  to decrease free AA pools. Additionally, all the AA CTL0225 may transport, specifically Ile, Leu, Val, Ala, Cys, and Ser, were decreased 24 hpi. These observations support the hypothesis that AA transporters, such as CTL0225, are essential for survival during IFN- $\gamma$  mediated persistence.

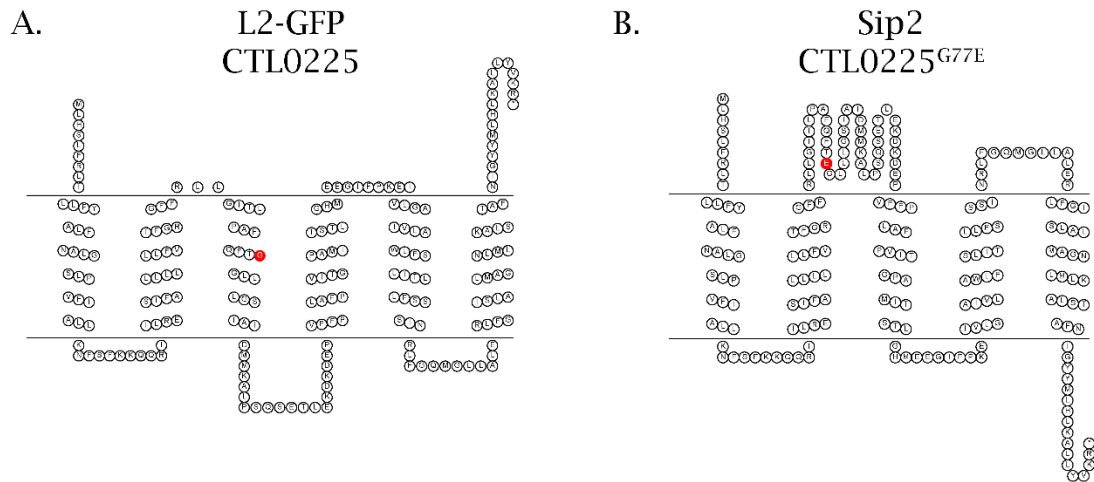


**Figure 21. G77E alters CTL0225 membrane topology. (A)** Membrane topology of wild type CTL0225. **(B)** G77E in Sip2 is predicted to disrupt the third transmembrane helix of CTL0225. TMHMM Server 2.0 predicted transmembrane orientation and TOPO2 display software.

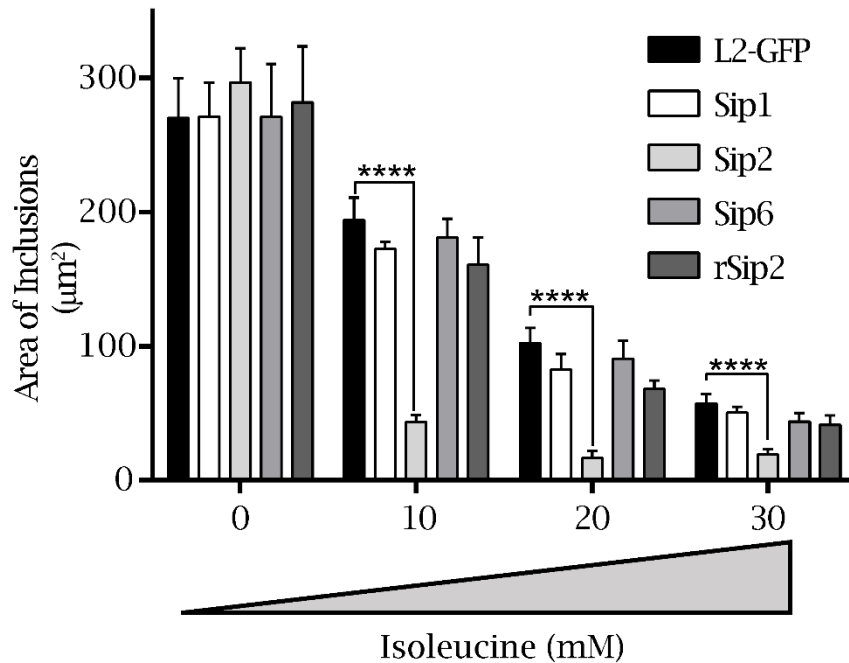


**Figure 22. Sip2 is sensitive to high concentrations of Ile.** All of the indicated strains make smaller inclusions in response to increasing concentrations of isoleucine. L2-GFP, Sip1, Sip6 and rSip2 make similar sized inclusions at the same Ile concentrations. In contrast, Sip2 makes significantly smaller inclusions when compared to L2-GFP. Bars represent mean inclusion size. n=3. At least 1000 inclusions for each strain were analyzed. Error bars indicate SD. \*\*\*\*,  $p < .0001$

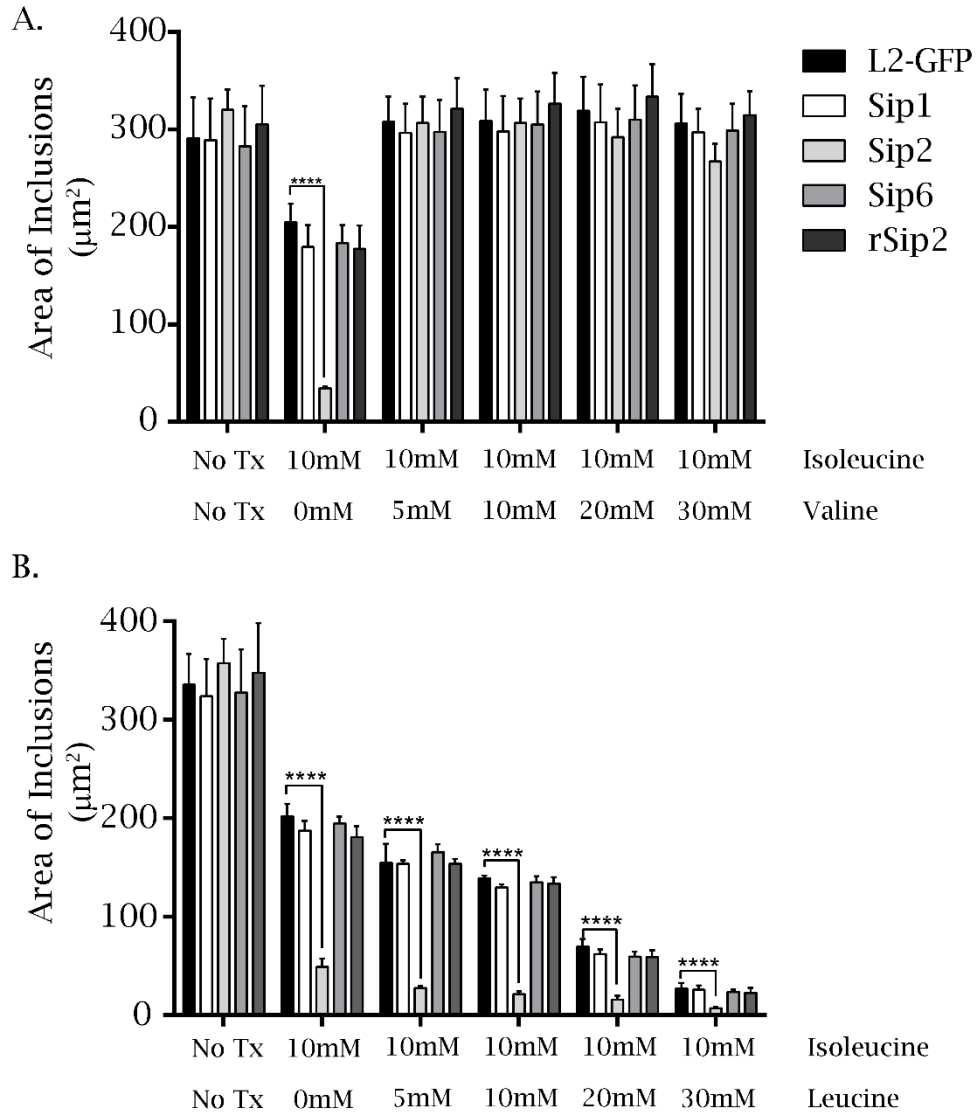


**Figure 23. Only Val reverses the Sip2 small inclusion phenotype.** The strains were treated with 10mM Ile in the presence of increasing concentrations of either (A) Val, or (B) Leu. The addition of 5mM Val was sufficient to allow Sip2 to form large inclusions when co-treated with 10mM Ile. However, increasing concentrations of Leu did not allow Sip2 to form large inclusions when co-treated with Ile. Bars represent mean inclusion size. n=3. At least 500 inclusions for each strain were analyzed. Error bars indicate SD. \*\*\*\*,  $p < .0001$

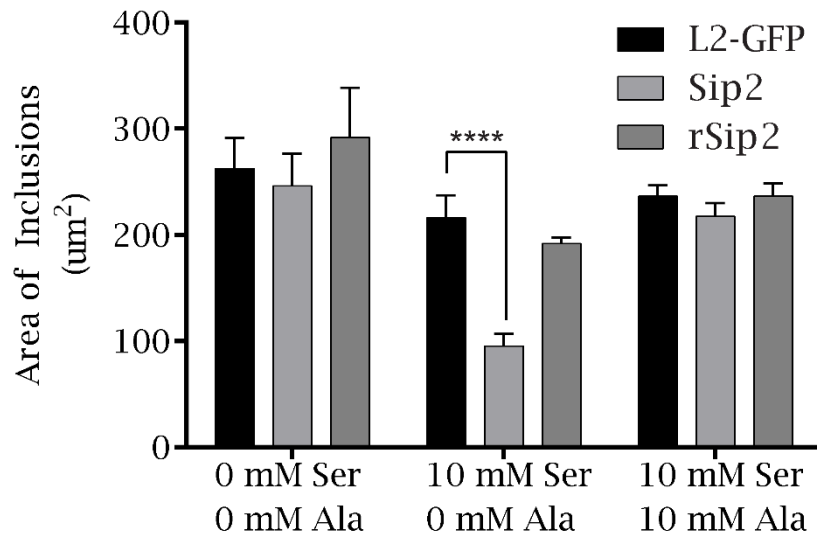


**Figure 24. Ala reverses formation of small inclusions induced by excess Ser.** HeLa cells were infected with the above strains and were either left untreated or treated with 10 mM Ser, or 10 mM Ser + Ala. Sip2 formed significantly smaller inclusions than L2-GFP and rSip2 strains when treated with Ser alone and this phenotype was reversed with the addition of 10 mM Ala. Bars represent the mean inclusion size of at least 1000 inclusions.  $n=3$ . Error bars indicate SD. \*\*\*\*,  $p < .0001$ .

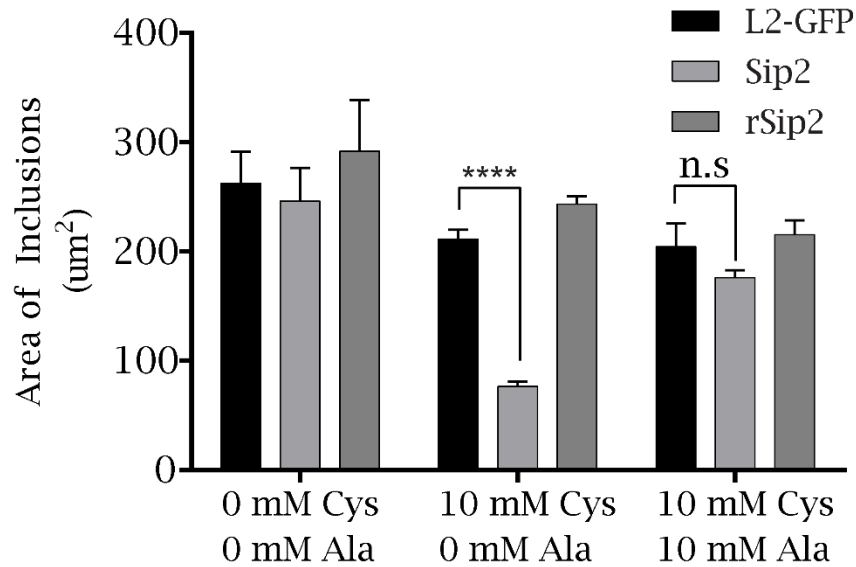


**Figure 25. Ala reverses Sip2 small inclusion phenotype caused by Cys.** HeLa cells were infected with the indicated strains and were either left untreated or treated with 10 mM Cys or 10 mM Cys + Ala. Sip2 formed significantly smaller inclusions than L2-GFP and rSip2 when treated with Cys alone. Sip2 formed large inclusions when co-treated with 10 mM Cys and Ala. Bars represent the mean inclusions size of at least 1000 inclusions.  $n=3$ . Error bars indicate SD. \*\*\*\*,  $p < .0001$ . n.s. non-significant.



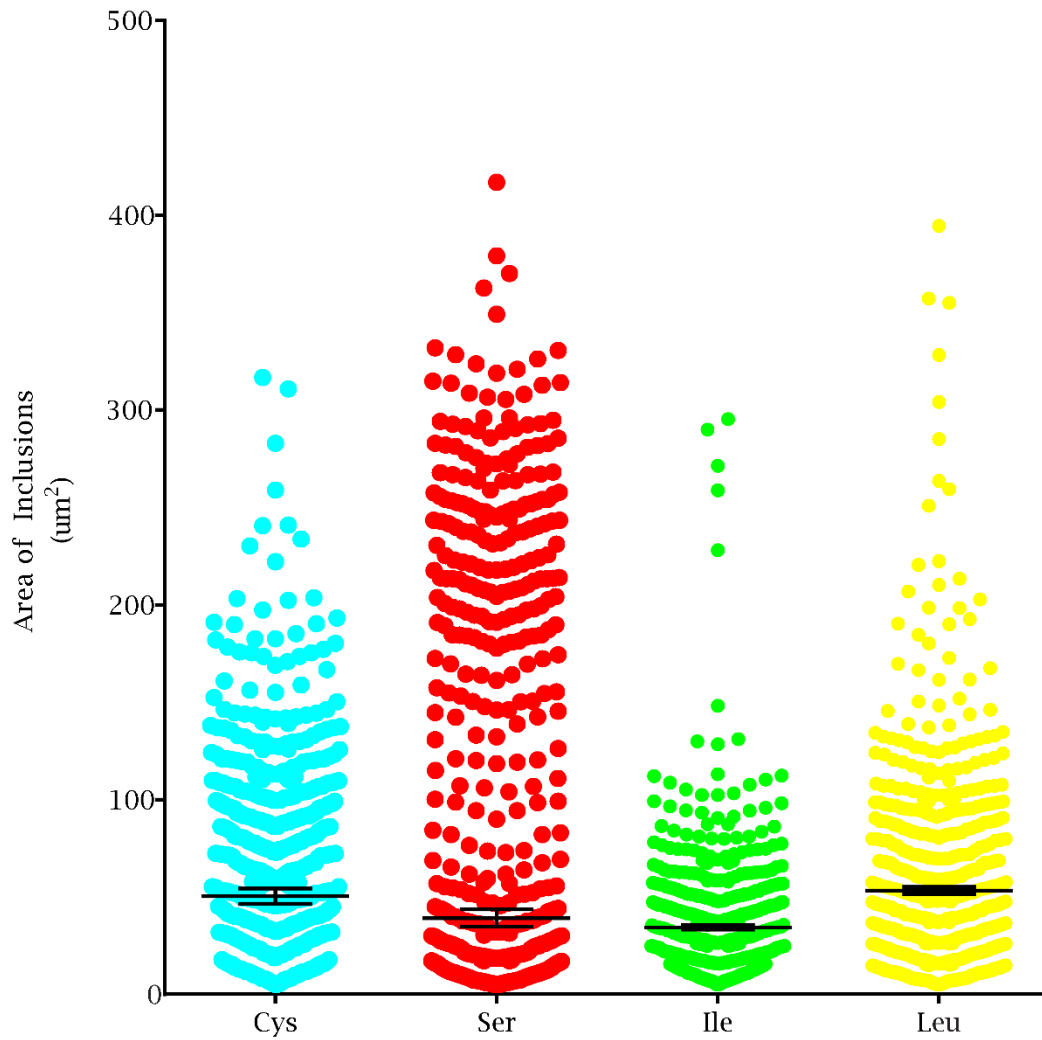


**Figure 26. Sip2 forms two populations of inclusions when treated with Ser.** Sip2 infected cells were treated with 10 mM Cys, Ser, Ile, or Leu. Infected monolayers were fixed 44-48 hpi, and the area of each inclusion was determined. Measurements of individual inclusion sizes are depicted. The average and standard deviation of inclusion sizes in each condition are represented by the indicated lines. At least 500 Sip2 inclusions were measured for each treatment condition.

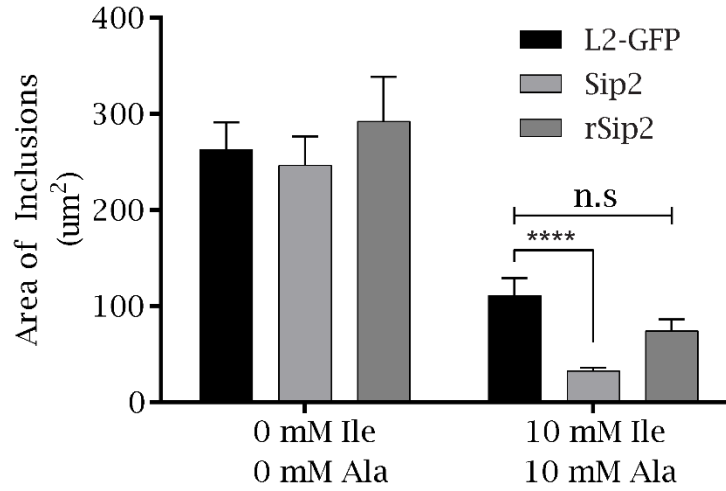


**Figure 27. Ala does not reverse the small inclusion phenotype caused by Ile.** HeLa cells were infected with L2-GFP, Sip2, and rSip2, and were either left untreated or treated with 10 mM Ile and Ala. The small inclusion phenotype caused by Ile treatment was not reversed with the addition of Ala. Bars represent the mean inclusions size of at least 1000 inclusions. n=3. Error bars indicate SD. \*\*\*\*,  $p < .0001$ . n.s. non-significant.

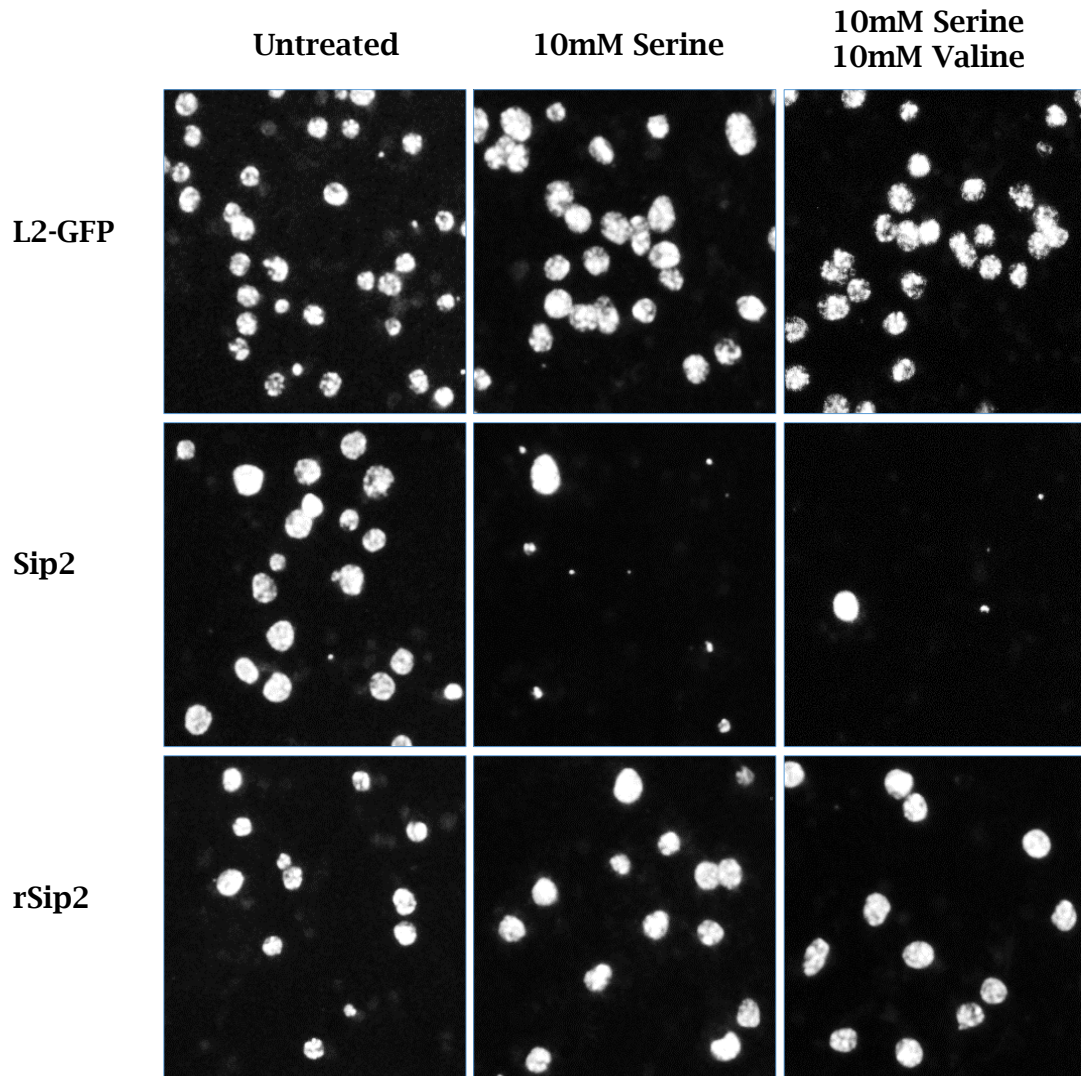


**Figure 28. Sip2 does not form large inclusions in the presence of Val + Ser.** The indicated strains were used to infect HeLa cells that were left untreated, treated with 10 mM Ser or 10 mM Ser + Val. These are representative images from one experiment. Inclusions were stained with anti-chlamydial LPS and Alexa Flour 488 secondary antibody. FIJI was used to adjust brightness and contrast.

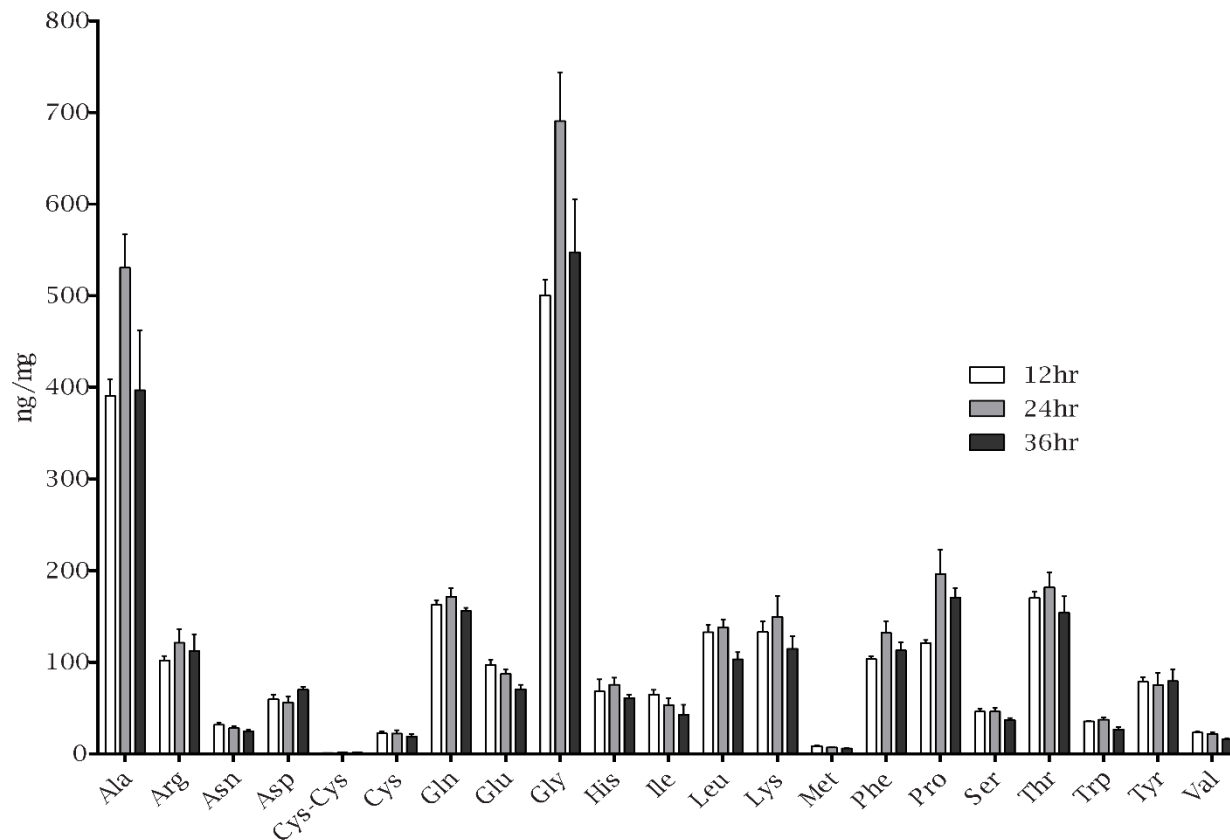


**Figure 29. Free AA concentrations remain stable over time.** Uninfected and untreated HeLa cells were harvested at the indicated time points and free AA were quantified using HPLC-Mass spectrometry. Concentrations were normalized to an internal standard, and mg cell weight. Bars represent the mean concentration from three replicate samples. Error bars indicated SD.

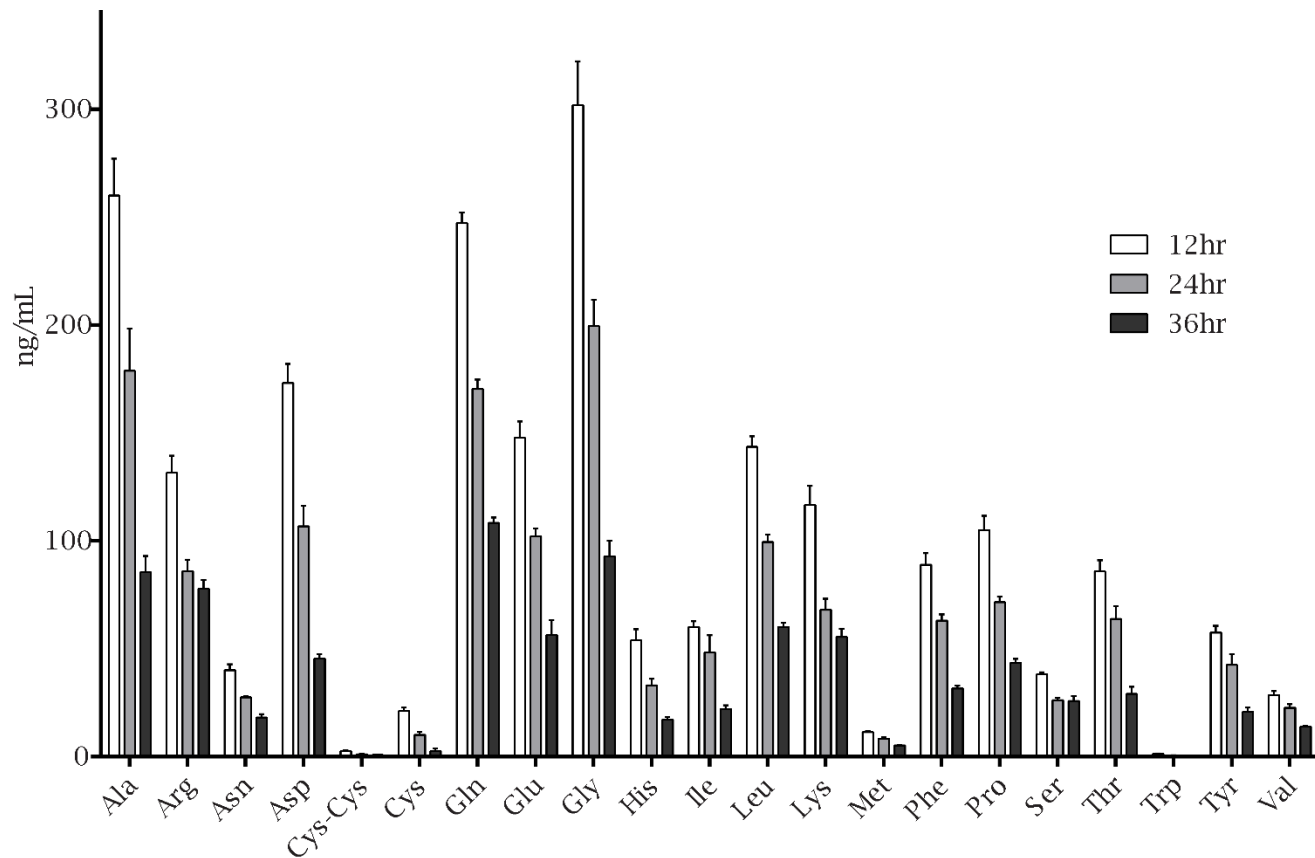


**Figure 30. Free AA decrease over time in IFN- $\gamma$  treated HeLa cells.** HeLa cells were treated for 24 hours with IFN- $\gamma$ . This time point was redefined as time zero. Free AA were collected and quantified at the indicated time points. Concentrations of the majority of the AAs decreased over time. Bars represent the mean of three replicate samples. Error bars indicated SD.

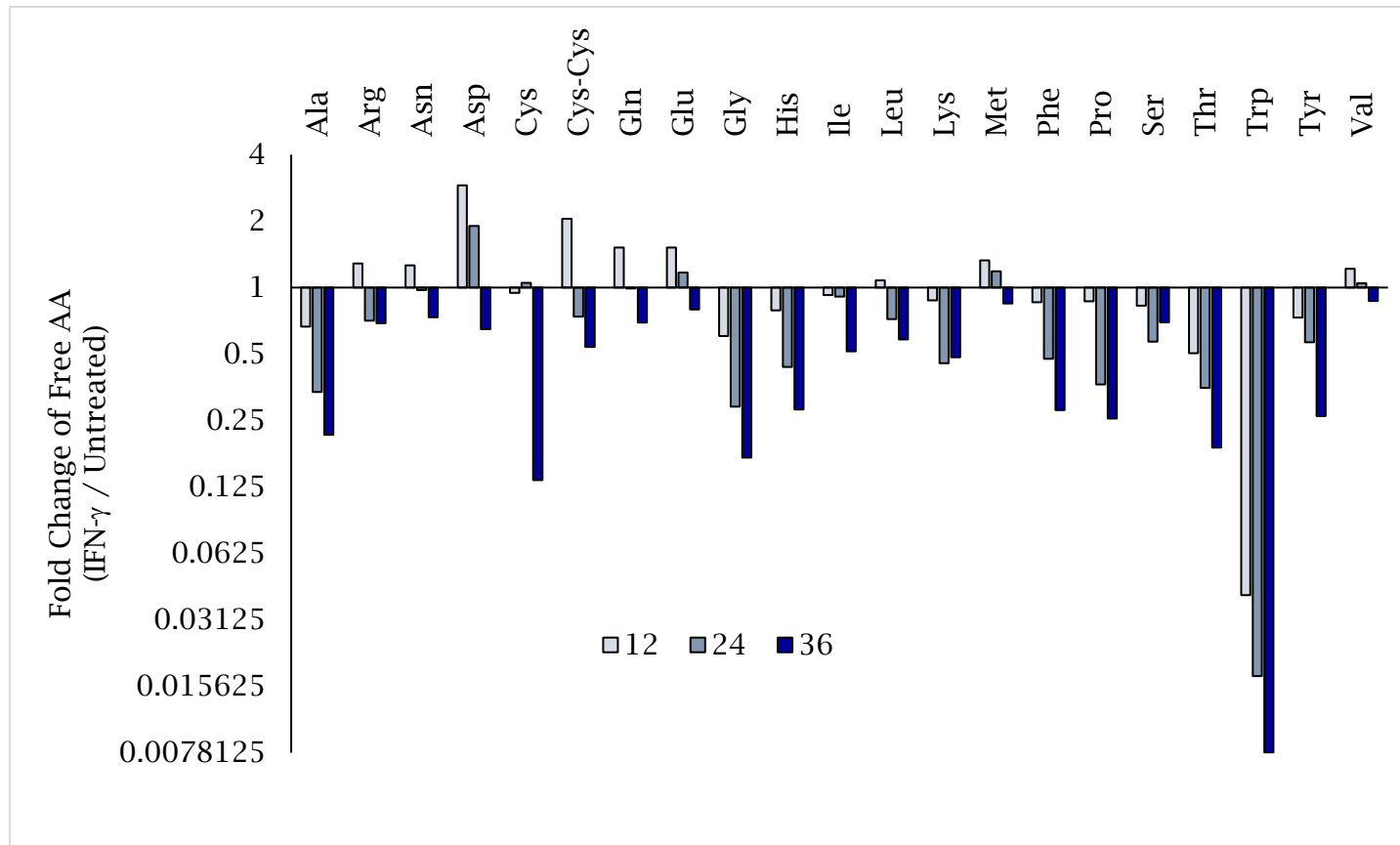


**Figure 31. IFN- $\gamma$  decreases free AA pools in HeLa cells.** Free AA concentrations were compared between untreated and IFN- $\gamma$  treated HeLa cells at the indicated time points. IFN- $\gamma$  treatment decreased all free AA pools by 36 hours. Bars represent the average free AA concentrations of three replicate samples normalized to uninfected HeLa cells.

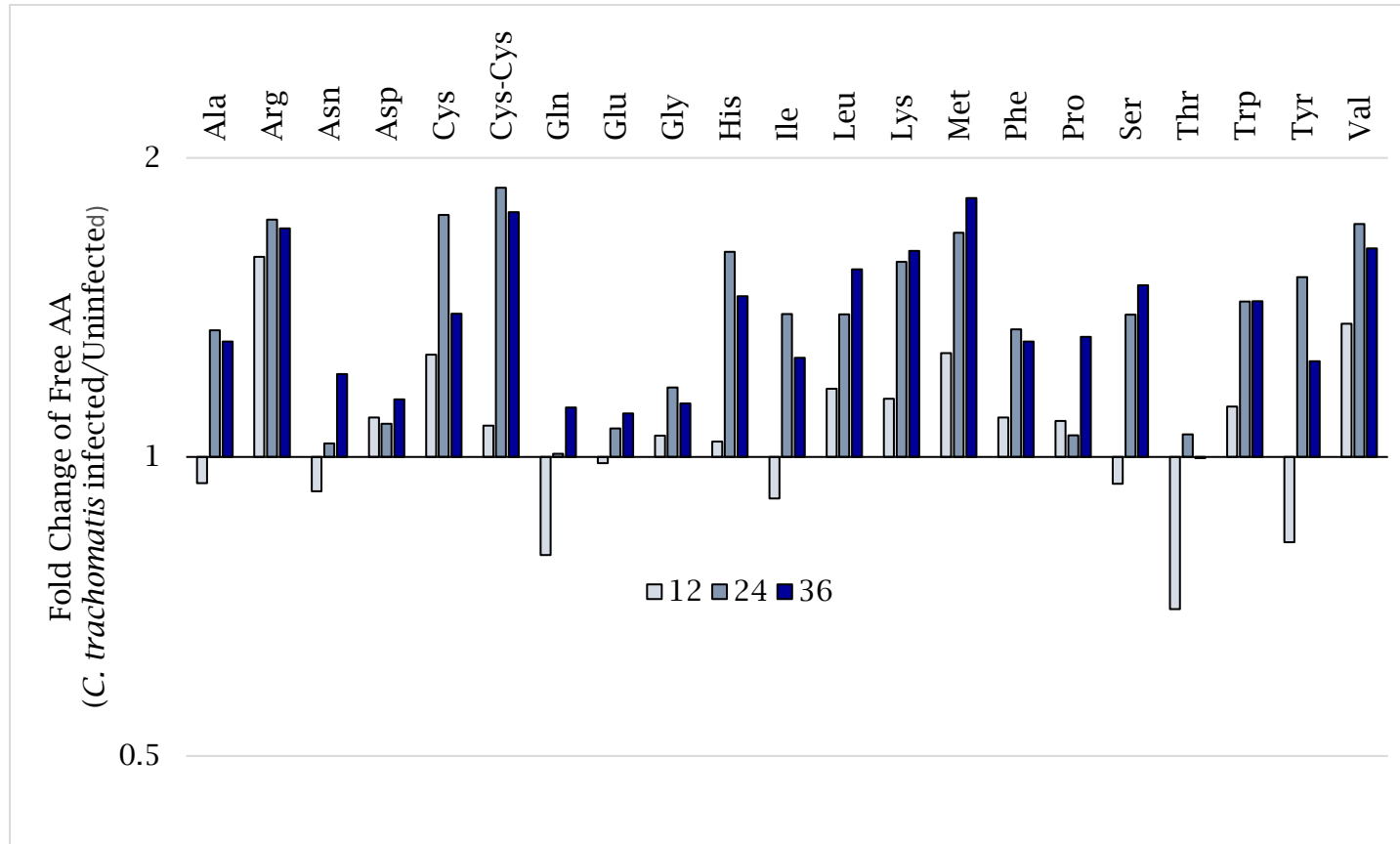


**Figure 32. *C. trachomatis* increases some free AA pools.** Free AA concentrations were compared between uninfected and L2-GFP infected HeLa cells. Pools of some AAs progressively increased in infected cells over time as compared to uninfected HeLa cells. Bars represent the average free AA concentrations of three replicate samples normalized to uninfected HeLa cells.

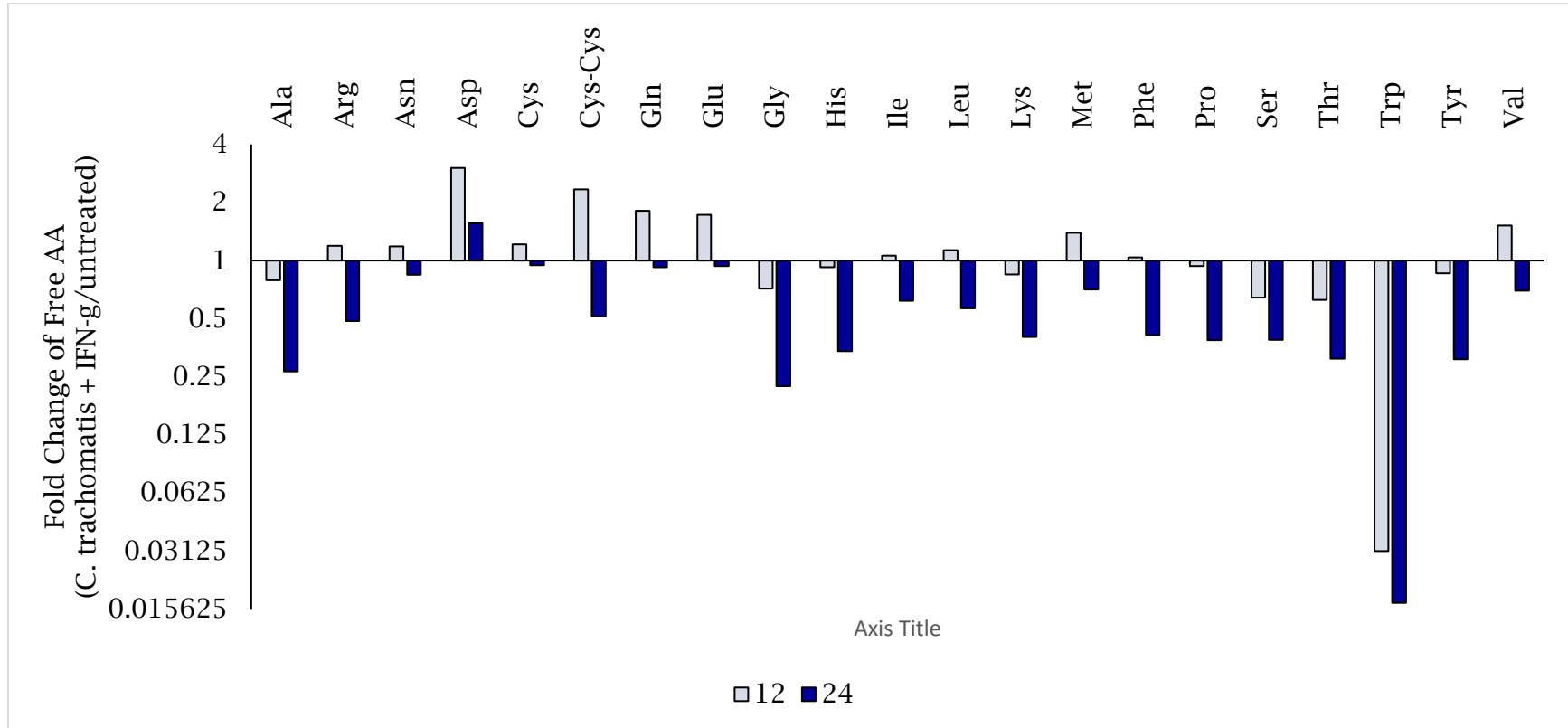


**Figure 33. Free AAs do not increase during IFN- $\gamma$  mediated persistence.** HeLa cells were treated with IFN- $\gamma$  for 24 hours and then infected with L2-GFP. Monolayers were collected, and the concentration of free AAs was determined as described above. Free AAs pools were compared between *C. trachomatis* infected + IFN- $\gamma$  treated HeLa cells and untreated HeLa cells. Most AA pools decreased over time. Bars represent the average free AA concentrations of three replicate samples normalized to uninfected HeLa cells.



## Chapter VI:

### Discussion

#### Caveats in chlamydial genetics

In the past decade, there have been significant advances in the development of chlamydial genetic tools such as transformation, complementation, and allele mapping [40, 100, 135, 136]. Despite these recent advances in chlamydial genetics, several challenges for genetically manipulating *Chlamydia* spp. remain.

CaCl<sub>2</sub> based transformation efficiency of strains containing the endogenous chlamydial plasmid and the transformation of large shuttle plasmids still needs improvement. Curing the endogenous plasmid may improve transformation efficiency, but this is a laborious process that takes many rounds of passaging with sub-inhibitory concentrations of novobiocin [137]. Reducing the shuttle plasmid size by eliminating nonessential *pgp* genes could increase transformation efficiency; however, the side effects of eliminating these genes has not been fully explored [138]. An alternative approach is to use a more efficient method of introducing large plasmids into *C. trachomatis*. A known method of transforming large plasmids into bacteria is electroporation [139]. Additionally, this approach has previously been used to transform *C. trachomatis* with shuttle plasmids [140]. Thus, electroporation may be worth revisiting as a more efficient method of introducing large plasmids into *Chlamydia*.

Complementation in *C. trachomatis* is another genetic tool that is in its infancy. Only three mutant genes have been complemented in *C. trachomatis* [100, 102, 106]. However, it is unknown how the overexpression of chlamydial

proteins affects chlamydial fitness. The problem with existing complementation methods is that they introduce the gene of interest at a non-physiological copy number. Gene dosage toxicity caused by overexpression of proteins has been observed in other organisms [141, 142], suggesting elevated concentrations of chlamydial proteins may be deleterious to chlamydial fitness.

A possible way to mitigate gene dosage toxicity is to use an inducible system. A Tet-inducible GFP system, recently developed in *C. trachomatis*, only expresses GFP when ATc is present in the medium [143]. However, the authors indicate this system is leaky. While this may not affect the results of complementation experiments, the “leakiness” of the Tet-inducible system should be considered when interpreting some results. A possible way of limiting the “leakiness” of the Tet promoter is to increase binding of the tetracycline repressor (TetR) to the shuttle plasmid by introducing additional Tet response elements upstream of the Tet promoter.

Mapping mutant alleles in *C. trachomatis* is challenging. Antibiotic LGT has been used to generate recombinants and map alleles [110, 116]. However, this method has some limitations such as the limited number of chromosomal genes that confer resistance to antibiotics and the fact that antibiotic resistance decreases chlamydial fitness [144, 145]. For example, *rpoB* and *gyrA* are routinely mutated to confer resistance to rifampicin and ofloxacin, respectively [110, 116, 144, 146, 147]. However, mutations in *rpoB* and *gyrA* inhibit growth and development [121, 122]. Additionally, mutating the chlamydial 16S rRNA gene confers resistance to spectinomycin and kasugamycin; however, mutating this gene also decreases chlamydial fitness [124, 148]. Thus, antibiotic LGT is not an ideal mapping strategy for mutants whose phenotype is tied to

development because recombinants generated using this method will have growth defects.

### **Limitations of identifying Sip mutants and mapping persistence genes**

The purpose of the persistence screen was to identify genes *C. trachomatis* uses to enter, maintain, and reactivate from IFN- $\gamma$  mediated persistence. We were only able to isolate six Sip mutants and all of these mutants had mutations in different genes, which suggests that our screen was not saturated. This result is likely linked to the concentration of EMS we used to mutate L2-GFP. We used a low concentration of EMS to mutate L2-GFP because we wanted fewer mutations in each Sip mutant [109]. Having fewer mutations per genome would make mapping the deleterious persistence mutations easier by LGT. Alternatively, mapping could have been facilitated by performing a screen of minimally mutagenized mutants but this would have increased screen size.

We chose not to use antibiotic LGT to map the deleterious persistence mutations in the Sip mutants because the persistence phenotype is related to chlamydial development and we found introducing resistance mutations into *rpoB* and *gyrA* confounded our persistence screen results. To circumvent the limitations of antibiotic LGT we developed a counterselection LGT approach, which does not use selective antibiotic markers. The main premise behind counterselection LGT is that chlamydiae naturally recombine their genomes at a low frequency [149]; however, the trick is enriching for these rare recombinants.

We have noticed counterselection LGT works best with mutants that have strong phenotypes related to EB production. For example, the Sip mutants that we could map (Sip1, Sip2, Sip6) generate almost no infectious progeny following

reactivation from persistence with indole. In contrast, we could not map the Sip mutants that made 25 to 50% of EBs (Sip3, Sip4, Sip5), as compared to L2-GFP (Figure 11). These results suggest the main limitation of counterselection LGT is that enrichment of recombinants depends heavily on mutant EB production, which influences the strength of selection. Additionally, these results indicate a more robust LGT technique needs to be developed to map the deleterious persistence mutation in these types of Sip mutants or the enrichment strategy needs to be more carefully designed. A possible way of improving upon counterselection LGT is to recombine mutants such as Sip3 with other mutants that make fewer EB such as Sip1, or with conditional temperature-sensitive mutants, which make little to no EB at 42°C [111].

#### **Mutant tryptophan synthase in Sip1 may be detrimental**

One of the Sip mutants identified in the persistence screen had a P221S mutation in TrpB (TrpB<sup>P221S</sup>). Isolating a Sip mutant with a mutation in a TS related gene was expected. However, this mutant does not fully reactivate from IFN- $\gamma$  mediated persistence with Trp (Figure 15). This result was surprising because a *C. trachomatis* serovar D mutant that contains a null mutation in TrpB can fully reactivate by Trp from IFN- $\gamma$  mediated persistence [109]. This result suggests that either the persistence model we used differs from the model used by Kari *et al.* or TrpB<sup>P221S</sup> may not ablate the function of TrpB but cause toxicity that is not resolved by the addition of Trp.

In the absence of indole, the  $\beta$ -subunit of TS favors a side reaction that hydrolyzes Ser into pyruvate, ammonia, and H<sub>2</sub>O [126]. Normally, indole is shuttled from the  $\alpha$ -subunit to the active site of the  $\beta$ -subunit through a hydrophobic tunnel. Once at the active site of the  $\beta$ -subunit, indole interacts

with an aminoacrylate intermediate, formed by the  $\beta$ -elimination of OH from Ser, to synthesize Trp [150-152]. However, disrupting the hydrophobic tunnel between the  $\alpha$ - and  $\beta$ -subunits can allow H<sub>2</sub>O molecules to enter the active site of the  $\beta$ -subunit. When this occurs, H<sub>2</sub>O hydrolyzes the aminoacrylate intermediate to produce pyruvate and ammonia [153].

We speculate that the P221S mutation, located on the periphery of TrpB, may cause a conformational change that prevents the shuttling of indole and may allow H<sub>2</sub>O to leak into the active site of the  $\beta$ -subunit. This hypothesis is supported by suppressor analysis, which indicates a suppressor mutation (Q52P), also located on the periphery of TrpB<sup>P221S</sup>, may restore the substrate tunnel (Figure 19). We observed that Sip1 genomes replicate more rapidly during Trp compared to indole reactivation. This result suggests that TrpR (repressor of TS operon) is dampening expression of TrpB<sup>P221S</sup>, resulting in lower ammonia production due to less TS expression. This hypothesis could be test by inducing expression of TrpR during IFN- $\gamma$  mediated persistence may allow Sip1 to reactivate with Trp [74, 109, 154, 155].

#### **CTL0694 may be involved in DNA damage repair**

CTL0694 is an oxidoreductase that is similar to CysJ. In *E. coli*, CysJ forms a multimeric complex with CysI (CysJ<sub>8</sub>CysI<sub>4</sub>) through its FMN domain and plays a critical role in the sulfite reductase pathway. However, CTL0694 lacks an FMN domain, and *C. trachomatis* does not encode an obvious CysI homologue, suggesting CTL0694 is not playing a role in sulfite reduction.

Recently, *E. coli* CysJ has been shown to have a secondary function. By forming a complex with YcbX, the CysJYcbX complex plays a critical role in detoxifying N-hydroxylated nucleobases, such as 6-N-hydroxylaminopurine

(HAP) [156, 157]. Enzymes that detoxify HAP-like nucleobases have been observed in phylogenetically diverse organisms ranging from green algae [158] to humans [159, 160], suggesting most organisms need to detoxify mutagenic nucleobase analogs.

Humans naturally generate HAP-like nucleobase analogs in the presence of oxidative radicals [161]. To reduce incorporation of toxic nucleobase analogs into replicating DNA, humans encode mitochondrial amidoxime reducing component (mARC) 2 which is capable of converting these toxic analogs into non-toxic bases. However, this system may become overwhelmed in the presence of IFN- $\gamma$  because IFN- $\gamma$  is known to increase the generation of oxidative radicals [162]. Thus, during IFN- $\gamma$  mediated persistence, *C. trachomatis* may need to rely on nucleobase detoxifying enzymes to prevent incorporation of toxic nucleobases during genome replication.

We speculate that CTL0694 is playing a critical role in preventing incorporation of toxic nucleobases into replicating genomes during IFN- $\gamma$  mediated persistence, as chlamydiae scavenge purines and pyrimidines from host nucleotide pools [163]. Failure to detoxify these nucleobases in the presence of IFN- $\gamma$  could explain why Sip6 makes smaller inclusions than L2-GFP in IFN- $\gamma$  + excess tryptophan conditions (Figure 16). Additionally, it could explain why Sip6 makes similar numbers of genomes as L2-GFP but produces fewer infectious progeny following reactivation with either Trp or indole (Figure 14). Lastly, we hypothesize that the P105L mutation in Sip6 may be inducing a conformational change that is preventing CTL0694 from binding to a YcbX-like protein. Protein-protein interaction assays could elucidate what CTL0694 binds

during IFN- $\gamma$  mediated persistence and provide insight into what role CTL0694 plays in IFN- $\gamma$   $\pm$  conditions.

### **Chlamydia increase AA during normal development**

Intracellular pathogens are known to encode effectors that increase the concentration of free AA. For example, *Legionella pneumophila* injects Ankyrin-B, a type IV effector, into the host cytoplasm to hijack host polyubiquitination and protein degradation machinery. When this occurs, degradation of host proteins increases, and there is a significant increase in free AA levels [164, 165]. Like *L. pneumophila*, *C. trachomatis* may increase free AA concentrations (Figure 32). However, it is unknown if the increase in free AA pools is caused by *C. trachomatis* or the host response to infection. Many of these host proteins are involved in cellular growth and proliferation [166], suggesting increased host AA transport may play a role in increasing free AA pools. Additionally, these results support the hypothesis that AA transporters, such as CTL0225, are dispensable during normal growth due to sufficient AA concentrations.

### **Amino acid transport in *Chlamydia***

There are only a few AA transporters annotated in the chlamydial genome. The chlamydial MtR homologue TyrP may transport Trp and tyrosine (Tyr), although this has never been verified. The only characterized chlamydial AA transporter is CTL0817, a BrnQ homolog. Chlamydial BrnQ transports Val and may be involved in the transport of Ile, Leu, Phe, and Met, as determined by AA competitive inhibition assays [67]. Notably, chlamydial BrnQ has expanded substrate specificity. In other bacteria, BrnQ only transports BCAA [132, 167], but in *Chlamydia* it may also transport Phe and Met [67]. Our results suggest CTL0225 is another AA transporter with expanded substrate specificity.

### **CTL0225 is likely a component of two AA transport systems**

Sip2 formed significantly smaller inclusions than L2-GFP when treated with a high concentration of Ile, Leu, Ser or Cys. As discussed in the introduction, a high concentration of one AA can block the transport of another similar AA. When competitive inhibition occurs, subsequent AA starvation induces *C. trachomatis* to form small inclusions. Consistent with this, when Sip2 is treated with Ile, Leu, Ala, or Ser it forms small inclusions. However, when Sip2 is co-treated with Val + either Ile or Leu, or Ala + either Ser or Cys, it forms large inclusions. Thus, CTL0225 is likely an AA transporter that is involved in the transport of BCAA, Ala, Cys, and Ser across the chlamydial inner membrane. These AAs have not been previously shown to be transported together [168, 169]. This observation suggests that CTL0225 may be a component of two distinct transporters.

CTL0225 has an upstream paralog, CTL0226. Both of these proteins are predicted to be members of the small neutral amino acid transporter (SNAT) family. This family of proteins is predicted to contain six transmembrane domains [170]. Like SnatA, CTL0226 is also predicted to contain six transmembrane domains.

SnatA family members are also predicted to transport neutral AAs. Recombinant SnatA transports Gly, whose transport can be competitively inhibited by a broad range of neutral AAs. Ala, Ser, and Cys, were amongst the strongest inhibitors (>80%) of Gly transport [171]. These observations are consistent with our competitive inhibition data that suggests CTL0225 may be involved in the transport of Ala, Ser, and Cys in *C. trachomatis*. Interestingly, Ile, Leu, and Val also weakly inhibit Gly transport. However, because most BCAA



transporters are predicted to have 12 transmembrane domains [134, 172], and Sip2 shows distinct competitive inhibition of Val transport by Ile and Leu, we speculate that CTL0225 may form a homodimer or heterodimer with its paralogue CTL0226 to transport BCAA.

SnatA mediated Gly transport was 60% inhibited by Trp [171]. We speculate that CLT0225 may also be involved in the transport of Trp. However, we were unable to test this because high concentrations were cytotoxic to HeLa cells. Additionally, we observed that the Sip2 mutant made fewer inclusions than L2-GFP following reactivation with Trp, suggesting Sip2 could not make proteins critical for survival and reactivation due to the inefficient transport of Trp and the above-mentioned AAs.

#### **IFN- $\gamma$ restricts host free AA pools**

Chlamydiae are auxotrophic for many AA and are highly dependent on their host cells for nutrients [78, 173]. Depleting or limiting the availability of AA, such as BCAA, Trp, and phenylalanine can inhibit chlamydial development and induce entry into persistence [72, 174, 175]. It is unknown how host AAs traverse the inclusion membrane or if chlamydiae actively or passively transport AAs once they are inside the inclusion lumen. However, it is known that cycloheximide can enhance chlamydial development by increasing free cytosolic AAs pools by inhibiting host protein synthesis [173, 176]. Additionally, chlamydiae incorporate radiolabeled AA added to cell culture medium [177]. These data suggest AA concentrations in the host cell cytoplasm can affect AA availability within the chlamydial inclusion. Thus, in AA limiting conditions chlamydial AA transporters may become important.

The broad specificity of AA substrates that CTL0225 may transport suggested AAs are limiting during IFN- $\gamma$  mediated persistence. Our metabolomics data indicate IFN- $\gamma$  treatment causes all free AAs to decrease over time as compared to untreated cells (Figure 30). This observation was surprising because IFN- $\gamma$  has not been shown to deplete AAs other than Trp [178]. Additionally, IFN- $\gamma$  induces autophagy, which maintains critical levels of AAs for cell host survival by degrading host proteins [179]. This is consistent with our metabolomic data, which suggests IFN- $\gamma$  treatment causes the depletion of AAs in HeLa cells over time. Additionally, these results support the hypothesis that *C. trachomatis* may encode multiple AA transporters and effectors to counter AA starvation caused by IFN- $\gamma$  mediated AA depletion.

Overall, we have validated the hypothesis that *C. trachomatis* has mechanisms, besides tryptophan synthesis, to circumvent the effects of IFN- $\gamma$  mediated persistence. We have identified two additional genes that play a role in IFN- $\gamma$  mediated persistence. We hypothesize that CTL0694 plays a critical role in *C. trachomatis* reactivating from persistence because Sip6 makes similar numbers of genomes as L2-GFP but is unable to transition from aberrant RB back into EB. Identifying the protein partner of CTL0694 is paramount to understanding its role during persistence. CTL0225 is an AA transporter with a broad substrate specificity that becomes necessary during AA limiting conditions. Metabolomics data indicate for the first time that free AA pools decreased over time in HeLa cells treated with IFN- $\gamma$  treatment, and that the active or passive mechanisms of AA depletion in eukaryotic cells should be investigated. Additionally, chlamydial effectors that increase AA concentrations should be identified and tested as they may function as nutritional virulence

factors. Lastly, we have described a TS mutant that may produce ammonia instead of Trp. This mutant could test the hypothesis that ocular strains of *Chlamydia* have inactivated TS to avoid ammonia production in the absence of indole.

## **Chapter VII:**

### **Future Directions**

#### **Constructing a larger library to screen for additional Sip mutants**

We identified only 6 Sip mutants from our persistence screen. These mutants did not have overlapping mutations, indicating the screen was unsaturated. A larger mutant library needs to be constructed to identify additional Sip mutants. However, making a larger library by plaque cloning is cost prohibitive, time-consuming, and labor-intensive. Fluorescence-activated cell sorting (FACS) is a fast and robust tool that has been used to sort cells infected with a GFP-expressing *Rickettsia prowazekii* [180] and cells containing fluorescently labeled *C. trachomatis* inclusions [181, 182]. Additionally, FACS has been used to sort single cells into individual wells [183, 184]. These studies indicate that cells infected with GFP-expressing *C. trachomatis* could be quickly sorted into individual wells by FACS to make a large mutant library.

#### **Mapping additional Sip mutant persistence alleles**

We were unable to map the deleterious persistence alleles in Sip3, Sip4, and Sip5 by recombining them with each other (Sip3 x Sip4, Sip3, x Sip5, Sip4 x Sip5). However, it may be possible to map these alleles by altering the recombination scheme. By recombining these mutants with mutants that make little to no EB, such as Sip1, or Sip6 it may be possible to map the remaining persistence alleles. Alternatively, reverse genetic techniques could also be used to map the deleterious persistence alleles.

#### **Determine if autophagy is involved in clearing persistent inclusions**

L2-GFP forms fewer inclusions following reactivation from persistence compared to when it infects untreated HeLa cells. However, it is unknown how

cells are clearing inclusions during persistence. A possible mechanism that cells use to clear inclusions is autophagy. IFN- $\gamma$  induces autophagy and the formation of autophagosomes that localize with lysosomes [185]. Additionally, IFN- $\gamma$  induces expression of human guanylate binding proteins 1 and 2, which associate with the chlamydial inclusion and facilitate fusion with autophagosomes [186]. These studies suggest that during IFN- $\gamma$  mediated persistence cells induce autophagy to clear chlamydial inclusions.

To test the hypothesis that IFN- $\gamma$  is inducing autophagy to clear inclusions during persistence, wild-type and KO cell lines lacking key autophagy proteins, such as ATG7 or ATG16, could be treated with IFN- $\gamma$  and infected with L2-GFP [187]. If autophagy is playing a key role in the clearance of inclusions during persistence, then the autophagy KO cell lines should have more inclusions than wild-type cells.

Fluorescent microscopy could also be used to monitor autophagosome formation in wild-type and autophagy KO cell lines. LC3 is an autophagosomal marker that associates with autophagosomes. If autophagosomes are clearing chlamydial inclusions in wild-type cells during persistence, then LC3 should colocalize with chlamydial inclusions. Conversely, in autophagy KO cell lines LC3 should not colocalize with chlamydial inclusions.

#### **Determine if Sip1 is degrading mutant TrpB**

We have not determined if TrpB<sup>P221S</sup> is being expressed at similar concentrations as wild-type TrpB during persistence. Western blot analysis can be used to compare expression of wild-type and mutant TrpB; however, we do not have an antibody to chlamydial TrpB. Alternatively, we can place an N- or C-terminal His-tag on TrpB and mutant TrpB, and express these proteins from a

shuttle plasmid, using their native promoter, in a  $\Delta trpB$  *C. trachomatis* background. An anti-His antibody could then be used to detect wild-type TrpB, and mutant TrpB by Western blot and relative expression could be quantified by densitometry [188].

#### **Assess if mutant TrpB produces ammonia**

In the absence of indole the  $\beta$ -subunit of TS can slowly hydrolyze Ser to pyruvate and ammonia [153]. We hypothesize that mutant TrpB (TrpB<sup>P221S</sup>) cannot utilize indole and is producing ammonia instead of Trp. Mutant and wild-type TS could be expressed and purified from *E. coli* [155]. By mixing purified wild-type and mutant TS with Ser and indole, ammonia and Trp should be produced [126, 189]. The concentration of ammonia and Trp can be quantified using HPLC [190].

#### **Determine if TrpB<sup>P221S</sup> expression is deleterious for chlamydial growth**

If TrpB<sup>P221S</sup> is deleterious to chlamydial growth, then strains that express TrpB<sup>P221S</sup> should make smaller inclusions and fewer EB than strains expressing TrpB. Wild-type and mutant *trpB* genes, placed under control of an inducible promoter, could be expressed from a shuttle vector in the presence of indole in a  $\Delta trpB$  *C. trachomatis* background. As a control,  $\Delta trpB$  *C. trachomatis*, harboring an empty vector, should be assessed in parallel with TrpB and TrpB<sup>P221S</sup>-expressing strains. If TrpB<sup>P221S</sup> is deleterious to chlamydial growth, then it should make smaller inclusions and less EB than strains expressing wild-type TrpB or the empty vector.

#### **Determine CTL0694 interacting partners and function**

CTL0694 is predicted to be an oxidoreductase that provides reducing electrons to an unknown protein during IFN- $\gamma$  mediated persistence.

Determining what protein CTL0694 binds to will help to define the role of CTL0694 during normal growth and IFN- $\gamma$  mediated persistence. By expressing wild-type and mutant CTL0694 (CTL0694<sup>P105L</sup>) in *C. trachomatis* during normal growth and IFN- $\gamma$  mediated persistence, co-immunoprecipitation assays could be used to isolate proteins that interact with CTL0694. Mass spectrometry and database mining could then be used to identify the interacting protein partners and help us to define the role CTL0694 plays during persistence. Additionally, we could also compare the binding partners between wild-type and CTL0694<sup>P105L</sup> to determine if the P105L mutation disrupts protein-protein interactions.

#### **Determine if Sip2 expresses CTL0225<sup>G77E</sup> during IFN- $\gamma$ mediated persistence**

Loss of the third transmembrane domain of CTL0225 likely inhibits AA transport function. However, it may be possible that the G77E mutation induces transcriptional degradation, translational silencing, or post-translational degradation of mutant CTL0225 (CTL0225<sup>G77E</sup>). Quantitative PCR can be used to detect mutant CTL0225 mRNA expression levels to confirm that CTL0225<sup>G77E</sup> is still being transcribed throughout normal development and during IFN- $\gamma$  mediated persistence. However, since we do not have an antibody to CTL0225, we cannot readily determine if CTL0225<sup>G77E</sup> is post-translationally degraded. An alternative approach to creating an antibody to CTL0225 would be to fuse an epitope tag to the N- or C- terminal end of CTL0225<sup>G77E</sup> and express it under its endogenous promoter from a shuttle plasmid. If this protein is being expressed and not degraded, it should be detectable by Western blot.

While it is suggestive that the G77E mutation causes the loss of function of CTL0225, it may be possible that this mutation causes translational silencing or post-translational degradation of mutant CTL0225. Quantitative PCR can be

used to detect mutant CTL0225 mRNA expression levels to confirm that CTL0225<sup>G77E</sup> is still being transcribed throughout normal development and during IFN- $\gamma$  mediated persistence. However, determining if Sip2 is post-translationally degrading CTL0225<sup>G77E</sup> is more challenging since we do not have a CTL0225 antibody. As an alternative approach to making an antibody, we could fuse an N- or C- terminal epitope tag to CTL0225 and CTL0225<sup>G77E</sup> and express these proteins under their endogenous promoter from a shuttle plasmid. If CTL0225<sup>G77E</sup> is being expressed and not degraded, it should be detectable by Western blot. Additionally, we can determine if CTL0225 forms a homodimer or heterodimer with CTL0226 by comparing native and SDS-PAGE gels.

#### **Confirm CTL0225 transports amino acids**

We hypothesize that the CTL0225 transports Ser, Cys, and Ala, while a homodimer or heterodimer of CTL0225 + CTL0226 is responsible for the transport of Leu, Ile, and Val. To directly assess the substrate specificity of those these proteins we could use radiolabeled (C<sup>14</sup>) AA in AA transport assays. We can clone these chlamydial genes into *E. coli* expression vectors and then transform these recombinant plasmids into strains of *E. coli* that cannot transport Ser or BCAA. By assessing radioactivity uptake in competitive inhibition assays with “cold AA,” we can determine how well these proteins transport each AA.

#### **Determine if Sip2 is sensitive to low concentrations of AA**

Metabolomics analysis of IFN- $\gamma$  treated HeLa cells suggest AA are limiting during IFN- $\gamma$  mediated persistence. Having multiple AA transporters may help to circumvent the effects of low AA concentrations. To test the hypothesis, HeLa cells could be incubated in DMEM-10 with no AA for 24 hours, to deplete AA,



and then infected with L2-GFP, Sip2, or rSip2. Inclusion sizes and EB production can then be compared at 24, 36, and 48, hpi. If Sip2 makes smaller inclusions and less EB than L2-GFP or rSip2, then it would suggest that Sip2 is not able to fully reactivate from persistence because of AA starvation and because it expresses a non-functional CTL0225.

## REFERENCES

1. Webb SG. Prehistoric eye disease (trachoma?) in Australian aborigines. *Am J Phys Anthropol.* 1990;81(1):91-100. doi: 10.1002/ajpa.1330810110. PubMed PMID: 2405692.
2. Nunn JF. *Ancient Egyptian Medicine*: University of Oklahoma Press; 2002.
3. Boldt J. *Trachoma*. London: Hodder & Stoughton; 1904.
4. Markel H. "The eyes have it": trachoma, the perception of disease, the United States Public Health Service, and the American Jewish immigration experience, 1897-1924. *Bull Hist Med.* 2000;74(3):525-60. PubMed PMID: 11016097.
5. Halberstädter L, von Prowazek, S. Zur Aetiologie des Trachoms. *Deutsche medizinische Wochenschrift.* 1907;33:1285-7.
6. Lindner K. Zur Trachomforschung. *Z Augenheilk.* 1909;22(547).
7. Halberstädter L, von Prowazek, S. Ueber Chlamydozoen befunde bei Blennorrhoea neonatorum non gonorrhoeica. *Berliner Klinische Wochenschrift.* 1909;46(1839).
8. Lindner K. Zur Atilogie der gonokokkenfreien Urethritis. *Wien klin Wochschr.* 1910;23(283).
9. Fritsch H, Hofstätter A., Lindner, K. Experimentelle Untersuchungen über die Beziehungen zwischen Einschlüssblennorrhoe und Trachom. *Z Augenheilk.* 1910;31(475).
10. Al-Rifai KMJ. Trachoma through history. *International Ophthalmology.* 1988;12(1):9-14. doi: 10.1007/bf00133774.
11. W.H.O. Trachoma: Fact Sheet: World Health Organization; 2016 [updated July 2016; cited 2016 September]. Available from: <http://www.who.int/mediacentre/factsheets/fs382/en/>.
12. TrachomaAtlas. Trachoma Atlas 2016 [cited 2016 September]. Available from: <http://www.trachomaatlas.org/>.
13. W.H.O. Sexually transmitted infections (STIs) Fact Sheet: World Health Organization; 2016 [updated August 2016; cited 2016 September]. Available from: <http://www.who.int/mediacentre/factsheets/fs110/en/>.
14. Carey AJ, Beagley KW. Chlamydia trachomatis, a hidden epidemic: effects on female reproduction and options for treatment. *Am J Reprod Immunol.* 2010;63(6):576-86. doi: 10.1111/j.1600-0897.2010.00819.x. PubMed PMID: 20192953.
15. Cunningham KA, Beagley KW. Male genital tract chlamydial infection: implications for pathology and infertility. *Biol Reprod.* 2008;79(2):180-9. doi: 10.1095/biolreprod.108.067835. PubMed PMID: 18480466.
16. Faro S. Chlamydia trachomatis infection in women. *J Reprod Med.* 1985;30(3 Suppl):273-8. PubMed PMID: 4020784.
17. Darville T, Hiltke TJ. Pathogenesis of genital tract disease due to Chlamydia trachomatis. *J Infect Dis.* 2010;201 Suppl 2:S114-25. PubMed PMID: 20524234; PubMed Central PMCID: PMC3150527.
18. Cates W, Jr., Wasserheit JN. Genital chlamydial infections: epidemiology and reproductive sequelae. *Am J Obstet Gynecol.* 1991;164(6 Pt 2):1771-81. PubMed PMID: 2039031.
19. Wollenhaupt HJ, Schneider C, Zeidler H, Krech T, Kuntz BM. [Clinical and serological characterization of Chlamydia-induced arthritis]. *Dtsch Med*

- Wochenschr. 1989;114(50):1949-54. doi: 10.1055/s-2008-1066852. PubMed PMID: 2598790.
20. Wollenhaupt J, Schmitz E, Zeidler H. [Chlamydia-induced arthritis: diagnosis--follow-up--therapy]. *Wien Med Wochenschr.* 1990;140(12):302-6. PubMed PMID: 2204211.
  21. Waalboer R, van der Snoek EM, van der Meijden WI, Mulder PG, Ossewaarde JM. Analysis of rectal *Chlamydia trachomatis* serovar distribution including L2 (lymphogranuloma venereum) at the Erasmus MC STI clinic, Rotterdam. *Sex Transm Infect.* 2006;82(3):207-11. doi: 10.1136/sti.2005.018580. PubMed PMID: 16731669; PubMed Central PMCID: PMCPMC2564739.
  22. van Liere GA, Hoebe CJ, Wolffs PF, Dukers-Muijers NH. High co-occurrence of anorectal chlamydia with urogenital chlamydia in women visiting an STI clinic revealed by routine universal testing in an observational study; a recommendation towards a better anorectal chlamydia control in women. *BMC Infect Dis.* 2014;14:274. doi: 10.1186/1471-2334-14-274. PubMed PMID: 24885306; PubMed Central PMCID: PMCPMC4032161.
  23. Rank RG, Yeruva L. Hidden in plain sight: chlamydial gastrointestinal infection and its relevance to persistence in human genital infection. *Infect Immun.* 2014;82(4):1362-71. doi: 10.1128/IAI.01244-13. PubMed PMID: 24421044; PubMed Central PMCID: PMCPMC3993372.
  24. Kong FY, Tabrizi SN, Fairley CK, Vodstrcil LA, Huston WM, Chen M, et al. The efficacy of azithromycin and doxycycline for the treatment of rectal chlamydia infection: a systematic review and meta-analysis. *J Antimicrob Chemother.* 2015;70(5):1290-7. doi: 10.1093/jac/dku574. PubMed PMID: 25637520.
  25. Matsumoto A. Structural characteristics of chlamydial bodies. *Chlamydia* Mo, editor. Boca Raton, FL: CRC Press; 1988. 25 p.
  26. Caldwell HD, Kromhout J, Schachter J. Purification and partial characterization of the major outer membrane protein of *Chlamydia trachomatis*. *Infect Immun.* 1981;31(3):1161-76. PubMed PMID: 7228399; PubMed Central PMCID: PMCPMC351439.
  27. Newhall WJ, Jones RB. Disulfide-linked oligomers of the major outer membrane protein of chlamydiae. *Journal of bacteriology.* 1983;154(2):998-1001. PubMed PMID: 6841322; PubMed Central PMCID: PMCPMC217558.
  28. Hatch TP, Vance DW, Jr., Al-Hossainy E. Identification of a major envelope protein in *Chlamydia* spp. *Journal of bacteriology.* 1981;146(1):426-9. PubMed PMID: 7217005; PubMed Central PMCID: PMCPMC217103.
  29. Matsumoto A. Fine structures of cell envelopes of *Chlamydia* organisms as revealed by freeze-etching and negative staining techniques. *Journal of bacteriology.* 1973;116(3):1355-63. PubMed PMID: 4127629; PubMed Central PMCID: PMCPMC246495.
  30. Betts HJ, Twiggs LE, Sal MS, Wyrick PB, Fields KA. Bioinformatic and biochemical evidence for the identification of the type III secretion system needle protein of *Chlamydia trachomatis*. *Journal of bacteriology.* 2008;190(5):1680-90. doi: 10.1128/JB.01671-07. PubMed PMID: 18165300; PubMed Central PMCID: PMCPMC2258694.

31. Clifton DR, Fields KA, Grieshaber SS, Dooley CA, Fischer ER, Mead DJ, et al. A chlamydial type III translocated protein is tyrosine-phosphorylated at the site of entry and associated with recruitment of actin. *Proc Natl Acad Sci U S A.* 2004;101(27):10166-71. doi: 10.1073/pnas.0402829101. PubMed PMID: 15199184; PubMed Central PMCID: PMCPMC454183.
32. Nans A, Saibil HR, Hayward RD. Pathogen-host reorganization during Chlamydia invasion revealed by cryo-electron tomography. *Cell Microbiol.* 2014;16(10):1457-72. doi: 10.1111/cmi.12310. PubMed PMID: 24809274; PubMed Central PMCID: PMCPMC4336559.
33. Engel J. Tarp and Arp: How Chlamydia induces its own entry. *Proc Natl Acad Sci U S A.* 2004;101(27):9947-8. doi: 10.1073/pnas.0403633101. PubMed PMID: 15226494; PubMed Central PMCID: PMCPMC454194.
34. Louis C, Nicolas G, Eb F, Lefebvre JF, Orfila J. Modifications of the envelope of Chlamydia psittaci during its developmental cycle: freeze-fracture study of complementary replicas. *Journal of bacteriology.* 1980;141(2):868-75. PubMed PMID: 7364718; PubMed Central PMCID: PMCPMC293698.
35. Nicholson TL, Olinger L, Chong K, Schoolnik G, Stephens RS. Global stage-specific gene regulation during the developmental cycle of Chlamydia trachomatis. *Journal of bacteriology.* 2003;185(10):3179-89. PubMed PMID: 12730178; PubMed Central PMCID: PMCPMC154084.
36. Shaw EI, Dooley CA, Fischer ER, Scidmore MA, Fields KA, Hackstadt T. Three temporal classes of gene expression during the Chlamydia trachomatis developmental cycle. *Molecular microbiology.* 2000;37(4):913-25. PubMed PMID: 10972811.
37. Belland RJ, Zhong G, Crane DD, Hogan D, Sturdevant D, Sharma J, et al. Genomic transcriptional profiling of the developmental cycle of Chlamydia trachomatis. *Proc Natl Acad Sci U S A.* 2003;100(14):8478-83. doi: 10.1073/pnas.1331135100. PubMed PMID: 12815105; PubMed Central PMCID: PMCPMC166254.
38. Rockey DD, Rosquist JL. Protein antigens of Chlamydia psittaci present in infected cells but not detected in the infectious elementary body. *Infect Immun.* 1994;62(1):106-12. PubMed PMID: 8262615; PubMed Central PMCID: PMCPMC186074.
39. Bannantine JP, Griffiths RS, Viratyosin W, Brown WJ, Rockey DD. A secondary structure motif predictive of protein localization to the chlamydial inclusion membrane. *Cell Microbiol.* 2000;2(1):35-47. PubMed PMID: 11207561.
40. Bauler LD, Hackstadt T. Expression and targeting of secreted proteins from Chlamydia trachomatis. *Journal of bacteriology.* 2014;196(7):1325-34. doi: 10.1128/JB.01290-13. PubMed PMID: 24443531; PubMed Central PMCID: PMCPMC3993338.
41. Rzomp KA, Scholtes LD, Briggs BJ, Whittaker GR, Scidmore MA. Rab GTPases are recruited to chlamydial inclusions in both a species-dependent and species-independent manner. *Infect Immun.* 2003;71(10):5855-70. PubMed PMID: 14500507; PubMed Central PMCID: PMCPMC201052.
42. Grieshaber SS, Grieshaber NA, Hackstadt T. Chlamydia trachomatis uses host cell dynein to traffic to the microtubule-organizing center in a p50

- dynamitin-independent process. *J Cell Sci.* 2003;116(Pt 18):3793-802. doi: 10.1242/jcs.00695. PubMed PMID: 12902405.
43. Mital J, Lutter EI, Barger AC, Dooley CA, Hackstadt T. Chlamydia trachomatis inclusion membrane protein CT850 interacts with the dynein light chain DYNLT1 (Tctex1). *Biochem Biophys Res Commun.* 2015;462(2):165-70. doi: 10.1016/j.bbrc.2015.04.116. PubMed PMID: 25944661; PubMed Central PMCID: PMC4449824.
  44. Saka HA, Thompson JW, Chen YS, Kumar Y, Dubois LG, Moseley MA, et al. Quantitative proteomics reveals metabolic and pathogenic properties of Chlamydia trachomatis developmental forms. *Molecular microbiology.* 2011;82(5):1185-203. doi: 10.1111/j.1365-2958.2011.07877.x. PubMed PMID: 22014092; PubMed Central PMCID: PMC3225693.
  45. Hackstadt T, Rockey DD, Heinzen RA, Scidmore MA. Chlamydia trachomatis interrupts an exocytic pathway to acquire endogenously synthesized sphingomyelin in transit from the Golgi apparatus to the plasma membrane. *EMBO J.* 1996;15(5):964-77. PubMed PMID: 8605892; PubMed Central PMCID: PMC449991.
  46. Moore ER. Sphingolipid trafficking and purification in Chlamydia trachomatis-infected cells. *Curr Protoc Microbiol.* 2012;Chapter 11:Unit 11A 2. doi: 10.1002/9780471729259.mc11a02s27. PubMed PMID: 23184593; PubMed Central PMCID: PMC3536446.
  47. Carabeo RA, Mead DJ, Hackstadt T. Golgi-dependent transport of cholesterol to the Chlamydia trachomatis inclusion. *Proc Natl Acad Sci U S A.* 2003;100(11):6771-6. doi: 10.1073/pnas.1131289100. PubMed PMID: 12743366; PubMed Central PMCID: PMC164522.
  48. Matsumoto A, Manire GP. Electron microscopic observations on the effects of penicillin on the morphology of Chlamydia psittaci. *Journal of bacteriology.* 1970;101(1):278-85. PubMed PMID: 5413965; PubMed Central PMCID: PMC250478.
  49. Abdelrahman Y, Ouellette SP, Belland RJ, Cox JV. Polarized Cell Division of Chlamydia trachomatis. *PLoS Pathog.* 2016;12(8):e1005822. doi: 10.1371/journal.ppat.1005822. PubMed PMID: 27505160; PubMed Central PMCID: PMC4978491.
  50. Liechti G, Kuru E, Packiam M, Hsu YP, Tekkam S, Hall E, et al. Pathogenic Chlamydia Lack a Classical Sacculus but Synthesize a Narrow, Mid-cell Peptidoglycan Ring, Regulated by MreB, for Cell Division. *PLoS Pathog.* 2016;12(5):e1005590. doi: 10.1371/journal.ppat.1005590. PubMed PMID: 27144308; PubMed Central PMCID: PMC4856321.
  51. Rosario CJ, Tan M. The early gene product EUO is a transcriptional repressor that selectively regulates promoters of Chlamydia late genes. *Molecular microbiology.* 2012;84(6):1097-107. doi: 10.1111/j.1365-2958.2012.08077.x. PubMed PMID: 22624851; PubMed Central PMCID: PMC3544401.
  52. Yu HH, Tan M. Sigma28 RNA polymerase regulates hctB, a late developmental gene in Chlamydia. *Molecular microbiology.* 2003;50(2):577-84. PubMed PMID: 14617180; PubMed Central PMCID: PMC2810255.
  53. Hybiske K, Stephens RS. Mechanisms of host cell exit by the intracellular bacterium Chlamydia. *Proc Natl Acad Sci U S A.* 2007;104(27):11430-5.

- doi: 10.1073/pnas.0703218104. PubMed PMID: 17592133; PubMed Central PMCID: PMCPMC2040915.
54. Yang C, Starr T, Song L, Carlson JH, Sturdevant GL, Beare PA, et al. Chlamydial Lytic Exit from Host Cells Is Plasmid Regulated. *MBio*. 2015;6(6):e01648-15. doi: 10.1128/mBio.01648-15. PubMed PMID: 26556273; PubMed Central PMCID: PMCPMC4659467.
  55. Chin E, Kirker K, Zuck M, James G, Hybiske K. Actin recruitment to the Chlamydia inclusion is spatiotemporally regulated by a mechanism that requires host and bacterial factors. *PLoS One*. 2012;7(10):e46949. doi: 10.1371/journal.pone.0046949. PubMed PMID: 23071671; PubMed Central PMCID: PMCPMC3469565.
  56. Lutter EI, Barger AC, Nair V, Hackstadt T. Chlamydia trachomatis inclusion membrane protein CT228 recruits elements of the myosin phosphatase pathway to regulate release mechanisms. *Cell Rep*. 2013;3(6):1921-31. doi: 10.1016/j.celrep.2013.04.027. PubMed PMID: 23727243; PubMed Central PMCID: PMCPMC3700685.
  57. Gerard HC, Krause-Opatz B, Wang Z, Rudy D, Rao JP, Zeidler H, et al. Expression of Chlamydia trachomatis genes encoding products required for DNA synthesis and cell division during active versus persistent infection. *Molecular microbiology*. 2001;41(3):731-41. PubMed PMID: 11532140.
  58. Byrne GI, Lehmann LK, Landry GJ. Induction of tryptophan catabolism is the mechanism for gamma-interferon-mediated inhibition of intracellular Chlamydia psittaci replication in T24 cells. *Infect Immun*. 1986;53(2):347-51. PubMed PMID: 3089936; PubMed Central PMCID: PMCPMC260881.
  59. Ghuysen JM, Goffin C. Lack of cell wall peptidoglycan versus penicillin sensitivity: new insights into the chlamydial anomaly. *Antimicrob Agents Chemother*. 1999;43(10):2339-44. PubMed PMID: 10508003; PubMed Central PMCID: PMCPMC89479.
  60. Chopra I, Storey C, Falla TJ, Pearce JH. Antibiotics, peptidoglycan synthesis and genomics: the chlamydial anomaly revisited. *Microbiology*. 1998;144 ( Pt 10):2673-8. doi: 10.1099/00221287-144-10-2673. PubMed PMID: 9802008.
  61. Raulston JE. Response of Chlamydia trachomatis serovar E to iron restriction in vitro and evidence for iron-regulated chlamydial proteins. *Infection and Immunity*. 1997;65(11):4539-47. PubMed PMID: PMC175652.
  62. Lloyd JB, Cable H, Rice-Evans C. Evidence that desferrioxamine cannot enter cells by passive diffusion. *Biochem Pharmacol*. 1991;41(9):1361-3. PubMed PMID: 2018567.
  63. Thompson CC, Carabeo RA. An optimal method of iron starvation of the obligate intracellular pathogen, Chlamydia trachomatis. *Front Microbiol*. 2011;2:20. doi: 10.3389/fmicb.2011.00020. PubMed PMID: 21687412; PubMed Central PMCID: PMCPMC3109288.
  64. Karayiannis P, Hobson D. Amino acid requirements of a Chlamydia trachomatis genital strain in McCoy cell cultures. *J Clin Microbiol*. 1981;13(3):427-32. PubMed PMID: 7240385; PubMed Central PMCID: PMCPMC273808.
  65. Kuo CC, Grayston JT. Amino acid requirements for growth of Chlamydia pneumoniae in cell cultures: growth enhancement by lysine or

- methionine depletion. *Journal of Clinical Microbiology*. 1990;28(6):1098-100. PubMed PMID: PMC267883.
66. Coles AM, Pearce JH. Regulation of *Chlamydia psittaci* (strain guinea pig inclusion conjunctivitis) growth in McCoy cells by amino acid antagonism. *J Gen Microbiol*. 1987;133(3):701-8. doi: 10.1099/00221287-133-3-701. PubMed PMID: 3655729.
  67. Braun PR, Al-Younes H, Gussmann J, Klein J, Schneider E, Meyer TF. Competitive inhibition of amino acid uptake suppresses chlamydial growth: involvement of the chlamydial amino acid transporter BrnQ. *Journal of bacteriology*. 2008;190(5):1822-30. doi: 10.1128/JB.01240-07. PubMed PMID: 18024516; PubMed Central PMCID: PMCPMC2258683.
  68. Romano JD, de Beaumont C, Carrasco JA, Ehrenman K, Bavoil PM, Coppens I. A novel co-infection model with *Toxoplasma* and *Chlamydia trachomatis* highlights the importance of host cell manipulation for nutrient scavenging. *Cell Microbiol*. 2013;15(4):619-46. doi: 10.1111/cmi.12060. PubMed PMID: 23107293; PubMed Central PMCID: PMCPMC3625693.
  69. Beatty WL, Byrne GI, Morrison RP. Morphologic and antigenic characterization of interferon gamma-mediated persistent *Chlamydia trachomatis* infection in vitro. *Proceedings of the National Academy of Sciences of the United States of America*. 1993;90(9):3998-4002. PubMed PMID: 8387206; PubMed Central PMCID: PMCPMC46433.
  70. Thomas SM, Garrity LF, Brandt CR, Schobert CS, Feng GS, Taylor MW, et al. IFN-gamma-mediated antimicrobial response. Indoleamine 2,3-dioxygenase-deficient mutant host cells no longer inhibit intracellular *Chlamydia* spp. or *Toxoplasma* growth. *Journal of immunology* (Baltimore, Md : 1950). 1993;150(12):5529-34. PubMed PMID: 8515074.
  71. Beatty WL, Morrison RP, Byrne GI. Reactivation of persistent *Chlamydia trachomatis* infection in cell culture. *Infect Immun*. 1995;63(1):199-205. PubMed PMID: 7806358; PubMed Central PMCID: PMCPMC172978.
  72. Leonhardt RM, Lee SJ, Kavathas PB, Cresswell P. Severe tryptophan starvation blocks onset of conventional persistence and reduces reactivation of *Chlamydia trachomatis*. *Infect Immun*. 2007;75(11):5105-17. doi: 10.1128/IAI.00668-07. PubMed PMID: 17724071; PubMed Central PMCID: PMCPMC2168275.
  73. Yasui H, Takai K, Yoshida R, Hayaishi O. Interferon enhances tryptophan metabolism by inducing pulmonary indoleamine 2,3-dioxygenase: its possible occurrence in cancer patients. *Proceedings of the National Academy of Sciences of the United States of America*. 1986;83(17):6622-6. PubMed PMID: 2428037; PubMed Central PMCID: PMCPMC386556.
  74. Caldwell HD, Wood H, Crane D, Bailey R, Jones RB, Mabey D, et al. Polymorphisms in *Chlamydia trachomatis* tryptophan synthase genes differentiate between genital and ocular isolates. *J Clin Invest*. 2003;111(11):1757-69. doi: 10.1172/JCI17993. PubMed PMID: 12782678; PubMed Central PMCID: PMCPMC156111.
  75. Fehlner-Gardiner C, Roshick C, Carlson JH, Hughes S, Belland RJ, Caldwell HD, et al. Molecular basis defining human *Chlamydia trachomatis* tissue tropism. A possible role for tryptophan synthase. *J Biol Chem*. 2002;277(30):26893-903. doi: 10.1074/jbc.M203937200. PubMed PMID: 12011099.

76. Carlson JH, Porcella SF, McClarty G, Caldwell HD. Comparative genomic analysis of *Chlamydia trachomatis* oculotropic and genitotropic strains. *Infect Immun*. 2005;73(10):6407-18. doi: 10.1128/IAI.73.10.6407-6418.2005. PubMed PMID: 16177312; PubMed Central PMCID: PMC1230933.
77. Harris SR, Clarke IN, Seth-Smith HM, Solomon AW, Cutcliffe LT, Marsh P, et al. Whole-genome analysis of diverse *Chlamydia trachomatis* strains identifies phylogenetic relationships masked by current clinical typing. *Nat Genet*. 2012;44(4):413-9. S1. doi: 10.1038/ng.2214. PubMed PMID: 22406642; PubMed Central PMCID: PMC3378690.
78. Stephens RS, Kalman S, Lammel C, Fan J, Marathe R, Aravind L, et al. Genome sequence of an obligate intracellular pathogen of humans: *Chlamydia trachomatis*. *Science*. 1998;282(5389):754-9. PubMed PMID: 9784136.
79. Sasaki-Imamura T, Yoshida Y, Suwabe K, Yoshimura F, Kato H. Molecular basis of indole production catalyzed by tryptophanase in the genus *Prevotella*. *FEMS microbiology letters*. 2011;322(1):51-9. doi: 10.1111/j.1574-6968.2011.02329.x. PubMed PMID: 21658104.
80. Romanik M, Martirosian G, Wojciechowska-Wieja A, Cieslik K, Kazmierczak W. [Co-occurrence of indole-producing bacterial strains in the vagina of women infected with *Chlamydia trachomatis*]. *Ginekologia polska*. 2007;78(8):611-5. PubMed PMID: 18050609.
81. Lloyd D, Lauritsen FR, Degn H. The parasitic flagellates *Trichomonas vaginalis* and *Tritrichomonas foetus* produce indole and dimethyl disulphide: direct characterization by membrane inlet tandem mass spectrometry. *Journal of general microbiology*. 1991;137(7):1743-7. doi: 10.1099/00221287-137-7-1743. PubMed PMID: 1955862.
82. Belland RJ, Nelson DE, Virok D, Crane DD, Hogan D, Sturdevant D, et al. Transcriptome analysis of chlamydial growth during IFN-gamma-mediated persistence and reactivation. *Proc Natl Acad Sci U S A*. 2003;100(26):15971-6. doi: 10.1073/pnas.2535394100. PubMed PMID: 14673075; PubMed Central PMCID: PMC307677.
83. Hogan RJ, Mathews SA, Mukhopadhyay S, Summersgill JT, Timms P. Chlamydial persistence: beyond the biphasic paradigm. *Infect Immun*. 2004;72(4):1843-55. PubMed PMID: 15039303; PubMed Central PMCID: PMC375192.
84. Wyrick PB. *Chlamydia trachomatis* persistence in vitro: an overview. *J Infect Dis*. 2010;201 Suppl 2:S88-95. doi: 10.1086/652394. PubMed PMID: 20470046; PubMed Central PMCID: PMC32878585.
85. Klos A, Thalmann J, Peters J, Gerard HC, Hudson AP. The transcript profile of persistent *Chlamydia pneumoniae* in vitro depends on the means by which persistence is induced. *FEMS Microbiol Lett*. 2009;291(1):120-6. Epub 2008/12/17. doi: 10.1111/j.1574-6968.2008.01446.x. PubMed PMID: 19077059.
86. Di Pietro M, Tramonti A, De Santis F, De Biase D, Schiavoni G, Filardo S, et al. Analysis of gene expression in penicillin G induced persistence of *Chlamydia pneumoniae*. *J Biol Regul Homeost Agents*. 2012;26(2):277-84. PubMed PMID: 22824742.



87. Papp JR, Shewen PE. Localization of chronic *Chlamydia psittaci* infection in the reproductive tract of sheep. *J Infect Dis.* 1996;174(6):1296-302. PubMed PMID: 8940221.
88. Yang YS, Kuo CC, Chen WJ. Reactivation of *Chlamydia trachomatis* lung infection in mice by cortisone. *Infect Immun.* 1983;39(2):655-8. PubMed PMID: 6832814; PubMed Central PMCID: PMCPMC348001.
89. Patton DL, Askienazy-Elbhar M, Henry-Suchet J, Campbell LA, Cappuccio A, Tannous W, et al. Detection of *Chlamydia trachomatis* in fallopian tube tissue in women with postinfectious tubal infertility. *Am J Obstet Gynecol.* 1994;171(1):95-101. PubMed PMID: 8030740.
90. Nanagara R, Li F, Beutler A, Hudson A, Schumacher HR, Jr. Alteration of *Chlamydia trachomatis* biologic behavior in synovial membranes. Suppression of surface antigen production in reactive arthritis and Reiter's syndrome. *Arthritis Rheum.* 1995;38(10):1410-7. PubMed PMID: 7575691.
91. Skowasch D, Yeghiazaryan K, Schrempf S, Golubnitschaja O, Welsch U, Preusse CJ, et al. Persistence of *Chlamydia pneumoniae* in degenerative aortic valve stenosis indicated by heat shock protein 60 homologues. *J Heart Valve Dis.* 2003;12(1):68-75. PubMed PMID: 12578339.
92. Lewis ME, Belland RJ, AbdelRahman YM, Beatty WL, Aiyar AA, Zea AH, et al. Morphologic and molecular evaluation of *Chlamydia trachomatis* growth in human endocervix reveals distinct growth patterns. *Front Cell Infect Microbiol.* 2014;4:71. doi: 10.3389/fcimb.2014.00071. PubMed PMID: 24959423; PubMed Central PMCID: PMCPMC4050528.
93. Read TD, Brunham RC, Shen C, Gill SR, Heidelberg JF, White O, et al. Genome sequences of *Chlamydia trachomatis* MoPn and *Chlamydia pneumoniae* AR39. *Nucleic Acids Res.* 2000;28(6):1397-406. PubMed PMID: 10684935; PubMed Central PMCID: PMCPMC111046.
94. Voigt A, Schofl G, Saluz HP. The *Chlamydia psittaci* genome: a comparative analysis of intracellular pathogens. *PLoS One.* 2012;7(4):e35097. doi: 10.1371/journal.pone.0035097. PubMed PMID: 22506068; PubMed Central PMCID: PMCPMC3323650.
95. Kalman S, Mitchell W, Marathe R, Lammel C, Fan J, Hyman RW, et al. Comparative genomes of *Chlamydia pneumoniae* and *C. trachomatis*. *Nat Genet.* 1999;21(4):385-9. doi: 10.1038/7716. PubMed PMID: 10192388.
96. Tam JE, Davis CH, Wyrick PB. Expression of recombinant DNA introduced into *Chlamydia trachomatis* by electroporation. *Can J Microbiol.* 1994;40(7):583-91. PubMed PMID: 8076253.
97. Wang Y, Kahane S, Cutcliffe LT, Skilton RJ, Lambden PR, Clarke IN. Development of a transformation system for *Chlamydia trachomatis*: restoration of glycogen biosynthesis by acquisition of a plasmid shuttle vector. *PLoS Pathog.* 2011;7(9):e1002258. doi: 10.1371/journal.ppat.1002258. PubMed PMID: 21966270; PubMed Central PMCID: PMCPMC3178582.
98. Song L, Carlson JH, Whitmire WM, Kari L, Virtaneva K, Sturdevant DE, et al. *Chlamydia trachomatis* plasmid-encoded Pgp4 is a transcriptional regulator of virulence-associated genes. *Infect Immun.* 2013;81(3):636-44. doi: 10.1128/IAI.01305-12. PubMed PMID: 23319558; PubMed Central PMCID: PMCPMC3584862.

99. Kari L, Whitmire WM, Olivares-Zavaleta N, Goheen MM, Taylor LD, Carlson JH, et al. A live-attenuated chlamydial vaccine protects against trachoma in nonhuman primates. *J Exp Med*. 2011;208(11):2217-23. doi: 10.1084/jem.20111266. PubMed PMID: 21987657; PubMed Central PMCID: PMC3201208.
100. Mueller KE, Wolf K, Fields KA. Gene Deletion by Fluorescence-Reported Allelic Exchange Mutagenesis in *Chlamydia trachomatis*. *MBio*. 2016;7(1):e01817-15. doi: 10.1128/mBio.01817-15. PubMed PMID: 26787828; PubMed Central PMCID: PMC4725004.
101. Lambowitz AM, Zimmerly S. Group II introns: mobile ribozymes that invade DNA. *Cold Spring Harb Perspect Biol*. 2011;3(8):a003616. doi: 10.1101/cshperspect.a003616. PubMed PMID: 20463000; PubMed Central PMCID: PMC3140690.
102. Johnson CM, Fisher DJ. Site-specific, insertional inactivation of *incA* in *Chlamydia trachomatis* using a group II intron. *PLoS One*. 2013;8(12):e83989. doi: 10.1371/journal.pone.0083989. PubMed PMID: 24391860; PubMed Central PMCID: PMC3877132.
103. Lowden NM, Yeruva L, Johnson CM, Bowlin AK, Fisher DJ. Use of aminoglycoside 3' adenylyltransferase as a selection marker for *Chlamydia trachomatis* intron-mutagenesis and in vivo intron stability. *BMC Res Notes*. 2015;8:570. doi: 10.1186/s13104-015-1542-9. PubMed PMID: 26471806; PubMed Central PMCID: PMC4606545.
104. Cupples CG, Miller JH. A set of *lacZ* mutations in *Escherichia coli* that allow rapid detection of each of the six base substitutions. *Proc Natl Acad Sci U S A*. 1989;86(14):5345-9. PubMed PMID: 2501784; PubMed Central PMCID: PMC297618.
105. Brenner S. The genetics of *Caenorhabditis elegans*. *Genetics*. 1974;77(1):71-94. PubMed PMID: 4366476; PubMed Central PMCID: PMC1213120.
106. Kokes M, Dunn JD, Granek JA, Nguyen BD, Barker JR, Valdivia RH, et al. Integrating chemical mutagenesis and whole-genome sequencing as a platform for forward and reverse genetic analysis of *Chlamydia*. *Cell Host Microbe*. 2015;17(5):716-25. doi: 10.1016/j.chom.2015.03.014. PubMed PMID: 25920978; PubMed Central PMCID: PMC4418230.
107. Rodolakis A, Souriau A. Response of ewes to temperature-sensitive mutants of *Chlamydia psittaci* (var *ovis*) obtained by NTG mutagenesis. *Ann Rech Vet*. 1983;14(2):155-61. PubMed PMID: 6614792.
108. Pastink A, Heemskerk E, Nivard MJ, van Vliet CJ, Vogel EW. Mutational specificity of ethyl methanesulfonate in excision-repair-proficient and -deficient strains of *Drosophila melanogaster*. *Mol Gen Genet*. 1991;229(2):213-8. PubMed PMID: 1921971.
109. Kari L, Goheen MM, Randall LB, Taylor LD, Carlson JH, Whitmire WM, et al. Generation of targeted *Chlamydia trachomatis* null mutants. *Proc Natl Acad Sci U S A*. 2011;108(17):7189-93. doi: 10.1073/pnas.1102229108. PubMed PMID: 21482792; PubMed Central PMCID: PMC3084044.
110. Nguyen BD, Valdivia RH. Virulence determinants in the obligate intracellular pathogen *Chlamydia trachomatis* revealed by forward genetic approaches. *Proc Natl Acad Sci U S A*. 2012;109(4):1263-8. doi: 10.1073/pnas.1117884109. PubMed PMID: 22232666; PubMed Central PMCID: PMC3268281.

111. Brothwell JA, Muramatsu MK, Toh E, Rockey DD, Putman TE, Barta ML, et al. Interrogating Genes That Mediate *Chlamydia trachomatis* Survival in Cell Culture Using Conditional Mutants and Recombination. *Journal of bacteriology*. 2016;198(15):2131-9. doi: 10.1128/JB.00161-16. PubMed PMID: 27246568; PubMed Central PMCID: PMC4944222.
112. Muramatsu MK, Brothwell JA, Stein BD, Putman TE, Rockey DD, Nelson DE. Beyond Tryptophan Synthase: Identification of Genes That Contribute to *Chlamydia trachomatis* Survival during Gamma Interferon-Induced Persistence and Reactivation. *Infect Immun*. 2016;84(10):2791-801. doi: 10.1128/IAI.00356-16. PubMed PMID: 27430273.
113. Jeffrey BM, Suchland RJ, Quinn KL, Davidson JR, Stamm WE, Rockey DD. Genome sequencing of recent clinical *Chlamydia trachomatis* strains identifies loci associated with tissue tropism and regions of apparent recombination. *Infect Immun*. 2010;78(6):2544-53. doi: 10.1128/IAI.01324-09. PubMed PMID: 20308297; PubMed Central PMCID: PMC2876530.
114. Joseph SJ, Didelot X, Gandhi K, Dean D, Read TD. Interplay of recombination and selection in the genomes of *Chlamydia trachomatis*. *Biol Direct*. 2011;6:28. doi: 10.1186/1745-6150-6-28. PubMed PMID: 21615910; PubMed Central PMCID: PMC3126793.
115. Joseph SJ, Didelot X, Rothschild J, de Vries HJ, Morre SA, Read TD, et al. Population genomics of *Chlamydia trachomatis*: insights on drift, selection, recombination, and population structure. *Mol Biol Evol*. 2012;29(12):3933-46. doi: 10.1093/molbev/mss198. PubMed PMID: 22891032; PubMed Central PMCID: PMC3494276.
116. Demars R, Weinfurter J, Guex E, Lin J, Potucek Y. Lateral gene transfer in vitro in the intracellular pathogen *Chlamydia trachomatis*. *Journal of bacteriology*. 2007;189(3):991-1003. doi: 10.1128/JB.00845-06. PubMed PMID: 17122345; PubMed Central PMCID: PMC1797294.
117. Matsumoto A, Izutsu H, Miyashita N, Ohuchi M. Plaque formation by and plaque cloning of *Chlamydia trachomatis* biovar trachoma. *J Clin Microbiol*. 1998;36(10):3013-9. PubMed PMID: 9738059; PubMed Central PMCID: PMC105103.
118. Putman TE, Suchland RJ, Ivanovitch JD, Rockey DD. Culture-independent sequence analysis of *Chlamydia trachomatis* in urogenital specimens identifies regions of recombination and in-patient sequence mutations. *Microbiology*. 2013;159(Pt 10):2109-17. doi: 10.1099/mic.0.070029-0. PubMed PMID: 23842467; PubMed Central PMCID: PMC3799229.
119. Ashburner M. *Drosophila: A Laboratory Handbook and Manual*. Two volumes 1989. xliii + 1331pp; 434pp p.
120. Song T, Park Y, Shamputa IC, Seo S, Lee SY, Jeon HS, et al. Fitness costs of rifampicin resistance in *Mycobacterium tuberculosis* are amplified under conditions of nutrient starvation and compensated by mutation in the beta' subunit of RNA polymerase. *Molecular microbiology*. 2014;91(6):1106-19. doi: 10.1111/mmi.12520. PubMed PMID: 24417450; PubMed Central PMCID: PMC3951610.
121. Schulz zur Wiesch P, Engelstadter J, Bonhoeffer S. Compensation of fitness costs and reversibility of antibiotic resistance mutations. *Antimicrob Agents Chemother*. 2010;54(5):2085-95. doi:

- 10.1128/AAC.01460-09. PubMed PMID: 20176903; PubMed Central PMCID: PMC2863634.
122. Melnyk AH, Wong A, Kassen R. The fitness costs of antibiotic resistance mutations. *Evol Appl.* 2015;8(3):273-83. doi: 10.1111/eva.12196. PubMed PMID: 25861385; PubMed Central PMCID: PMC4380921.
  123. Colicchio R, Pagliuca C, Pastore G, Cicatiello AG, Pagliarulo C, Tala A, et al. Fitness Cost of Rifampin Resistance in *Neisseria meningitidis*: In Vitro Study of Mechanisms Associated with rpoB H553Y Mutation. *Antimicrob Agents Chemother.* 2015;59(12):7637-49. doi: 10.1128/AAC.01746-15. PubMed PMID: 26416867; PubMed Central PMCID: PMC4649176.
  124. Binet R, Maurelli AT. Fitness Cost Due to Mutations in the 16S rRNA Associated with Spectinomycin Resistance in *Chlamydia psittaci* 6BC. *Antimicrobial Agents and Chemotherapy.* 2005;49(11):4455-64. doi: 10.1128/AAC.49.11.4455-4464.2005. PubMed PMID: PMC1280162.
  125. Schneider WM, Chevillotte MD, Rice CM. Interferon-stimulated genes: a complex web of host defenses. *Annu Rev Immunol.* 2014;32:513-45. doi: 10.1146/annurev-immunol-032713-120231. PubMed PMID: 24555472; PubMed Central PMCID: PMC4313732.
  126. Anderson KS, Kim AY, Quillen JM, Sayers E, Yang XJ, Miles EW. Kinetic characterization of channel impaired mutants of tryptophan synthase. *J Biol Chem.* 1995;270(50):29936-44. PubMed PMID: 8530393.
  127. Fernandez E, Torrents D, Zorzano A, Palacin M, Chillaron J. Identification and functional characterization of a novel low affinity aromatic-preferring amino acid transporter (arpAT). One of the few proteins silenced during primate evolution. *J Biol Chem.* 2005;280(19):19364-72. doi: 10.1074/jbc.M412516200. PubMed PMID: 15757906.
  128. Russ WP, Engelman DM. The GxxxG motif: a framework for transmembrane helix-helix association. *J Mol Biol.* 2000;296(3):911-9. doi: 10.1006/jmbi.1999.3489. PubMed PMID: 10677291.
  129. Piperno JR, Oxender DL. Amino acid transport systems in *Escherichia coli* K-12. *J Biol Chem.* 1968;243(22):5914-20. PubMed PMID: 4880290.
  130. Daniels VG, Newey H, Smyth DH. Stereochemical specificity of neutral amino acid transfer systems in rat small intestine. *Biochim Biophys Acta.* 1969;183(3):637-9. PubMed PMID: 5822832.
  131. Robbins JC, Oxender DL. Transport systems for alanine, serine, and glycine in *Escherichia coli* K-12. *Journal of bacteriology.* 1973;116(1):12-8. PubMed PMID: 4583203; PubMed Central PMCID: PMC246384.
  132. Guardiola J, Iaccarino M. *Escherichia coli* K-12 mutants altered in the transport of branched-chain amino acids. *Journal of bacteriology.* 1971;108(3):1034-44. PubMed PMID: 4945181; PubMed Central PMCID: PMC247185.
  133. Hoshino T, Kose-Terai K, Uratani Y. Isolation of the braZ gene encoding the carrier for a novel branched-chain amino acid transport system in *Pseudomonas aeruginosa* PAO. *Journal of bacteriology.* 1991;173(6):1855-61. PubMed PMID: 1900503; PubMed Central PMCID: PMC207713.
  134. Kaiser JC, Omer S, Sheldon JR, Welch I, Heinrichs DE. Role of BrnQ1 and BrnQ2 in branched-chain amino acid transport and virulence in *Staphylococcus aureus*. *Infect Immun.* 2015;83(3):1019-29. doi: 10.1128/IAI.02542-14. PubMed PMID: 25547798; PubMed Central PMCID: PMC4333469.

135. Agaisse H, Derre I. A *C. trachomatis* cloning vector and the generation of *C. trachomatis* strains expressing fluorescent proteins under the control of a *C. trachomatis* promoter. *PLoS One*. 2013;8(2):e57090. doi: 10.1371/journal.pone.0057090. PubMed PMID: 23441233; PubMed Central PMCID: PMC3575495.
136. Xu S, Battaglia L, Bao X, Fan H. Chloramphenicol acetyltransferase as a selection marker for chlamydial transformation. *BMC Res Notes*. 2013;6:377. doi: 10.1186/1756-0500-6-377. PubMed PMID: 24060200; PubMed Central PMCID: PMC3849861.
137. O'Connell CM, Nicks KM. A plasmid-cured *Chlamydia muridarum* strain displays altered plaque morphology and reduced infectivity in cell culture. *Microbiology*. 2006;152(Pt 6):1601-7. doi: 10.1099/mic.0.28658-0. PubMed PMID: 16735724.
138. Gong S, Yang Z, Lei L, Shen L, Zhong G. Characterization of *Chlamydia trachomatis* plasmid-encoded open reading frames. *Journal of bacteriology*. 2013;195(17):3819-26. doi: 10.1128/JB.00511-13. PubMed PMID: 23794619; PubMed Central PMCID: PMC3754608.
139. Ohse M, Takahashi K, Kadowaki Y, Kusaoke H. Effects of plasmid DNA sizes and several other factors on transformation of *Bacillus subtilis* ISW1214 with plasmid DNA by electroporation. *Biosci Biotechnol Biochem*. 1995;59(8):1433-7. doi: 10.1271/bbb.59.1433. PubMed PMID: 7549093.
140. Binet R, Maurelli AT. Transformation and isolation of allelic exchange mutants of *Chlamydia psittaci* using recombinant DNA introduced by electroporation. *Proc Natl Acad Sci U S A*. 2009;106(1):292-7. doi: 10.1073/pnas.0806768106. PubMed PMID: 19104068; PubMed Central PMCID: PMC2629194.
141. Daniel J. Measuring the toxic effects of high gene dosage on yeast cells. *Mol Gen Genet*. 1996;253(3):393-6. PubMed PMID: 9003327.
142. Bhattacharyya S, Bershtein S, Yan J, Argun T, Gilson AI, Trauger SA, et al. Transient protein-protein interactions perturb *E. coli* metabolome and cause gene dosage toxicity. *Elife*. 2016;5. doi: 10.7554/eLife.20309. PubMed PMID: 27938662; PubMed Central PMCID: PMC5176355.
143. Wickstrum J, Sammons LR, Restivo KN, Hefty PS. Conditional gene expression in *Chlamydia trachomatis* using the tet system. *PLoS One*. 2013;8(10):e76743. doi: 10.1371/journal.pone.0076743. PubMed PMID: 24116144; PubMed Central PMCID: PMC3792055.
144. DeMars R, Weinfurter J. Interstrain gene transfer in *Chlamydia trachomatis* in vitro: mechanism and significance. *Journal of bacteriology*. 2008;190(5):1605-14. doi: 10.1128/JB.01592-07. PubMed PMID: 18083799; PubMed Central PMCID: PMC2258673.
145. Sandoz KM, Rockey DD. Antibiotic resistance in *Chlamydiae*. *Future Microbiol*. 2010;5(9):1427-42. doi: 10.2217/fmb.10.96. PubMed PMID: 20860486; PubMed Central PMCID: PMC3075073.
146. Nguyen B, Valdivia R. A chemical mutagenesis approach to identify virulence determinants in the obligate intracellular pathogen *Chlamydia trachomatis*. *Methods Mol Biol*. 2014;1197:347-58. doi: 10.1007/978-1-4939-1261-2\_20. PubMed PMID: 25172291.
147. Suchland RJ, Sandoz KM, Jeffrey BM, Stamm WE, Rockey DD. Horizontal transfer of tetracycline resistance among *Chlamydia* spp. in vitro.

- Antimicrob Agents Chemother. 2009;53(11):4604-11. doi: 10.1128/AAC.00477-09. PubMed PMID: 19687238; PubMed Central PMCID: PMCPMC2772348.
148. Binet R, Maurelli AT. The chlamydial functional homolog of KsgA confers kasugamycin sensitivity to *Chlamydia trachomatis* and impacts bacterial fitness. *BMC Microbiol.* 2009;9:279. doi: 10.1186/1471-2180-9-279. PubMed PMID: 20043826; PubMed Central PMCID: PMCPMC2807437.
  149. Gomes JP, Bruno WJ, Borrego MJ, Dean D. Recombination in the genome of *Chlamydia trachomatis* involving the polymorphic membrane protein C gene relative to *ompA* and evidence for horizontal gene transfer. *Journal of bacteriology.* 2004;186(13):4295-306. doi: 10.1128/JB.186.13.4295-4306.2004. PubMed PMID: 15205432; PubMed Central PMCID: PMCPMC421610.
  150. Dunn MF, Aguilar V, Brzovic P, Drewe WF, Jr., Houben KF, Leja CA, et al. The tryptophan synthase bienzyme complex transfers indole between the alpha- and beta-sites via a 25-30 A long tunnel. *Biochemistry.* 1990;29(37):8598-607. PubMed PMID: 2271543.
  151. Miles EW. Tryptophan synthase: a multienzyme complex with an intramolecular tunnel. *Chem Rec.* 2001;1(2):140-51. PubMed PMID: 11893063.
  152. Cash MT, Miles EW, Phillips RS. The reaction of indole with the aminoacrylate intermediate of *Salmonella typhimurium* tryptophan synthase: observation of a primary kinetic isotope effect with 3-[(2)H]indole. *Arch Biochem Biophys.* 2004;432(2):233-43. doi: 10.1016/j.abb.2004.09.027. PubMed PMID: 15542062.
  153. Hilario E, Caulkins BG, Huang YM, You W, Chang CE, Mueller LJ, et al. Visualizing the tunnel in tryptophan synthase with crystallography: Insights into a selective filter for accommodating indole and rejecting water. *Biochim Biophys Acta.* 2016;1864(3):268-79. doi: 10.1016/j.bbapap.2015.12.006. PubMed PMID: 26708480; PubMed Central PMCID: PMCPMC4732270.
  154. Carlson JH, Wood H, Roshick C, Caldwell HD, McClarty G. In vivo and in vitro studies of *Chlamydia trachomatis* TrpR:DNA interactions. *Molecular microbiology.* 2006;59(6):1678-91. doi: 10.1111/j.1365-2958.2006.05045.x. PubMed PMID: 16553875; PubMed Central PMCID: PMCPMC2808116.
  155. Akers JC, Tan M. Molecular mechanism of tryptophan-dependent transcriptional regulation in *Chlamydia trachomatis*. *Journal of bacteriology.* 2006;188(12):4236-43. doi: 10.1128/JB.01660-05. PubMed PMID: 16740930; PubMed Central PMCID: PMCPMC1482941.
  156. Kozmin SG, Leroy P, Pavlov YI, Schaaper RM. YcbX and yiiM, two novel determinants for resistance of *Escherichia coli* to N-hydroxylated base analogues. *Molecular microbiology.* 2008;68(1):51-65. doi: 10.1111/j.1365-2958.2008.06128.x. PubMed PMID: 18312271; PubMed Central PMCID: PMCPMC2740630.
  157. Kozmin SG, Wang J, Schaaper RM. Role for CysJ flavin reductase in molybdenum cofactor-dependent resistance of *Escherichia coli* to 6-N-hydroxylaminopurine. *Journal of bacteriology.* 2010;192(8):2026-33. doi: 10.1128/JB.01438-09. PubMed PMID: 20118259; PubMed Central PMCID: PMCPMC2849459.

158. Chamizo-Ampudia A, Galvan A, Fernandez E, Llamas A. The *Chlamydomonas reinhardtii* molybdenum cofactor enzyme crARC has a Zn-dependent activity and protein partners similar to those of its human homologue. *Eukaryot Cell*. 2011;10(10):1270-82. doi: 10.1128/EC.05096-11. PubMed PMID: 21803866; PubMed Central PMCID: PMCPMC3187064.
159. Havemeyer A, Lang J, Clement B. The fourth mammalian molybdenum enzyme mARC: current state of research. *Drug Metab Rev*. 2011;43(4):524-39. doi: 10.3109/03602532.2011.608682. PubMed PMID: 21942410.
160. Krompholz N, Krischkowski C, Reichmann D, Garbe-Schonberg D, Mendel RR, Bittner F, et al. The mitochondrial Amidoxime Reducing Component (mARC) is involved in detoxification of N-hydroxylated base analogues. *Chem Res Toxicol*. 2012;25(11):2443-50. doi: 10.1021/tx300298m. PubMed PMID: 22924387.
161. Simandan T, Sun J, Dix TA. Oxidation of DNA bases, deoxyribonucleosides and homopolymers by peroxy radicals. *Biochem J*. 1998;335 ( Pt 2):233-40. PubMed PMID: 9761719; PubMed Central PMCID: PMCPMC1219774.
162. Aune TM, Pogue SL. Inhibition of tumor cell growth by interferon-gamma is mediated by two distinct mechanisms dependent upon oxygen tension: induction of tryptophan degradation and depletion of intracellular nicotinamide adenine dinucleotide. *The Journal of clinical investigation*. 1989;84(3):863-75. doi: 10.1172/JCI114247. PubMed PMID: 2503544; PubMed Central PMCID: PMCPMC329730.
163. Hatch TP. Utilization of L-cell nucleoside triphosphates by *Chlamydia psittaci* for ribonucleic acid synthesis. *Journal of bacteriology*. 1975;122(2):393-400. PubMed PMID: 1168632; PubMed Central PMCID: PMCPMC246069.
164. Price CT, Al-Quadani T, Santic M, Rosenshine I, Abu Kwaik Y. Host proteasomal degradation generates amino acids essential for intracellular bacterial growth. *Science*. 2011;334(6062):1553-7. doi: 10.1126/science.1212868. PubMed PMID: 22096100.
165. Niu H, Xiong Q, Yamamoto A, Hayashi-Nishino M, Rikihisa Y. Autophagosomes induced by a bacterial Beclin 1 binding protein facilitate obligatory intracellular infection. *Proc Natl Acad Sci U S A*. 2012;109(51):20800-7. doi: 10.1073/pnas.1218674109. PubMed PMID: 23197835; PubMed Central PMCID: PMCPMC3529060.
166. Tan GM, Lim HJ, Yeow TC, Movahed E, Looi CY, Gupta R, et al. Temporal proteomic profiling of *Chlamydia trachomatis*-infected HeLa-229 human cervical epithelial cells. *Proteomics*. 2016;16(9):1347-60. doi: 10.1002/pmic.201500219. PubMed PMID: 27134121.
167. Kiritani K. Mutants of *Salmonella typhimurium* defective in transport of branched-chain amino acids. *Journal of bacteriology*. 1974;120(3):1093-101. PubMed PMID: 4373435; PubMed Central PMCID: PMCPMC245887.
168. Cho BK, Federowicz S, Park YS, Zengler K, Palsson BO. Deciphering the transcriptional regulatory logic of amino acid metabolism. *Nat Chem Biol*. 2011;8(1):65-71. doi: 10.1038/nchembio.710. PubMed PMID: 22082910; PubMed Central PMCID: PMCPMC3777760.
169. Short SA, White DC, Kaback HR. Mechanisms of active transport in isolated bacterial membrane vesicles. IX. The kinetics and specificity of

- amino acid transport in *Staphylococcus aureus* membrane vesicles. *J Biol Chem.* 1972;247(23):7452-8. PubMed PMID: 4636316.
170. Drew D, Sjostrand D, Nilsson J, Urbig T, Chin CN, de Gier JW, et al. Rapid topology mapping of *Escherichia coli* inner-membrane proteins by prediction and PhoA/GFP fusion analysis. *Proc Natl Acad Sci U S A.* 2002;99(5):2690-5. doi: 10.1073/pnas.052018199. PubMed PMID: 11867724; PubMed Central PMCID: PMCPMC122409.
  171. Akahane S, Kamata H, Yagisawa H, Hirata H. A novel neutral amino acid transporter from the hyperthermophilic archaeon *Thermococcus* sp. KS-1. *J Biochem.* 2003;133(2):173-80. PubMed PMID: 12761179.
  172. Adams MD, Wagner LM, Graddis TJ, Landick R, Antonucci TK, Gibson AL, et al. Nucleotide sequence and genetic characterization reveal six essential genes for the LIV-I and LS transport systems of *Escherichia coli*. *J Biol Chem.* 1990;265(20):11436-43. PubMed PMID: 2195019.
  173. Hatch TP. Competition between *Chlamydia psittaci* and L cells for host isoleucine pools: a limiting factor in chlamydial multiplication. *Infect Immun.* 1975;12(1):211-20. PubMed PMID: 1095493; PubMed Central PMCID: PMCPMC415269.
  174. Harper A, Pogson CI, Jones ML, Pearce JH. Chlamydial Development Is Adversely Affected by Minor Changes in Amino Acid Supply, Blood Plasma Amino Acid Levels, and Glucose Deprivation. *Infection and Immunity.* 2000;68(3):1457-64. PubMed PMID: PMC97301.
  175. Allan I, Pearce JH. Differential amino acid utilization by *Chlamydia psittaci* (strain guinea pig inclusion conjunctivitis) and its regulatory effect on chlamydial growth. *J Gen Microbiol.* 1983;129(7):1991-2000. doi: 10.1099/00221287-129-7-1991. PubMed PMID: 6415225.
  176. Ripa KT, Mardh PA. Cultivation of *Chlamydia trachomatis* in cycloheximide-treated McCoy cells. *J Clin Microbiol.* 1977;6(4):328-31. PubMed PMID: 562356; PubMed Central PMCID: PMCPMC274768.
  177. Allan I, Pearce JH. Radiolabelling of *Chlamydia psittaci* (strain guinea pig inclusion conjunctivitis) to high specific activity using <sup>14</sup>C-labelled amino acids. *FEMS Microbiology Letters.* 1982;13(1):69-73. doi: 10.1111/j.1574-6968.1982.tb08229.x.
  178. Turco J, Winkler HH. Gamma-interferon-induced inhibition of the growth of *Rickettsia prowazekii* in fibroblasts cannot be explained by the degradation of tryptophan or other amino acids. *Infect Immun.* 1986;53(1):38-46. PubMed PMID: 3087883; PubMed Central PMCID: PMCPMC260072.
  179. Onodera J, Ohsumi Y. Autophagy is required for maintenance of amino acid levels and protein synthesis under nitrogen starvation. *J Biol Chem.* 2005;280(36):31582-6. doi: 10.1074/jbc.M506736200. PubMed PMID: 16027116.
  180. Driskell LO, Tucker AM, Woodard A, Wood RR, Wood DO. Fluorescence Activated Cell Sorting of *Rickettsia prowazekii*-Infected Host Cells Based on Bacterial Burden and Early Detection of Fluorescent Rickettsial Transformants. *PLoS One.* 2016;11(3):e0152365. doi: 10.1371/journal.pone.0152365. PubMed PMID: 27010457; PubMed Central PMCID: PMCPMC4807063.
  181. Alzhanov DT, Suchland RJ, Bakke AC, Stamm WE, Rockey DD. Clonal isolation of chlamydia-infected cells using flow cytometry. *J Microbiol*



- Methods. 2007;68(1):201-8. doi: 10.1016/j.mimet.2006.07.012. PubMed PMID: 16997404.
182. Vicetti Miguel RD, Henschel KJ, Duenas Lopez FC, Quispe Calla NE, Cherpes TL. Fluorescent labeling reliably identifies *Chlamydia trachomatis* in living human endometrial cells and rapidly and accurately quantifies chlamydial inclusion forming units. *J Microbiol Methods*. 2015;119:79-82. doi: 10.1016/j.mimet.2015.10.003. PubMed PMID: 26453947; PubMed Central PMCID: PMC4993108.
  183. Osborne GW. Recent advances in flow cytometric cell sorting. *Methods Cell Biol*. 2011;102:533-56. doi: 10.1016/B978-0-12-374912-3.00021-3. PubMed PMID: 21704853.
  184. Schulte R, Wilson NK, Prick JC, Cossetti C, Maj MK, Gottgens B, et al. Index sorting resolves heterogeneous murine hematopoietic stem cell populations. *Exp Hematol*. 2015;43(9):803-11. doi: 10.1016/j.exphem.2015.05.006. PubMed PMID: 26051918; PubMed Central PMCID: PMC4571925.
  185. Li P, Du Q, Cao Z, Guo Z, Evankovich J, Yan W, et al. Interferon-gamma induces autophagy with growth inhibition and cell death in human hepatocellular carcinoma (HCC) cells through interferon-regulatory factor-1 (IRF-1). *Cancer Lett*. 2012;314(2):213-22. doi: 10.1016/j.canlet.2011.09.031. PubMed PMID: 22056812; PubMed Central PMCID: PMC3487386.
  186. Al-Zeer MA, Al-Younes HM, Lauster D, Abu Lubad M, Meyer TF. Autophagy restricts *Chlamydia trachomatis* growth in human macrophages via IFNG-inducible guanylate binding proteins. *Autophagy*. 2013;9(1):50-62. doi: 10.4161/auto.22482. PubMed PMID: 23086406; PubMed Central PMCID: PMC3542218.
  187. Selleck EM, Orchard RC, Lassen KG, Beatty WL, Xavier RJ, Levine B, et al. A Noncanonical Autophagy Pathway Restricts *Toxoplasma gondii* Growth in a Strain-Specific Manner in IFN-gamma-Activated Human Cells. *MBio*. 2015;6(5):e01157-15. doi: 10.1128/mBio.01157-15. PubMed PMID: 26350966; PubMed Central PMCID: PMC4600106.
  188. Taylor SC, Berkelman T, Yadav G, Hammond M. A defined methodology for reliable quantification of Western blot data. *Mol Biotechnol*. 2013;55(3):217-26. doi: 10.1007/s12033-013-9672-6. PubMed PMID: 23709336; PubMed Central PMCID: PMC3840294.
  189. Tang XF, Ezaki S, Atomi H, Imanaka T. Biochemical analysis of a thermostable tryptophan synthase from a hyperthermophilic archaeon. *Eur J Biochem*. 2000;267(21):6369-77. PubMed PMID: 11029579.
  190. Bravo M, Eran H, Zhang FX, McKenna CE. A rapid, sensitive high-performance liquid chromatography analysis of ammonia and methylamine for nitrogenase assays. *Anal Biochem*. 1988;175(2):482-91. PubMed PMID: 3239773.

## CURRICULUM VITAE

Matthew Kazuyuki Muramatsu

### EDUCATION

- Ph.D. Microbiology** 2013-2017  
Department of Microbiology and Immunology  
Indiana University, Indianapolis, IN
- Ph.D. Microbiology** 2011-2012  
Department of Biology-Microbiology Program  
Indiana University, Bloomington, IN
- B.S. Microbiology** 2005-2009  
Department of Microbiology  
University of Washington, Seattle, WA

### RESEARCH EXPERIENCE

- Graduate Research Assistant** 2013-2017  
Department of Microbiology and Immunology  
Indiana University School of Medicine, Indianapolis, IN  
PI: **David Nelson, Ph.D.**
- Investigating the different mechanisms *C. trachomatis* uses to circumvent intracellular stressors such as nutrient deprivation and the effects of IFN- $\gamma$  mediated persistence.
- Graduate Research Assistant** 2011-2012  
Department of Biology  
Indiana University, Bloomington, IN  
PI: **David Nelson, Ph.D.**
- Optimized transformation, plasmid curing, and chemical mutagenesis conditions for *C. trachomatis*.
- Research Scientist** 2010-2011  
Department of Immunology  
University of Washington, Seattle, WA  
PI: **Michael Gale Jr., Ph.D.** NIAID: 272200900035C-2-0-1
- Investigated how novel adjuvant compounds stimulated the innate immune system in cell culture and animal models.
- Undergraduate Research Technician** 2008-2009  
Northwest Fisheries Science Center  
National Oceanic and Atmospheric Administration, Seattle, WA  
P.I.: **Mark Strom, Ph.D.**
- Used Multi-Locus Sequence Typing to determine the genetic phylogeny of *Vibrio parahaemolyticus* isolates.

## PROFESSIONAL EXPERIENCE

**Microbiologist** 2009-2010

Institute of Environmental Health, Lake Forest Park, WA

- Co-led a Federal Drug Administration project investigating the number and type of bacteria found in ready to eat leafy greens.
- Used molecular and culture based techniques to identify harmful pathogens present in food.

## GRANT & AWARD

**Microbial Pathogenesis and Host Response Travel Award** 2015

Cold Spring Harbor Laboratory, Cold Spring Harbor, NY

**Genetic, Cellular and Molecular Sciences Training Grant** 2011-2012

National Institute of General Medical Sciences, National Institute of Health

NIGMS Training Grant 5T32GM007757-32

## PUBLICATIONS

1. **Muramatsu MK**, Brothwell JA, Stein BD, Putman TE, Rockey DD, Nelson DE. 2016. Beyond tryptophan synthase: identification of genes that contribute to *Chlamydia trachomatis* survival during gamma interferon-induced persistence and reactivation. *Infect Immun* 84:2791-2801.
2. Brothwell JA, **Muramatsu MK**, Toh E, Rockey DD, Putman TE, Barta ML, Hefty PS, Suchland RJ, Nelson DE. 2016. Interrogating genes that mediate *Chlamydia trachomatis* survival in cell culture using conditional mutants and recombination. *J Bacteriol* 198:2131-2139.

## INVITED TALK

1. **Muramatsu MK**, Brothwell JA, Putman TE, Rockey DD, Stein BD, Nelson DE. Identification and characterization of novel persistence genes in *Chlamydia trachomatis*. European Society for Chlamydia Research, 2016. Oxford, United Kingdom.

## CONFERENCE PRESENTATIONS

1. **Muramatsu MK**, Brothwell JA, Putman TE, Rockey DD, Stein BD, Nelson DE. Identification of genes important for *Chlamydia trachomatis* persistence. Poster. Microbial Pathogenesis and Host Response, 2015. Cold Spring Harbor, NY.
2. **Muramatsu MK**, Brothwell JA, Putman TE, Rockey DD, Nelson DE. Identifying novel persistence genes in *Chlamydia trachomatis*. Poster. Midwest Microbial Pathogenesis Conference, 2015, Indianapolis, IN.

3. Brothwell JA, **Muramatsu MK**, Toh E, Putman TE, Rockey DD, Nelson DE. Exploiting temperature sensitive alleles to investigate chlamydial essential gene functions and generate isogenic recombinants. Paper. 7<sup>th</sup> Chlamydia Basic Research Society, 2015, New Orleans, LA.
4. Brothwell JA, **Muramatsu MK**, Toh E, Putman TE, Rockey DD, Nelson DE. Generation of *Chlamydia trachomatis* recombinants via negative selection. Poster. Midwest Microbial Pathogenesis Conference, 2015, Indianapolis, IL.
5. **Muramatsu MK**, Putman TE, Rockey DD, Suchland RJ, Nelson DE. Unraveling *Chlamydia trachomatis* persistence: A Forward Genetic Approach. Poster. Midwest Microbial Pathogenesis Conference, 2014, Chicago, IL.
6. Brothwell JA, **Muramatsu MK**, Toh E, Nelson DE. Uncovering chlamydia essential genes: screen and genetic analyses of temperature sensitive *Chlamydia trachomatis* mutants. Poster. Midwest Microbial Pathogenesis Conference, 2014, Chicago, IL.
7. **Muramatsu MK**, Brothwell JA, Nelson DE. A Forward Genetic Approach to Identify Novel Persistence Genes in *Chlamydia trachomatis*. Poster. American Society for Microbiology 114<sup>th</sup> General Meeting, 2014. Boston, MA.
8. **Muramatsu MK**. Analyzing the phylogenetic relationships of *Vibrio parahaemolyticus* in the Northwest region of the U.S. by Multi Locus Sequence Typing. Poster. 12<sup>th</sup> Annual University of Washington Undergraduate Research Symposium, 2009. Seattle, WA.

#### TEACHING EXPERIENCE

**Associate Instructor**

**Fall 2011**

Evolution and Diversity, Indiana University, Bloomington, IN

#### AFFILIATION

The American Society of Microbiology: Member

**2009-Pres.**

#### SERVICE

Research in progress award committee chair

**2014**